# EVALUATION OF STRESS DROP OF THE AUGUST 2, 1974 GEORGIA-SOUTH CAROLINA EARTHQUAKE AND AFTERSHOCK SEQUENCE

A THESIS

Presented to

The Faculty of the Division of Graduate

Studies and Research

By

Samuel Rutt Bridges

In Partial Fulfillment

of the Requirements for the Degree

Master of Science in Geophysical Sciences

Georgia Institute of Technology

August, 1975

EVALUATION OF STRESS DROP OF THE AUGUST 2, 1974 GEORGIA-SOUTH CAROLINA EARTHQUAKE AND AFTERSHOCK SEQUENCE

Approved:

L.T.Long, Chairman

G.L.Maynard

J.M.Wampler

Date approved by Chairman Aug 20 1975

# ACKNOWLEDGMENTS

This research was conducted under the direction of Dr. Leland Timothy Long, to whom the author is indebted for many useful criticisms and insights into both the field operations and data analysis. His understanding of the problems involved in this investigation ranged from the nuts and bolts of instrumentation to the theoretical significance of the results, and the author is most grateful for this expert and practical guidance. Thanks are also extended to Dr. G. Lafayette Maynard for his input into the field operations as well as his helpful suggestions for editing the manuscript. Dr. J. Marion Wampler's critical review of the manuscript is also appreciated.

Dr. C. O. Pollard's loan of his boat and motor for several weeks following the main shock was instrumental in acquiring good aftershock data. Dr. Pollard also gave of his own time in the geologic field reconnaissance following the August 2, 1974 earthquake. His unselfish contributions are greatly appreciated.

Mr. James M. Butler has assisted with all aspects of the field operations and much of the analysis. A good portion of his efforts, particularly those just following the main shock, were not financially compensated due to lack of funding in the early stages of the study. I offer my heartfelt thanks to James for his kind and generous nature. Mr. Richard L. Garfield also gave free time to the project during the crucial early stages, and this is gratefully acknowledged.

The author is also grateful to Mr. and Mrs. J. W. Champion who gave freely of their time and efforts to provide gravity data in the immediate epicentral area. Mr. Allen Wyatt has done an excellent job in keeping the instruments operating and in preparing us for the many field excursions.

The author also wishes to acknowledge the aid of Mr. H. E. Denman through his definitive study on the seismic and geologic background of the Clark Hill Reservoir. Mr. Peter Scheffeler, Dr. Pradeep Talwani and others at the University of South Carolina provided intensity data. Law Engineering and Testing Company also provided supplementary intensity data. Ranger W. A. Hamilton of the Corps of Engineers aided in the distribution of intensity forms as well as arranging the acquisition of water level data for the reservoir.

Colonel Earl Bradley, U.S. Army (Ret) provided the use of his cabin on the reservoir as a base of operations for many weeks following the August 2, 1974 event. His generosity and enthusiasm are warmly appreciated. Sgt. Fred R. Timblin provided the use of his storage room adjacent to his cabin on the reservoir. The magnetic tape data obtained at this recording site was essential in recognizing the high stress drop nature of the aftershock activity. The author is most grateful to Sgt. Timblin for his trust in providing us with access to these facilities.

Dr. Peter Leary and Mr. Peter Malin of Princeton University provided the author with preliminary results of seismic refraction studies they carried out during March and April, 1975. This free

exchange of data in the true spirit of scientific investigation is thankfully acknowledged.

I gratefully acknowledge the help of Miss Katherine P. Gennusa who assisted with many aspects of the project. Her unselfish, encouraging nature and tireless labors are responsible for many of the successes of this project.

Thanks are due to Mr. Terry McGee, who operated our magnetic tape seismic recorder in his home during the first week following the August 2, 1974 event. The author is especially appreciative of the kind efforts of Mr. Tim Standard and his father. Their operation of a smoked paper recorder from September, 1974 through January, 1975 provided valuable data on aftershock activity levels. Their cheerful acceptance of this sometimes tiresome daily chore reflects their generous natures. The author is also indebted to Ranger Fred Pless and his associates at Bobby Brown State Park for the operation of a smoked paper recorder from January through March, 1975. These data have helped verify the lack of migration of activity with time, and so were valuable in the development of this thesis. Mr. David Dunbar, a graduate research assistant at Georgia Tech, aided in the data analysis and instrumentation calibrations.

This thesis was typed by Miss Barbara A. Haas. Her patience and understanding is greatly appreciated.

This research was supported by grant AJ(40-1)4822 with the Nuclear Regulatory Commission (Formerly the Atomic Energy Commission).

TABLE OF CONTENTS

TABLE OF CONTENTS (Continued)

# LIST OF TABLES

# LIST OF ILLUSTRATIONS

LIST OF ILLUSTRATIONS (Continued)

## SUMMARY

On August 2, 1974 at 8:52 GMT, a magnitude $m_b = 4.3$ earthquake occurred near the northern portion of the Clark Hill Reservoir. Detailed aftershock monitoring following this event has provided the most extensive documentation of an aftershock sequence ever obtained for a southeastern United States earthquake. The data include smoked paper seismograms which have been used to establish activity levels and to locate individual microearthquakes, and magnetic tape data which have provided information on both location of aftershocks and microearthquake particle displacement spectra. On the basis of these aftershock data the change in stress occurring along a fault during an earthquake was evaluated. The stress drop of selected aftershocks was calculated using the following five published stress drop-dependent relations; (1) the theoretical relations between spectral corner frequencies as a function of magnitude and stress drop, (2) the empirical relations between stress drop, magnitude of the main shock and duration of aftershock activity, (3) the relations between stress drop and "b" value as a function of the difference between the magnitude of the main shock and the magnitude of the largest aftershock, (4) the comparison of the "b" value of the aftershock sequence to "b" values of numerous other well-studied aftershock sequences (of New Zealand and California) for which the main event's stress drop is known, and (5) the comparison of the magnitude of the main shock to its fault dimensions as estimated

from the size of the aftershock zone. All five methods imply a high stress drop for the August 2, 1974 event and its aftershocks. The stress drop values are much larger than had previously been reported for earthquakes of about the same magnitude in other areas. The data indicate that high stress conditions remained in the aftershock hypocentral area after the August 2, 1974 $m_b = 4.3$ event. The direct methods of Randall (1973) indicated stress drops several times larger than those obtained by Gibowicz's (1973) statistical methods.

The scatter of aftershock hypocenters indicated that faulting was not occurring along a single plane. Instead, the distribution of hypocenters suggest that faulting was occurring along two or more planes. The faulting was assumed to be at depths less than 1.5 km since no hypocenters deeper than 1.5 km were found. Relative to their magnitudes, the intensities of the aftershocks were high. This may be due in part to the shallow hypocenters and the competence of the rock. Two possible explanations for this activity are suggested; one involves the rupture of brittle rocks during bending of the crust, while the other entails thermal perturbation of the stress field due to circulating groundwater.

# CHAPTER I

## INTRODUCTION

On August 2, 1974 at 4:52 a.m. EDT (8:52 GMT) an earthquake of magnitude $m_b$ = 4.3 (Earthquake Data Report, United States Geological Survey) occurred in the northern portion of the Clark Hill Reservoir Area (CHRA). Locally the earthquake was felt with intensities V and VI (Modified Mercalli Intensity) and as far away as Augusta (70 km) with intensity III-IV (Figure 1). Following the main shock, portable seismic recorders were moved into the epicentral area to record aftershocks. An abnormally large number of aftershocks were recorded on both smoked paper and magnetic tape recording instruments to provide an unusually well-documented set of aftershock data for this southeastern United States earthquake.

Stress drop is a measure of the decrease in stress which occurs along a fault during an earthquake. It is a critical factor in the understanding of the tectonic mechanism causing this and perhaps other southeastern United States earthquakes. The object of this thesis is to evaluate the stress drop of the August 2, 1974 event and some of its aftershocks.

### Seismic History of the Clark Hill Reservoir Area

The only minor ($m_b \geq 4.0$) earthquake known to have occurred in the Clark Hill Reservoir Area prior to the August 2, 1974 event was

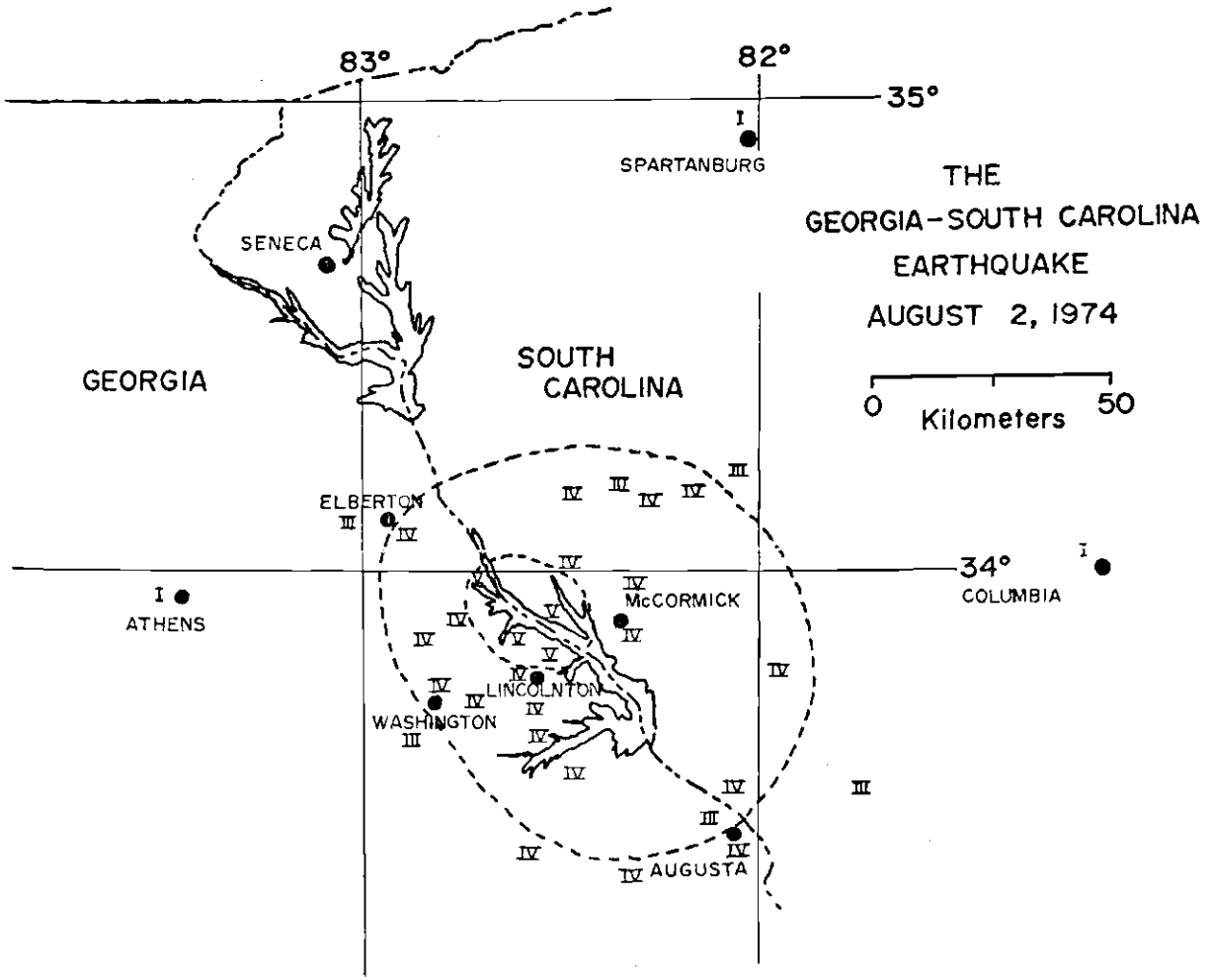


Figure 1. Intensity Map of the August 2, 1974 4:52 a.m. EDT Earthquake.

the November 1, 1875 earthquake of Modified Mercalli Intensity VI. Based upon somewhat sketchy intensity data (Rockwood, 1876; Atlanta Constitution, 1875), the epicenter was placed somewhere between Lincolnton, Georgia and Washington, Georgia (Figure 2). Prior to installation of the Worldwide Standard Seismograph Station ATL in 1963, events smaller than local magnitude ($M_L$) 3.5 probably would not have been reported. Low level seismic activity may possibly have been occurring in this area for many years. In this sparsely populated area such activity would likely have gone unnoticed or have been passed off as large blasts from one of the numerous Elberton granite quarries.

Since the installation of the ATL seismic station near Lovejoy, Georgia in 1963, the minimum detection level for events in the CHRA has been local magnitude ($M_L$) 1.8 ± 0.3. This improved seismic detection capability has revealed sporadic low-level seismic activity in the vicinity of the CHRA. At least 15 events in the magnitude range of $M_L$ = 2.6 to 3.4 have occurred in the CHRA between July, 1963 and July, 1974 (Table 1). In addition, about 40 events in the magnitude range of 1.8 to 3.4 occurred during April through August, 1969 (Long, 1974). This swarm included four of the above 15 events. This swarm exhibited a "b" value of 1.3 ± 0.5.

The data shown in Table 1 (after Denman, 1974) indicate that these events are not all from the same epicentral area. S-P times recorded at ATL vary by as much as 2.52 seconds, indicating a radial scatter of activity of as much as 22.4 km. However, these S-P data cluster around two distinct values, 19.34 ± 0.02 sec. and 21.45 ± 0.40 sec. This apparently indicates at least two separate areas of activity.

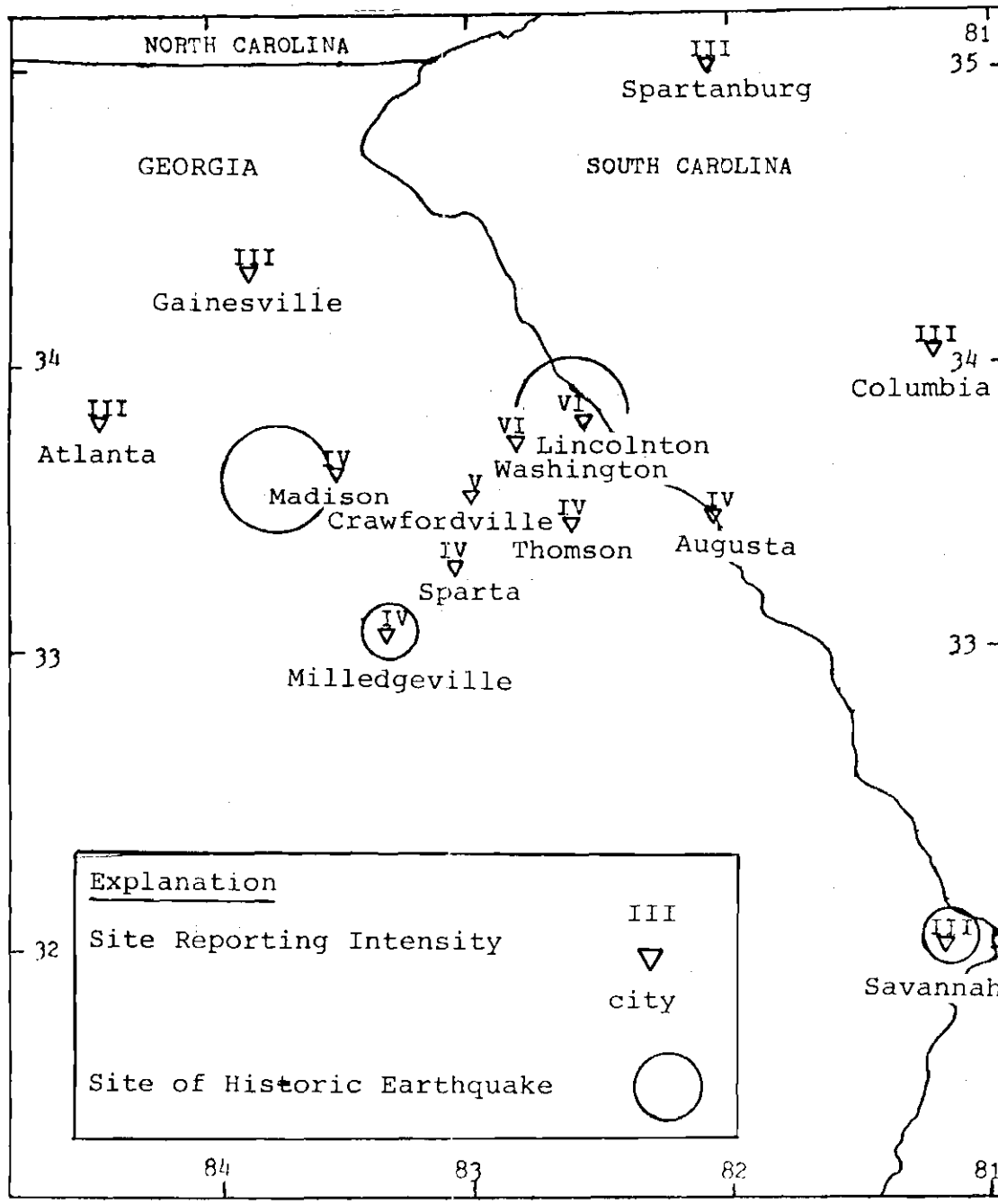


Figure 2. Intensities of the November 1, 1875 Earthquake and Epicenters of Earthquakes of Intensity V or Greater in Georgia (Rockwood, 1876; Atlanta Constitution, 1875; After Denman, 1974).

Table 1. Catalog of Clark Hill Events,

July, 1963 Through July, 1974

| Date | Time (GMT) P at ATL[+] | S-P Seconds | Distance Kilometers[++] | $M_{BLG}$ |
|---|---|---|---|---|
| 7/04/74 | 02:18 | 21.60 | 192.4 ± 10 | 2.6 |
| 2/13/74 | 06:56 | 21.50 | 191.5 ± 10 | 2.7 |
| 10/08/73 | 13:38 | 21.30 | 189.7 ± 10 | 3.3 |
| 4/26/71 | 09:04 | 21.44 | 190.9 ± 10 | 2.7 |
| 4/16/71 | 07:31 | 21.22 | 188.9 ± 10 | 3.3 |
| 5/18/69 | 10:56 | 21.66 | 192.9 ± 10 | 3.2 |
| 5/18/69 | 10:54 | 21.65 | 192.8 ± 10 | 3.4 |
| 5/09/69 | 12:14 | 21.47 | 191.2 ± 10 | 3.2 |
| 5/05/69 | 22:39 | 21.60 | 192.4 ± 10 | 2.7 |
| 4/07/65 | 07:41 | 21.10 | 187.9 ± 10 | 3.5 |
| 4/06/65 | 21:19 | 19.36 | 172.4 ± 10 | 2.6 |
| 12/29/64 | 07:16 | 21.69 | 193.2 ± 10 | 3.2 |
| 12/28/64 | 17:33 | 21.83 | 194.4 ± 10 | 2.9 |
| 3/07/64 | 18:03 | 19.31 | 172.0 ± 10 | 3.6 |
| 10/07/63 | 06:02 | 21.04 | 187.4 ± 10 | 3.4 |

[+]P wave arrival at ATL to the nearest minute.

[++]Accuracy is ± 10 km based on a ± 0.1 sec error in the measured S-P times.

The seismic history of the CHRA prior to the August 2, 1974 event is discussed in more detail by Denman (1974). The August 2, 1974 event and its aftershocks are the subject of this study.

## The Geology of the Clark Hill Reservoir

The CHRA is located on the Savannah River about 80 km northwest of Augusta, Georgia. The reservoir falls within the Piedmont Physiographic Province. The rocks of the CHRA are of both metamorphic and igneous origin. The metamorphic rocks, which are Precambrian to Paleozoic in age, consist of both metasedimentary and metaigneous rocks. Some of the rocks (Denman, 1974) have been through as many as four major metamorphic events (approximately 1100, 550, 450 and 250 million years before present). In general, the original features of the rocks are greatly obscured. The texture of most of the rocks of the CHRA is gneissic. Basalt or diabase dikes of Mesozoic age cut through the metamorphic rocks and generally trend northwest. Additional information and references for the regional geology of the CHRA are given by Denman (1974).

## The Geology of the Epicentral Area

In the immediate epicentral area of the August 2, 1974 event, the rocks are commonly coarse grained and gneissic in texture with numerous quartzite veins ranging up to a meter in thickness. Feldspar phenocrysts with diameters ranging up to a centimeter or two are quite common. Because of their marked lateral variability Crickmay (1952) has interpreted these rocks as largely metasedimentary in origin. The

metamorphic grade implies formation under moderately high temperature and pressure (amphibolite facies).

In the immediate epicentral area, one of the most perplexing characteristics of these rocks is their cracked and jointed texture, readily observed at the surface. This is particularly perplexing since such fractured rocks would not ordinarily be expected to sustain high shear stress.

# CHAPTER II

## INSTRUMENTATION AND EQUIPMENT

Typically, a seismic recording system (Figure 3) consists of a seismometer which generates a voltage proportional to the particle velocity of the earth, a voltage amplifier which may increase the seismometer output voltage by a factor as high as 100,000, a timing system accurate to within ± 0.1 second per day, 12 volt battery power supplies and a smoked paper or magnetic tape recorder. Such systems may also employ electronic filters to attenuate sixty hertz noise or to narrow the bandpass of the system.

### Magnetic Tape Recorders

Magnetic tape recordings (Figure 4) were used for the investigation of the spectral character of the microearthquakes. In the field, signal levels were set by the use of a portable oscilloscope so that at the tape input the level of seismic background noise corresponded to approximately forty millivolts peak to peak; the tape saturation level of four volts peak to peak provided a dynamic range of 42 dB or 100:1 for this system. Unfortunately, at the time of this study, chronometers had not yet been installed in these systems. However, by playing back individual microearthquakes on a strip chart recorder at 125 millimeters per second S-P times accurate to ± 0.01 second were easily obtained. This represents an error of aftershock location distance of less than 100 meters.

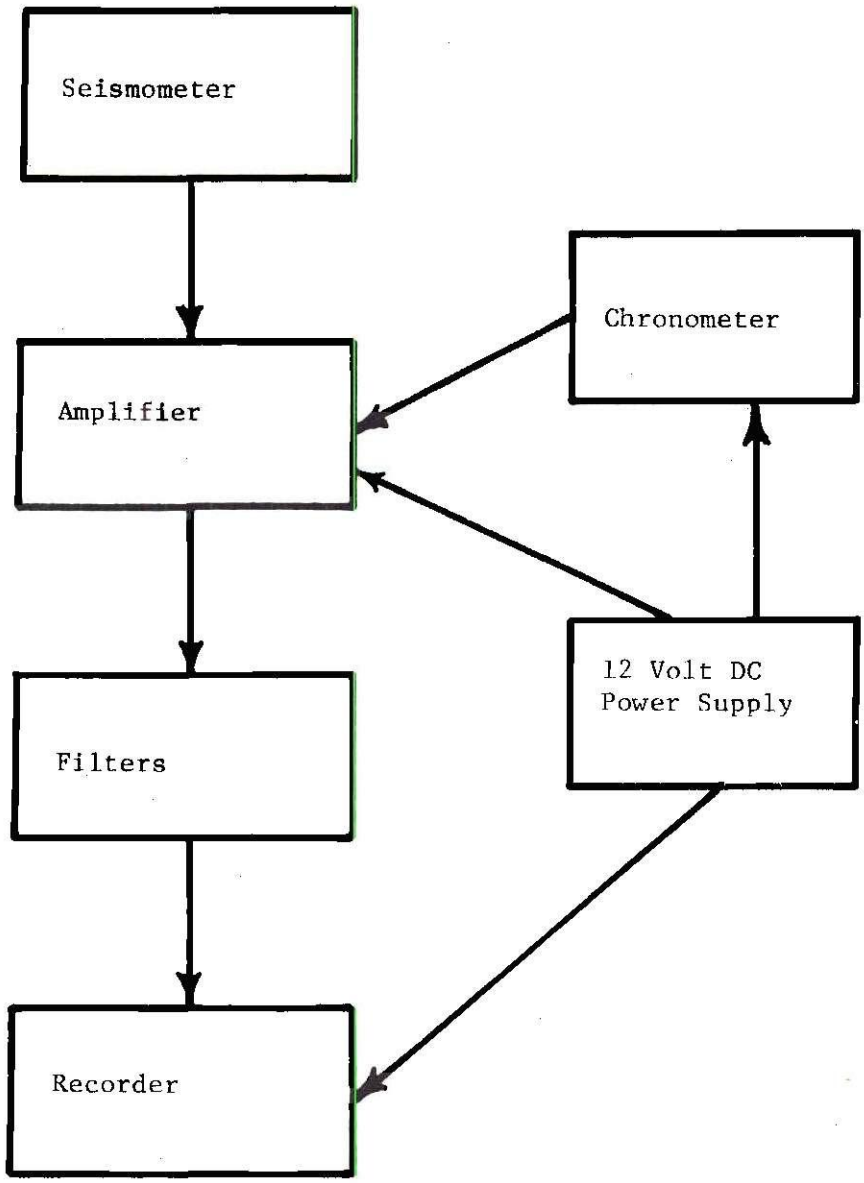


Figure 3. Schematic Diagram of an Earthquake Seismograph.

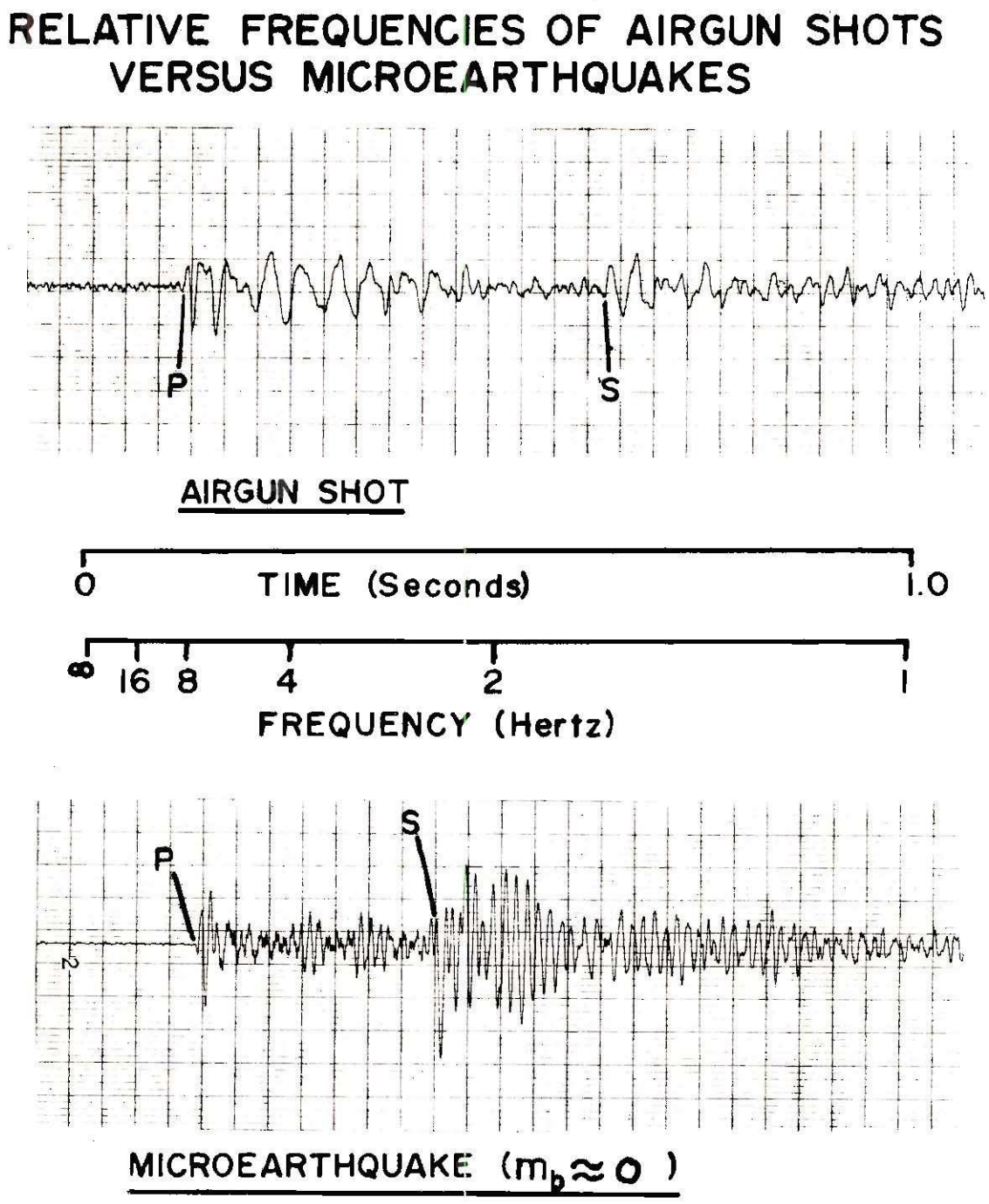


Figure 4. Strip Chart Playback of Events Recorded on Magnetic Tape. Note that the Microearthquake Energy is in High Frequencies (~100 hz). For Comparison, the Characteristic Frequency of the Airgun is About 20 Hertz.

Examination of magnetic tape data was facilitated by playing back the tapes into a smoked paper recorder with time marks from a chronometer (Figure 5). A stable recording and playback speed was assumed. These smoked paper seismograms were then compared to other smoked paper seismograms from the same time period to correlate individual microearthquakes.

Tape recorders used included a Honeywell 8100 half-inch, reel-to-reel, seven-channel FM recorder and a Sony RC-800B one-quarter inch reel-to-reel portable AM recorder. The Honeywell recorder's frequency response was DC to 600 Hertz (at 1 7/8 ips); the Sony tape recorder's frequency response, however, was 20 to 4000 Hertz (at 15/16 ips). Seismograms from the Honeywell FM recorder established that the corner frequencies of the aftershocks were always several times greater than twenty hertz; hence, the low frequency cut off of the Sony recorder did not affect the evaluation of aftershock corner frequencies. Frequency response curves for the Honeywell and Sony tape recorders as well as the Hewlett Packard Strip Chart Recorder are given in Appendix I.

## Smoked Paper Recorders

Smoked paper recorders provide a simple visual mode for producing seismograms. First, a sheet of smooth finish paper is taped or rubber cemented to a cylindrical drum. This drum is then rotated over a sooty kerosene flame until the paper is coated with carbon black. The recording is effected by a stylus attached to a penmotor that produces displacements that are proportional to the current output

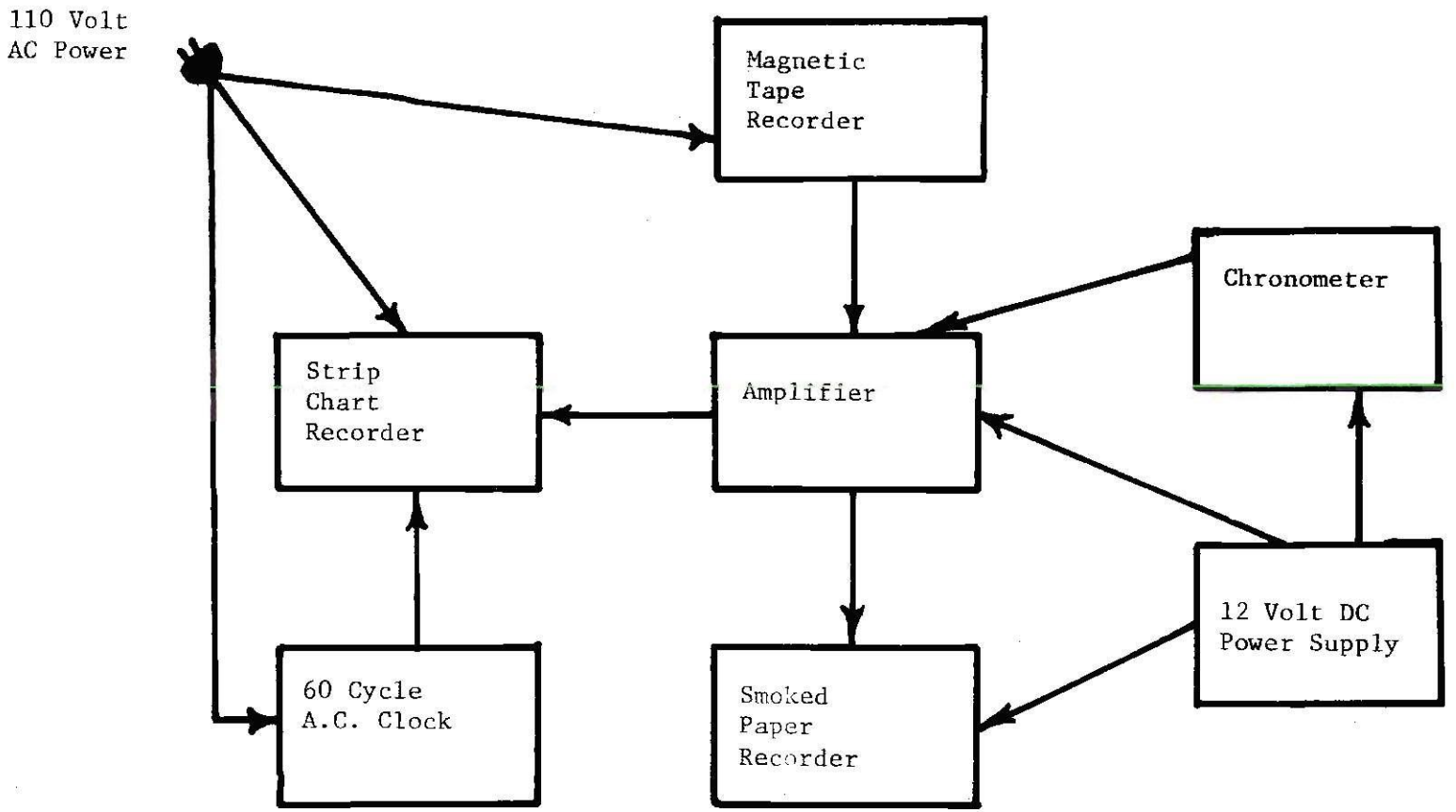


Figure 5. Schematic Diagram for Magnetic Tape Data Playback.

of the seismometer-amplifier system. Hence, a displacement of the ground (such as may be caused by a tremor or a footstep) produces a proportional displacement of the stylus. As the drum rotates, the penmotor and stylus are translated along the length of the drum, producing a helical recording (Figure 9). The paper is then removed from the drum and "fixed" by coating it with a mixture of twenty parts alcohol to one part shellac. The alcohol evaporates, leaving a permanent shellac coating on the smoked paper record. Details of the instrumentation of these smoked paper seismographs are given in Appendix I.

# CHAPTER III

# PROCEDURE

## Field Operations

Following the August 2, 1974 event, several portable microearthquake stations were deployed in a pattern around the epicenter. Aftershock monitoring with three or more stations was carried out until September 21, 1974. A high level of microearthquake activity continued throughout this period. As late as September 21, 1974, 500 microearthquakes having local magnitudes of zero or greater were being recorded each day within a five km radius of the epicentral zone (Figure 6). During this period, microearthquake recording stations were continuously relocated to improve resolution of the events. At first travel was by truck, but due to difficulty of road access to desirable recording sites, a boat was later used. Except during high winds and foul weather, boat travel proved to be a very effective method for conducting a microearthquake survey due to the many convenient waterways in the epicentral area.

From September 22, 1974 through January 21, 1975 a smoked paper seismograph station was located in Danburg, Georgia approximately 18 km west of the epicentral area. The station had a magnitude threshold of local magnitude $1.5 \pm 0.2$. From January 25, 1975 until March 15, 1975 epicentral seismic coverage consisted primarily of smoked paper seismograms from a station located at Bobby Brown State

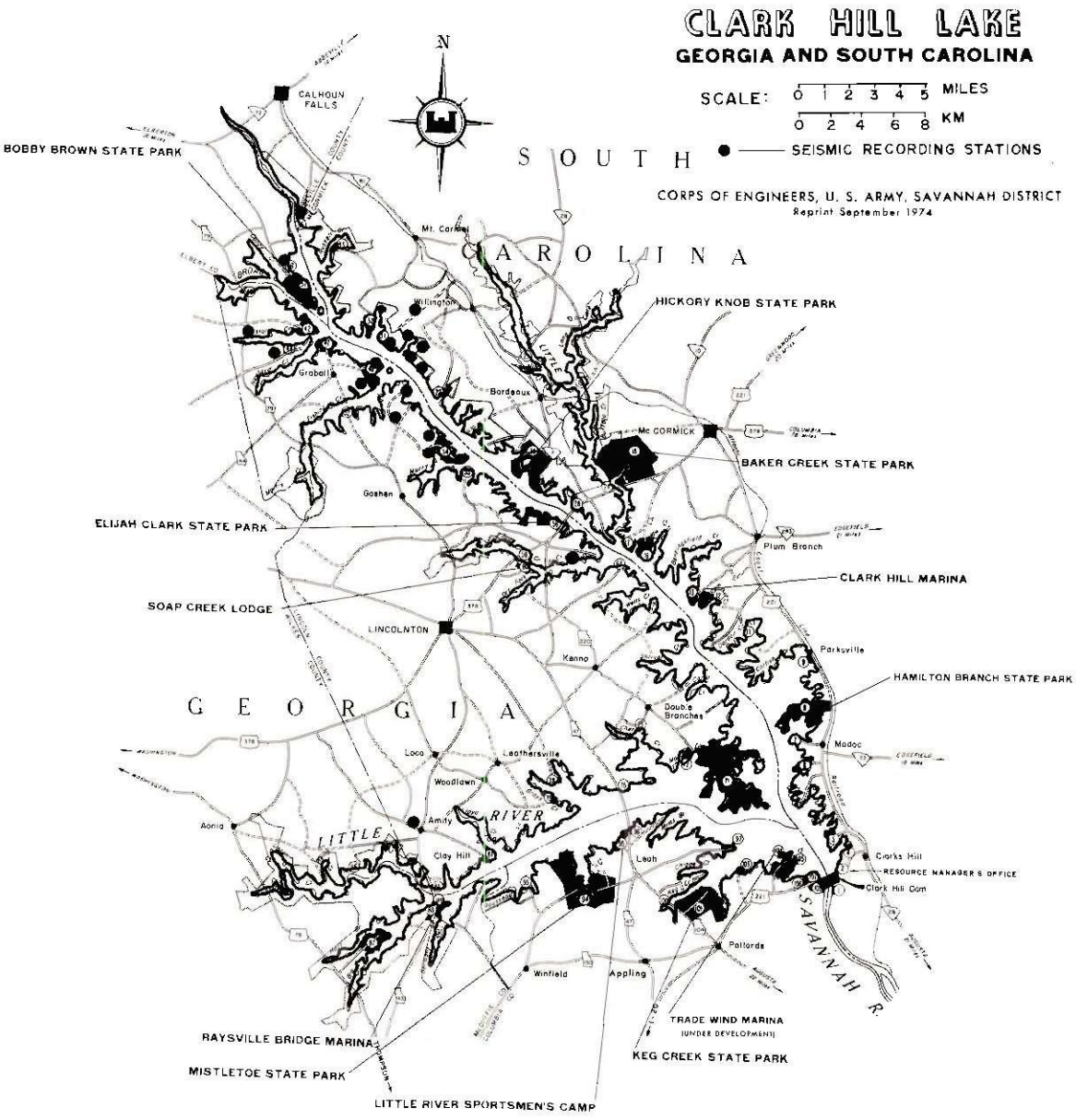


Figure 6. Clark Hill Lake, Station Locations.

Park, nine km north of the epicentral area. This station had a magnitude threshold of local magnitude 0.5 ± 0.2. Since March monthly weekend and occasional quarter-break recording trips of 2-4 day duration have provided supplementary data. Appendix II contains details of these trips as well as seismic recording station data.

# CHAPTER IV

# RESULTS

## Earthquake Frequency of Occurrence and Magnitude

The distribution of earthquakes as a function of magnitude may be represented by the recurrence equation (Richter, 1958)

$$\log_{10}(N_c) = a - bM \tag{1}$$

where $N_c$ is the number of shocks of magnitude M or greater per unit time and a and b are generally observed to be constants. The magnitude M is usually assumed to be the Richter local magnitude $M_L$. Evernden (1970) has shown this linear relationship to be valid for most areas. For most areas, the "b" value is between 0.8 and 1.0 (Richter, 1958; Gibowicz, 1973); this means that the frequency of occurrence of shocks of a given magnitude is eight to ten times the frequency of occurrence of shocks one magnitude unit higher.

## Magnitudes

Local magnitudes ($M_L$) are used by both Randall (1973) and Gibowicz (1973) for the evaluation of stress drop. For this study, magnitudes were evaluated using a local magnitude scale ($M_{LSE}$) devised by Long (1973). This scale employs a local attenuation function derived from more than 100 quarry blasts and natural events occurring

in the southeastern United States. The $M_{LSE}$ scale is based on the trace amplitude for the largest recorded phase of period near one second on the short period vertical ATL seismogram. Because of the similarity of the World Wide Standard short period vertical seismometer's frequency response to that of the Wood-Anderson torsion seismometer (used by Richter's scale), and because of the similarity of the definition of Richter's local magnitude ($M_L$) to Long's $M_{LSE}$, these two magnitudes are assumed to be equivalent. Magnitude relations derived for the smoked paper seismograms from station TDS and SUM are based on the local magnitude $M_{LSE}$.

When possible, magnitudes were also calculated by Nuttli's (1973) $M_{BLG}$ scale. The theoretical trace amplitude of a zero magnitude event at the distance range of the CHRA is within ± 0.3 magnitude units for both $M_{LSE}$ and $M_{BLG}$. For magnitudes in the range 2.0 to 3.5, this study has found these two scales to be within ± 0.3 magnitude units of each other. The reported (Earthquake Data Report, United States Geological Survey) $M_{BLG}$ magnitude for the August 2, 1974 event was 4.8; this was the assumed value for local magnitude used in the stress drop calculations. Båth (1973) and Gibowicz (1972) give plots of $M_L$ versus $m_b$ for statistically significant numbers of earthquakes. Båth's results indicate that a body wave magnitude $m_b = 4.3$ earthquake is approximately equal to a local magnitude $M_L = 4.6$ earthquake; Gibowicz's data indicate that an $m_b = 4.3$ earthquake is approximately equal to an $M_L = 4.8$ earthquake. Based on the similarity among $M_L$, $M_{LSE}$ and $M_{BLG}$, these results indicate that our assumed value of

$M_L$ = 4.8 for the August 2, 1974 earthquake is a good estimate, since its body wave magnitude ($m_b$) based on nine reporting stations was 4.3 (Earthquake Data Report, United States Geological Survey).

## Evaluation of Stress Drop Using Gibowicz's Empirical Relations

Gibowicz (1973) made a statistical study of aftershock sequences and developed empirical relations between stress drop and (1) "b" value, (2) aftershock activity duration and (3) difference in magnitude between the main shock and the largest aftershock. He found that high stress drop led to high "b" value, low magnitude of the largest aftershock, long duration of aftershock activity, and conversely. In addition, larger magnitude events generally had higher stress drops.

In order to utilize these empirical relations, computation of "a" and "b" values for the recurrence relation of equation (1) was necessary. Using the ATL records, a catalog of events was constructed for the first month and a half following the August 2, 1974 event (Table 2). Using this catalog of events, a plot of recurrence rate versus magnitude (Figure 7) was obtained. A straight line fitted by eye indicated a "b" value of 1.77 $\pm$ 0.3 and a value for "a" (the logarithm of the number of magnitude zero or greater events occurring per month) of 4.70 $\pm$ 1.0. This would indicate that for the month and a half following the August 2, 1974 event there were approximately 1600 events of magnitude zero or greater occurring per day and one event of magnitude two or greater occurring every two days.

Table 2. Catalog of Major Aftershocks of the August 2, 1974 $M_L$ = 4.3 Clark Hill Reservoir Earthquake

| Date | Arrival Time of P Wave at ATL | S-P (sec) | $M_L$ | Date | Arrival Time of P Wave at ATL | S-P (sec) | $M_L$ |
|---|---|---|---|---|---|---|---|
| 8- 2-74 | 11:14:52.2 | 21.61 | 2.00 | 8-12-74 | 14:57:24.24 | 21.3 | 1.96 |
| 8- 2-74 | 11:40:00 | ? | 2.00 | 8-13-74 | 10:33:53.75 | 21.7 | 2.18 |
| 8- 2-74 | 12:09:23.0 | 21.61 | 2.27 | 8-22-74 | 19:16:57.48 | 21.9 | 2.36 |
| 8- 2-74 | 13:31:10.56 | 21.1 | 1.88 | 8-25-74 | 10:59:00 | ? | 1.78 |
| 8- 2-74 | 13:31:19.01 | 21.6 | 2.02 | 8-27-74 | 08:46:19.56 | 21.8 | 2.29 |
| 8- 2-74 | 13:34:34.70 | ? | 2.18 | 8-27-74 | 08:47:37.31 | 22.0 | 2.73 |
| 8- 2-74 | 14:23:23.94 | 21.9 | 2.22 | 8-27-74 | 08:52:55.66 | 21.7 | 1.78 |
| 8- 2-74 | 15:30:00 | ? | 1.88 | 9- 1-74 | 03:19:00 | ? | 2.18 |
| 8- 2-74 | 16:23:45.87 | 22.1 | 2.81 | 9-21-74 | 06:23:43.06 | 21.6 | 2.41 |
| 8- 2-74 | 17:04:00 | ? | 2.02 | 9-21-74 | 07:43:48.40 | 21.7 | 1.88 |
| 8- 2-74 | 18:14:00 | ? | 1.88 | 9-22-74 | 04:57:00 | ? | 1.66 |
| 8- 3-74 | 08:35:10.36 | 21.5 | 1.78 | 9-22-74 | 02:37:00 | ? | 1.78 |
| 8- 3-74 | 11:35:00 | ? | 1.66 | 9-22-74 | 17:50:00 | ? | 2.02 |
| 8- 4-74 | 00:19:04.02 | 21.4 | 1.88 | 9-22-74 | 20:19:11.90 | 21.7 | 2.18 |
| 8- 4-74 | 03:44:00 | ? | 1.78 | 9-22-74 | 20:19:51.93 | 21.6 | 2.08 |
| 8- 4-74 | 04:07:00 | ? | 1.88 | 9-23-74 | 06:16:28.13 | 22.29 | 2.15 |
| 8- 4-74 | 06:14:00 | ? | 1.66 | 9-23-74 | 07:26:16.69 | 21.98 | 2.29 |
| 8- 7-74 | 04:06:57.25 | 23.5 | 2.08 | 9-23-74 | 09:03:00 | ? | 1.94 |
| 8- 7-74 | 08:23:25.65 | 21.5 | 2.08 | | | | |
| 8- 8-74 | 16:20:00 | ? | 1.88 | | | | |
| 8-11-74 | 18:55:57.43 | 22.1 | 1.78 | | | | |

Table 2. Catalog of Major Aftershocks of the August 2, 1974 $M_L$ = 4.3 Clark Hill Reservoir Earthquake (Continued)

| Date | Arrival Time of P Wave at TDS | S-P (sec) | $M_L$ | Date | Arrival Time of P Wave at TDS | S-P (sec) | $M_L$ |
|---|---|---|---|---|---|---|---|
| 9-23-74 | 23:49:58.04 | 2.06 | 2.00 | 10-8-74 | 23:22:00.00 | 2.13 | 3.22 |
| 9-24-74 | 00:03:40.27 | 2.07 | 1.77 | 10-13-74 | 22:01:51.71 | 2.09 | 1.92 |
| 9-24-74 | 04:34:33.18 | 2.08 | 1.92 | 10-15-74 | 07:40:51.13 | 2.17 | 2.38 |
| 9-24-74 | 06:28:19.55 | 2.05 | 1.92 | 10-17-74 | 12:28:28.63 | 2.16 | 2.35 |
| 9-24-74 | 06:29:25.54 | 2.07 | 1.83 | 10-17-74 | 13:09:23.59 | 2.08 | 1.57 |
| 9-24-74 | 07:31:31.64 | 2.19 | 2.43 | 10-17-74 | 17:05:46.10 | 1.99 | 1.71 |
| 9-24-74 | 14:16:25.89 | 2.21 | 2.08 | 10-21-74 | 15:05:41.64 | 2.04 | 2.52 |
| 9-24-74 | 16:32:50.67 | 2.17 | 2.30 | 10-22-74 | 20:30:18.18 | 2.35 | 2.89 |
| 9-24-74 | 21:57:51.67 | 2.10 | 2.08 | 10-23-74 | 17:09:21.39 | 2.05 | 1.57 |
| 9-25-74 | 02:15:23.14 | 2.15 | 2.08 | 10-31-74 | 00:42:36.13 | 1.95 | 1.97 |
| 9-25-74 | 09:18:05.09 | 2.17 | 2.53 | 11- 1-74 | 16:39:27.30 | 2.38 | 2.00 |
| 9-25-74 | 15:48:15.81 | 2.17 | 2.25 | 11- 4-74 | 04:31:11.08 | 2.07 | 1.77 |
| 9-25-74 | 15:58:13.80 | 2.21 | 1.65 | 11- 5-74 | 02:02:14.32 | 2.34 | 3.25 |
| 9-25-74 | 16:55:00 | ? | 2.08 | 11- 5-74 | 02:22:41.15 | 2.07 | ? |
| 9-25-74 | 17:05:59.30 | 2.08 | 2.00 | 11- 5-74 | 05:17:20.77 | 2.59 | 1.77 |
| 9-26-74 | 13:31:44.89 | 2.12 | 1.48 | 11- 9-74 | 13:16:56.81 | 2.26 | 2.70 |
| 9-26-74 | 19:52:42.77 | 2.05 | 1.88 | 11-10-74 | 14:02:30.06 | 2.03 | 2.17 |
| 9-28-74 | 22:41:35.68 | 2.03 | 1.97 | 11-16-75 | 07:41:32.27 | 2.18 | 1.92 |
| 9-30-74 | 18:51:08.26 | 2.14 | 2.11 | 11-19-74 | 21:07:01 | 2.1 | 1.77 |
| 10- 8-74 | 02:16:38.99 | 2.02 | 1.77 | 11-21-74 | 03:31:01 | 2.1 | 1.92 |
| 10- 8-74 | 22:35:07.74 | 2.07 | 2.17 | 11-25-74 | 16:36:37 | 2.1 | 2.08 |

Table 2. Catalog of Major Aftershocks of the August 2, 1974 $M_L$ = 4.3 Clark Hill Reservoir Earthquake (Continued)

| Date | Arrival Time of P Wave at TDS | S-P (sec) | $M_L$ | Date | Arrival Time of P Wave at TDS | S-P (sec) | $M_L$ |
|---|---|---|---|---|---|---|---|
| 11-25-74 | 14:27:04 | 2.1 | 2.69 | 1- 8-75 | 14:00:00 | 2.1 | 1.92 |
| 12- 3-74 | 07:24:00 | 2.27 | 3.28 | 1-10-75 | 10:00:00 | 1.0 | ? |
| 12-12-74 | 03:00:00* | 2.1 | 2.00 | 1-22-75 | 23:00:00 | 2.1 | 1.48 |
| 12-15-74 | 04:00:00 | 2.1 | 2.35 | 1-23-75 | 02:00:00 | 2.1 | 1.48 |
| 12-24-74 | 13:00:00 | 2.1 | 2.48 | 1-23-75 | 02:00:00 | 2.1 | 1.92 |
| 12-27-74 | 19:00:00 | 2.1 | 2.40 | 1-23-75 | 23:00:00 | 2.1 | 1.77 |
| 12-29-74 | 04:00:00 | 2.1 | 1.71 | | | | |

*Arrival times on the following 11 events are approximate due to clock malfunction.

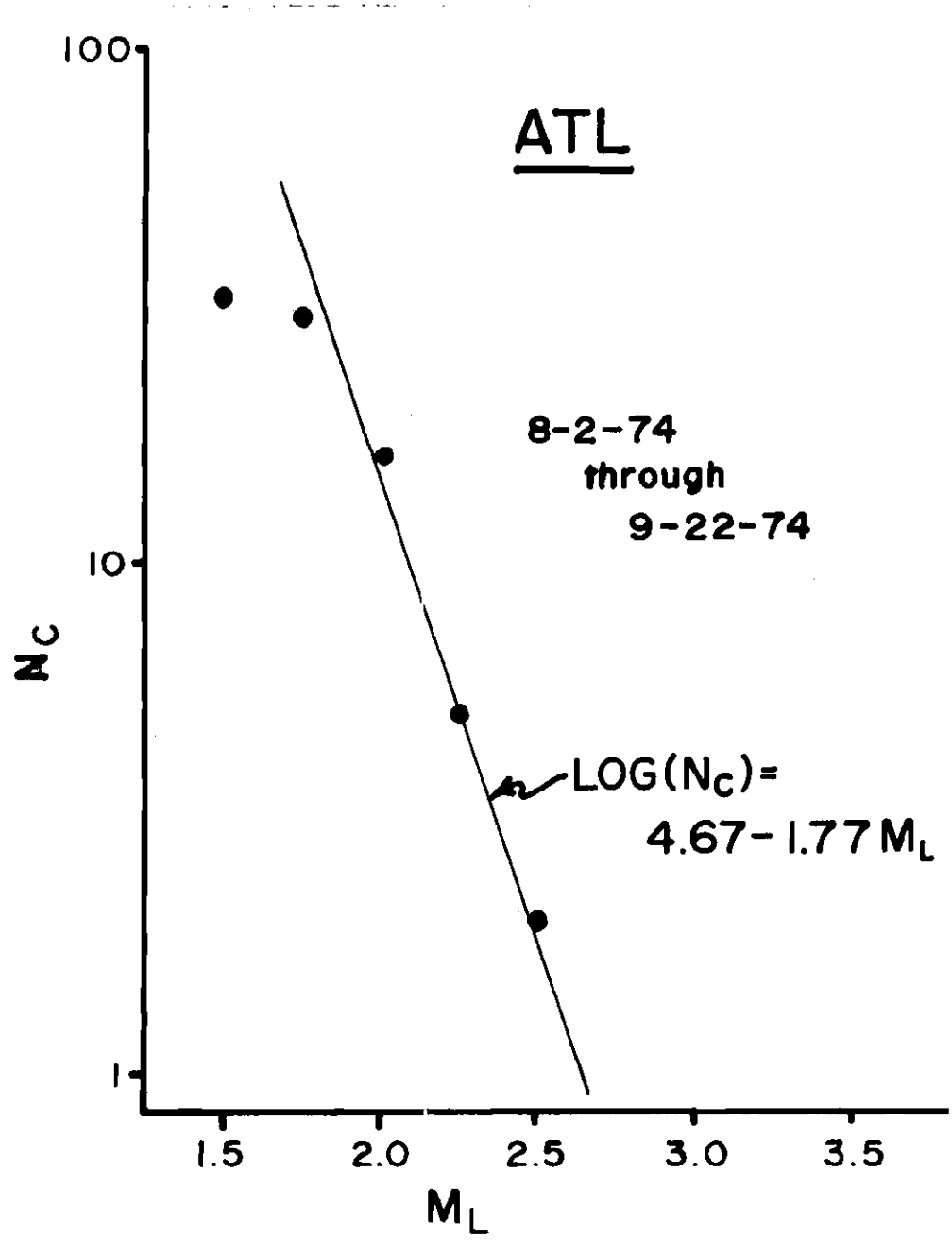


Figure 7. Aftershock Recurrence Relation, August 2 - September 20, 1974.

Gibowicz (1973) provides the following empirical formula for evaluating stress drop from "b" value

$$b = 0.84 + \log_{10}\left(\frac{\Delta\sigma o}{\Delta\sigma m}\right) \tag{2}$$

where $\Delta\sigma o$ is the observed stress drop in the main shock and $\Delta\sigma m$ is a normal stress drop for an earthquake of the same magnitude. This emperical formula had a correlation coefficient of 0.63. Using this formula with a "b" value of 1.77 gives a $\frac{\Delta\sigma o}{\Delta\sigma m}$ ratio of 8.5. That is, based on this calculation, the August 2, 1974 event had a stress drop which was 8.5 times that of a "normal" event. Gibowicz also develops an empirical relation through which he defines "normal" stress drop, $\Delta\sigma m$, as follows

$$M_L = (5.0 \pm 0.4) + (1.5 \pm 0.4)\log_{10}(\Delta\sigma m). \tag{3}$$

Using $M_L = 4.8$, a normal stress drop ($\Delta\sigma m$) of 0.74 bars is obtained, hence, a stress drop of 6.3 bars is indicated for the August 2, 1974 event.

In addition, Gibowicz obtained an empirical formula which relates the "b" value and the difference between the magnitude of the main shock and the largest aftershock to the stress drop. His equation is

$$b(M_L - M_1) = 1.0 + 2\log_{10}\left(\frac{\Delta\sigma o}{\Delta\sigma m}\right) \tag{4}$$

where $M_L$ is the local magnitude of the main shock and $M_1$ is the local magnitude of the largest aftershock. This empirical formula had a data correlation coefficient of 0.64. Using $M_L = 4.8$, $M_1 = 3.3$, $b = 1.77$ and $\Delta\sigma m = 0.74$, a stress drop of 5.0 bars is obtained.

According to a relation often called Båth's law, the normal difference in magnitude between the main shock and the largest aftershock is 1.2 magnitude units; in this study the difference was 1.5. According to Gibowicz, in general, the greater the stress drop, the larger the magnitude difference. A plot from Gibowicz (1973) data of magnitude differences versus the magnitude of the main shocks (Figure 8, Table 3) indicates a random relationship; hence, the magnitude difference appears to be independent of the magnitude of the main shock.

Gibowicz explains the relationship between the magnitude differences and stress drop as follows, "The difference between the magnitudes of the main shock and the largest aftershock is small when the stress drop of the main shock is low, or the remaining stress high, and conversely." In the case of the August 2, 1974 event, there may have been a substantial amount of remaining stress, since several relatively large aftershocks were observed (two $M_L = 3.2$ and one $M_L = 3.3$). A high level of remaining stress would also explain the long duration of aftershock activity (Figure 9). Further evidence for this idea is given in a later section on the source dimensions of the August 2, 1974 event.

Gibowicz defines the duration of aftershock activity as the

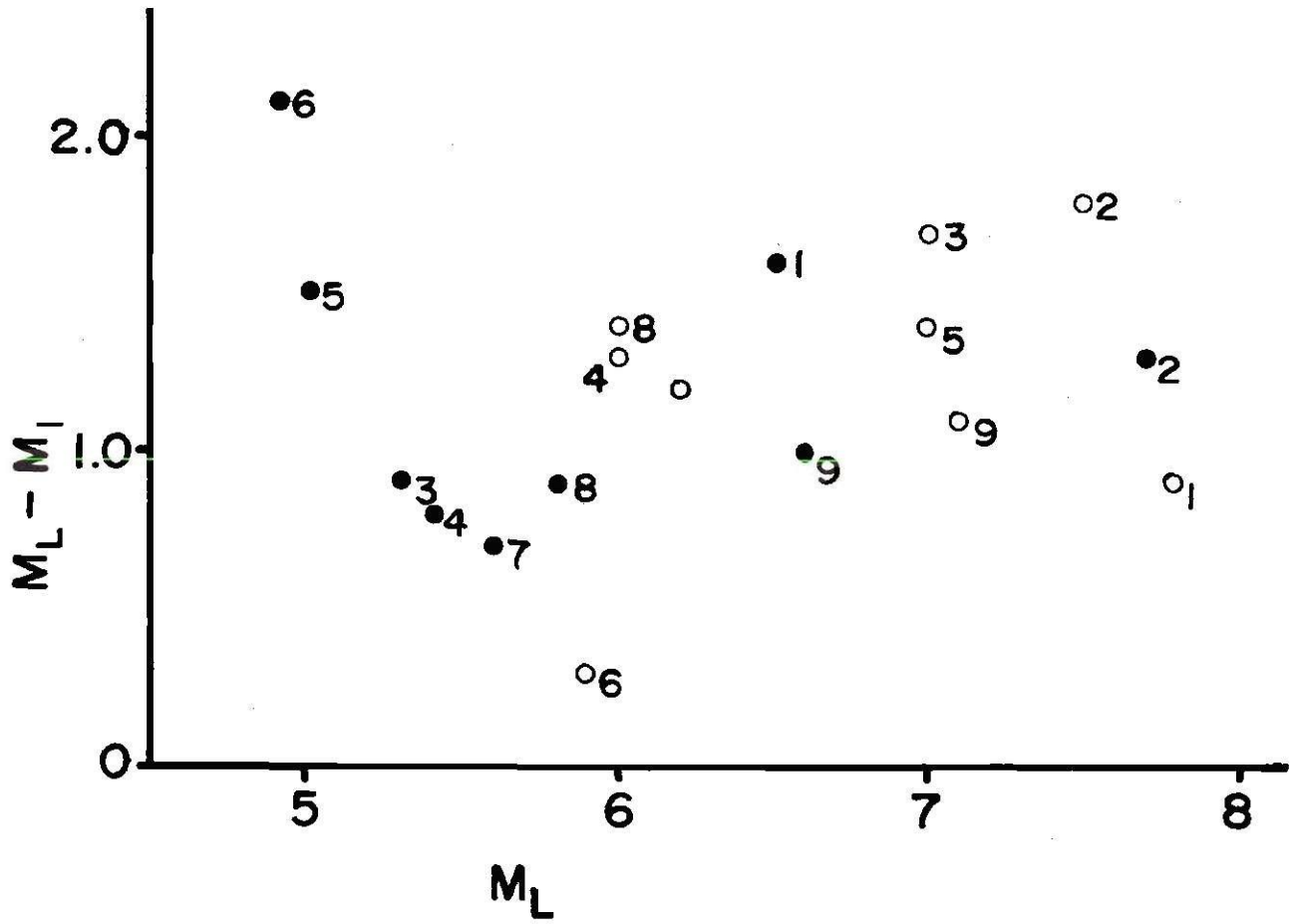


Figure 8. Difference in Magnitude Between the Main Shock and Largest Aftershock ($M_L$-$M_1$) Versus the Magnitude of the Main Shock. Full and Open Circles Represent California and New Zealand Earthquakes, Respectively. Event Numbers are Identified in Table 3 (After Gibowicz, 1973).

Table 3. Aftershock Data for California and New Zealand Earthquakes (After Gibowicz, 1973)

| Event # | Location | Date | $M_L$* | $M_1$+ | $M_L - M_1$ |
|---|---|---|---|---|---|
| | CALIFORNIA | | | | |
| 1 | Desert Hot Springs | 12- 4-48 | 6.5 | 4.9 | 1.6 |
| 2 | Kern County | 7-21-52 | 7.7 | 6.4 | 1.3 |
| 3 | San Francisco | 3-27-57 | 5.3 | 4.4 | 0.9 |
| 4 | Watsonville | 9-14-63 | 5.4 | 4.6 | 0.8 |
| 5 | Corralitos | 11-16-64 | 5.0 | 3.5 | 1.5 |
| 6 | Antioch | 9-10-65 | 4.9 | 2.8 | 2.1 |
| 7 | Parkfield | 1-28-66 | 5.6 | 4.9 | 0.7 |
| 8 | Truckee | 9-12-66 | 5.8 | 4.9 | 0.9 |
| 9 | San Fernando | 2- 9-71 | 6.6 | 5.5 | 1.1 |
| | NEW ZEALAND | | | | |
| 1 | Hawke's Bay | 2- 2-31 | 7.8 | 6.9 | 0.9 |
| 2 | Pahiatua | 3- 5-34 | 7.5 | 5.7 | 1.8 |
| 3 | Wairarapa | 1-24-42 | 7.0 | 5.3 | 1.7 |
| 4 | Wairarapa | 12- 2-42 | 6.0 | 4.7 | 1.3 |
| 5 | Fiordland | 5-24-60 | 7.0 | 5.6 | 1.4 |
| 6 | Westport | 5-10-62 | 5.9 | 5.6 | 0.3 |
| 7 | Gisborne | 3- 4-66 | 6.2 | 5.0 | 1.2 |
| 8 | Seddon | 4-23-66 | 6.0 | 4.6 | 1.4 |
| 9 | Inanguhua | 5-23-68 | 7.1 | 6.0 | 1.1 |

*Magnitude of the main shock

+Magnitude of the largest aftershock

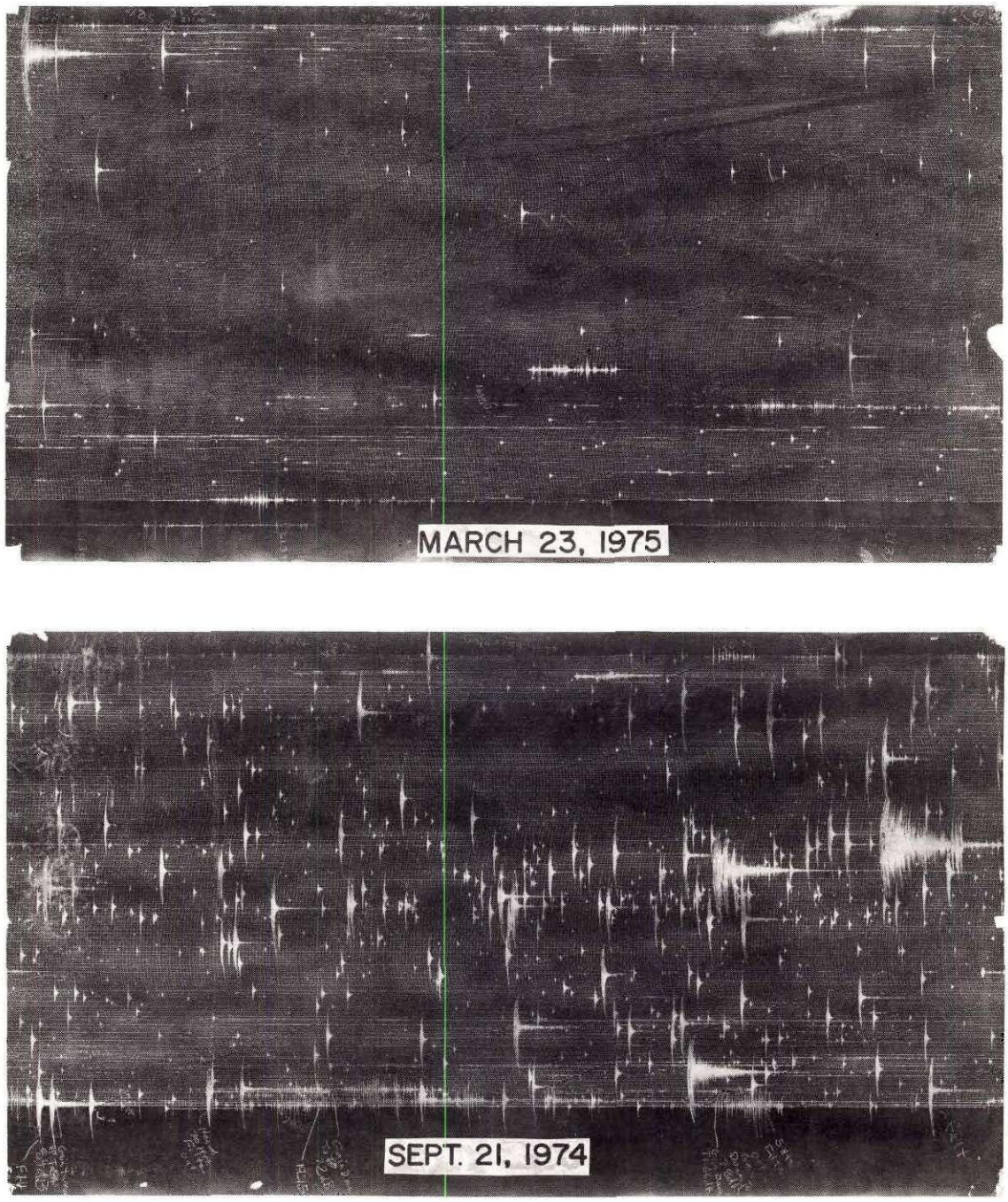


Figure 9. Smoked Paper Records, Station SUM. Each Seismogram Represents 24 Hours of Recording. The Minimum Observable Event's Magnitude is about $M_L$ = 0.3.

time following the main shock required for the rate of aftershock activity to fall to less than one magnitude 3.0 event per day. Gibowicz obtained the following empirical relation for the calculation of aftershock duration

$$\log_{10}\left(\frac{t_o}{t_A}\right) = 3\log_{10}\left(\frac{\Delta\sigma o}{\Delta\sigma m}\right) , \qquad (5)$$

where $t_o$ is the duration of activity in days for a given sequence, and $t_A$ is the duration in days expected for a given fault area. An expression for the calculation $t_A$ (Gibowicz, 1973) is given as

$$\log_{10}(t_A) = 1.3\log_{10}(A) - 2.4 , \qquad (6)$$

where A is the fault area in square kilometers. The correlation coefficient for the data on which both of these empirical formulas are based was given as 0.78.

In order to use these formulae, we must first estimate the area of the fault from its aftershock zone. The length of the fault plane is taken as the longest dimension of the area in which the aftershocks occur (Liebermann and Pomeroy, 1970); the width of the fault plane is taken as the depth of the deepest aftershock, and is corrected for the dip of the fault plane whenever possible. A plot of aftershock locations (Figure 10) indicates a maximum fault length of five kilometers and a maximum depth of 1.5 kilometers (see Appendix III for details of the aftershock hypocenter calculations). Using equation (6), the

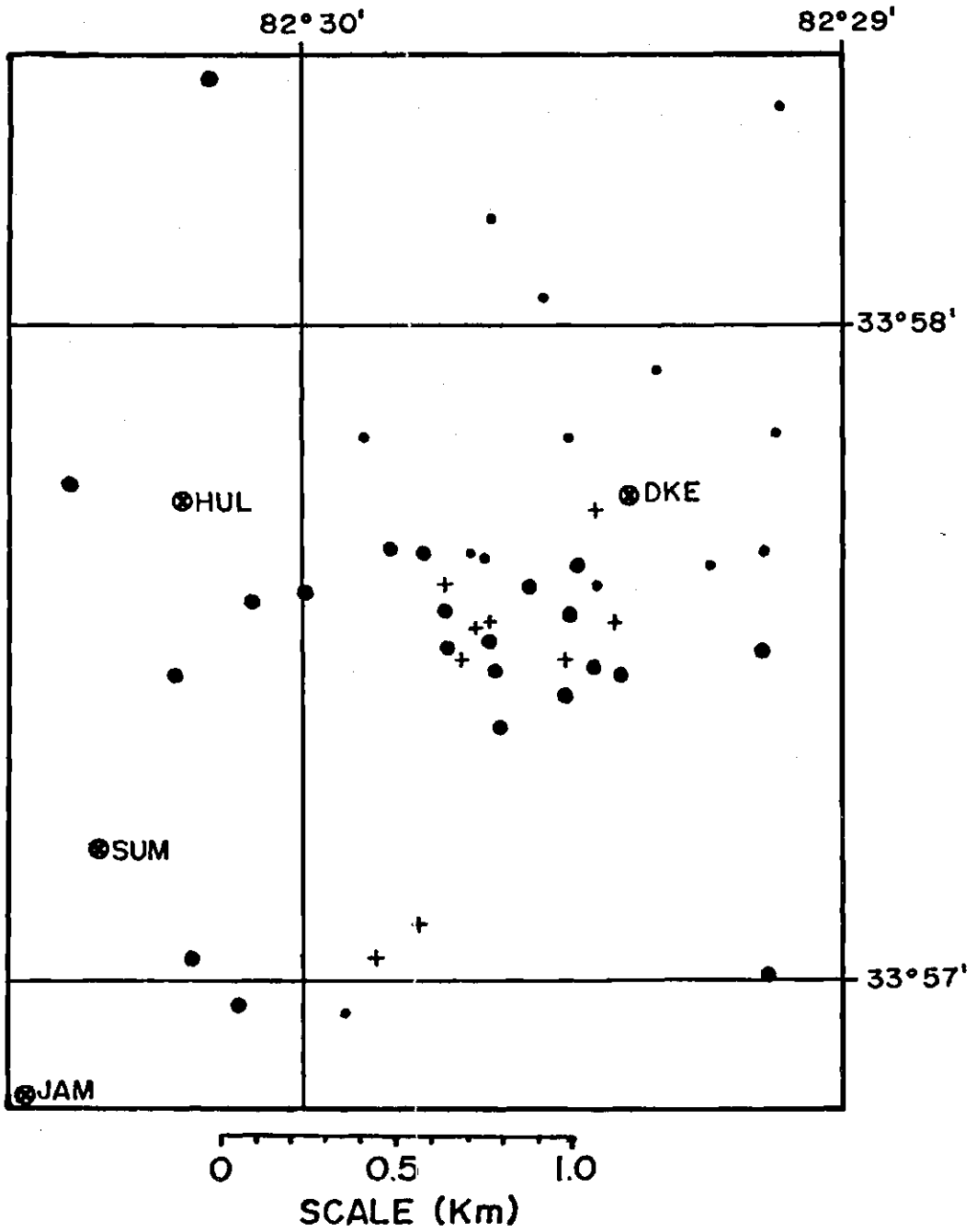


Figure 10. Aftershock Epicenter Map. Epicenter Errors Are As Follows: Crosses, ± 0.1 km; Large Closed Circles, ± 0.2 km; Small Closed Circles, ± 0.5 km. Circles Crosses Indicate Station Locations.

predicted duration for the August 2, 1974 event's aftershock sequence was 0.054 days, or 1.3 hours. It should be reiterated that this is for the occurrence of one magnitude 3.0 or larger event per day.

To determine when the activity level had fallen below one magnitude three or larger event per day, Gibowicz plotted the number of events per day above the minimum magnitude detection level for a particular aftershock sequence. A relation of the form

$$n = n_1(t)^{-p} \tag{7}$$

where n = the number of events per day, $n_1$ = the number of events on the first day, t = the number of days since the main shock and p is a parameter called the decay coefficient, was fitted to Gibowicz's data. However, the small sample size of the August 2, 1974 aftershock rate of occurrence data (Figure 11) prevented accurate computation of the constants in equation (7). A relation (equation (7)) with $n_1$ = 11 and p = 1.7 was visually fitted to the data in Figure 11. The data were not considered adequate for statistical analysis of the precision of this fit. The minimum detection level for the data from ATL which was used in Figure 11 was $M_L$ = 1.8. Using a "b" value of 1.77 (Figure 7), we may predict that when there is one magnitude 3.0 or greater event occurring per day, there are 133 magnitude 1.8 or greater events occurring per day. Applying this value (n = 133) to equation (8) gives t = 0.23 days until the activity falls to less than an average of one magnitude three or greater event per day.

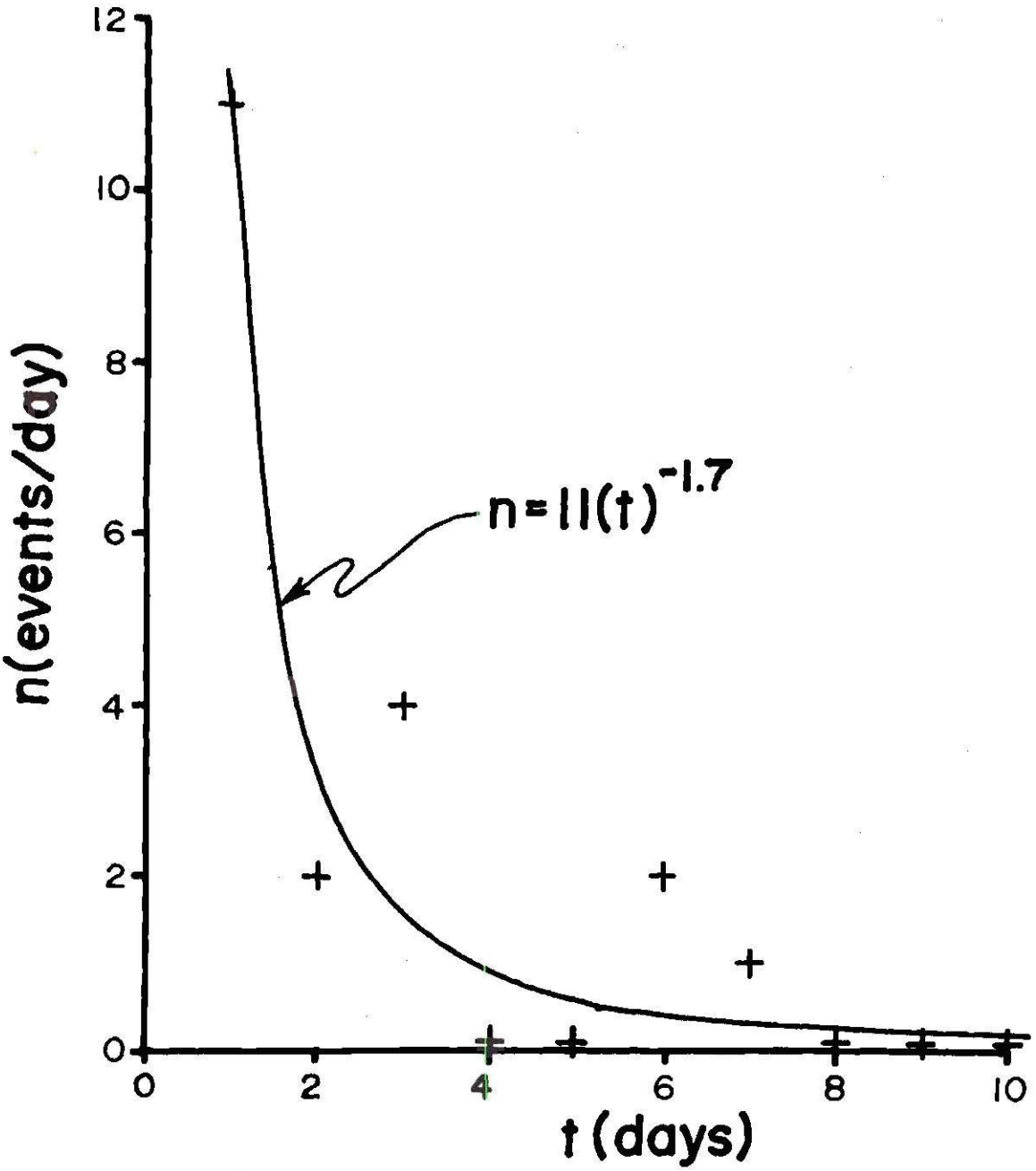


Figure 11. Decay Plot of August 2, 1974 Aftershock Sesquence.

Using the duration (t = 0.23 days, extrapolated from rate of occurrence data) in equations (5) and (6) gives $\frac{\Delta\sigma o}{\Delta\sigma m} = 1.62$, or $\Delta\sigma o = 1.2$ bars. While this is a slightly high stress drop, the validity of Gibowicz's equations in this low of a magnitude range ($M_L = 4.8$) is questionable, since Gibowicz's study had a mean magnitude of 6.3 and a minimum magnitude of 4.9. Therefore, extrapolation of his results to this study is subject to substantial doubt and computations using his equations are presented more for the purpose of a comparative evaluation than for their merit as individual independent measures of the stress drop.

Evaluation of Stress Drop Using Theoretical Relations

Based on a circular dislocation model, Brune (1970) developed relationships between earthquake source parameters and seismic spectra. Randall (1973) generalized these relations by showing that the far field results of Brune's spectral theory are largely independent of his dislocation source model. Randall derived expressions for seismic spectral energy and characteristic stress which were independent of assumptions about the source model. He also derived a theoretical relationship between fault size, local magnitude and stress drop (Figure 12); this relationship was used to evaluate the stress drop of the August 2, 1974 event and its aftershocks. In addition, Randall showed that this theoretical relation (Figure 12) was consistent with empirical relations between magnitude and fault size, and between seismic energy and magnitude. His theoretical relationship for the calculation of stress drop was found to give results that agree well

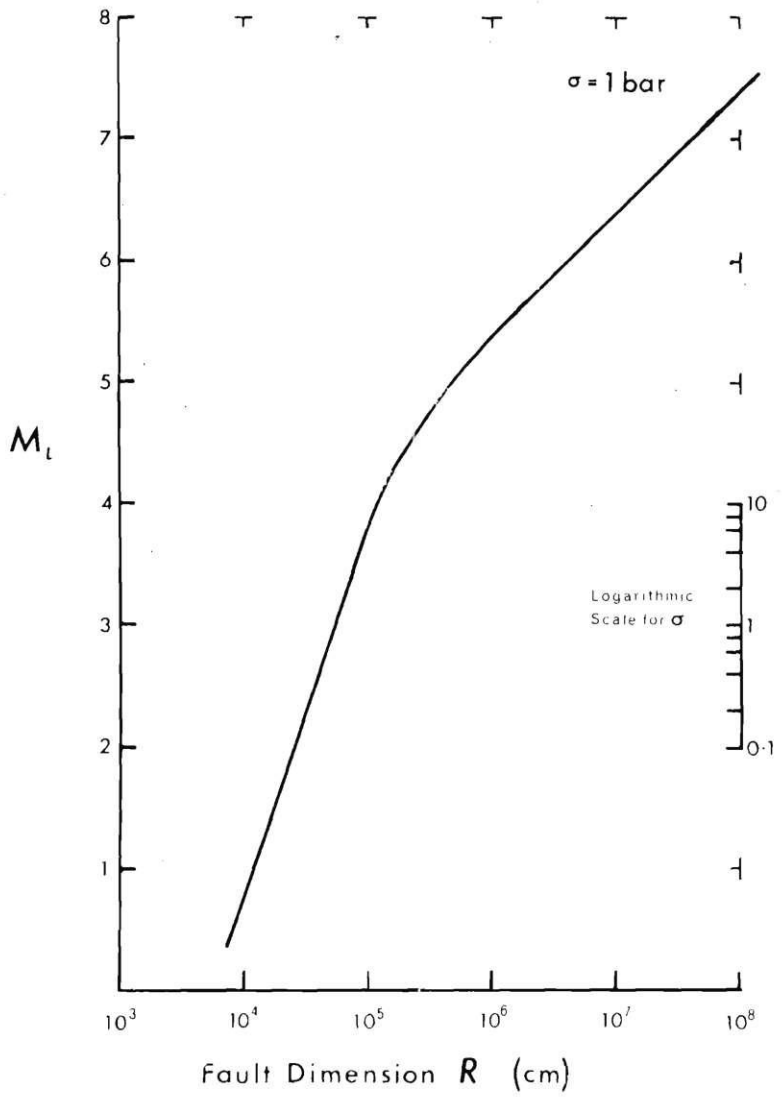


Figure 12. Theoretical Relationship Between Fault Radius (R) and Local Mangitude ($M_L$) as a Function of Stress Drop ($\sigma$). Stress Drop of an Event May Be Determined by Measuring Vertical Displacement from $\sigma$ = 1 Curve Using Logarithmic Scale for $\sigma$ (Randall, 1973).

with those obtained from spectral estimates of seismic moment and fault size for earthquakes with local magnitudes ranging from 1.0 to 7.0.

We define a characteristic fault radius, r, according to Randall (1973) as

$$r = \left(\frac{A}{\pi}\right)^{\frac{1}{2}}. \tag{8}$$

Using our previous estimate of 7.5 square kilometers for the fault area, A, of the August 2, 1974 event, we obtain a characteristic fault radius of 1.54 kilometers. Using Randall's relationship (Figure 12), we obtain a stress drop of 5.0 bars for the August 2, 1974 event.

Theoretical fault radii are also commonly calculated from spectral corner frequencies; conversely, theoretical corner frequencies may also be calculated from fault radii. Based on circular dislocation theory, Brune (1970) provides the following theoretical relation for the calculation of corner frequency ($\nu$) from fault radius (r)

$$2\pi\nu = 2.34\beta/r, \tag{9}$$

where $\beta$ is the rupture velocity (generally accepted to be the shear wave velocity). If we assume a fault radius of 1.54 kilometers based on aftershock activity and a rupture velocity of 3.5 kilometers per second, we may calculate a theoretical corner frequency of 0.85 hertz for the August 2, 1974 event.

In an attempt to determine the corner frequency of the August 2, 1974 event, a four-second portion of the compressional wave train recorded at AMG was digitized by the method described in Appendix IV. A spectrum for this wave form was then calculated (Figure 13). A corner frequency may exist at around 1.4 hertz. However, the noise level of digitization was too high to allow observation of a clear corner frequency. The digitization interval for this analysis was 0.04 seconds; hence, we would not expect to resolve frequencies higher than about four hertz which is one third of the folding frequency. Above five or six hertz, the spectrum probably represents white noise. The relative amplitude of the spectrum at frequencies of 8 to 12 hertz increases at the same slope as the inverse of the instrument response curve (dashed line in Figure 13). Since the spectrum of white noise is flat, the application of the instrument response correction would explain these equal slopes. The increase in the relative amplitude of the left hand portion of the spectrum may be partially due to D.C. shifts in the digitized data.

If we accept a corner frequency of 1.4 hertz, and assume a rupture velocity of 3.5 km/sec, the characteristic fault radius of the August 2, 1974 event may be evaluated as 0.93 km (equation (9)). This indicates that the fault area of the August 2, 1974 shock may have been considerably smaller than the zone of aftershocks or that the rupture velocity was higher than the assumed 3.5 km/sec. Using our calculated characteristic fault radius based on corner frequency 0.93 kilometers, we may return to Randall's (1973) curves (Figure 12)

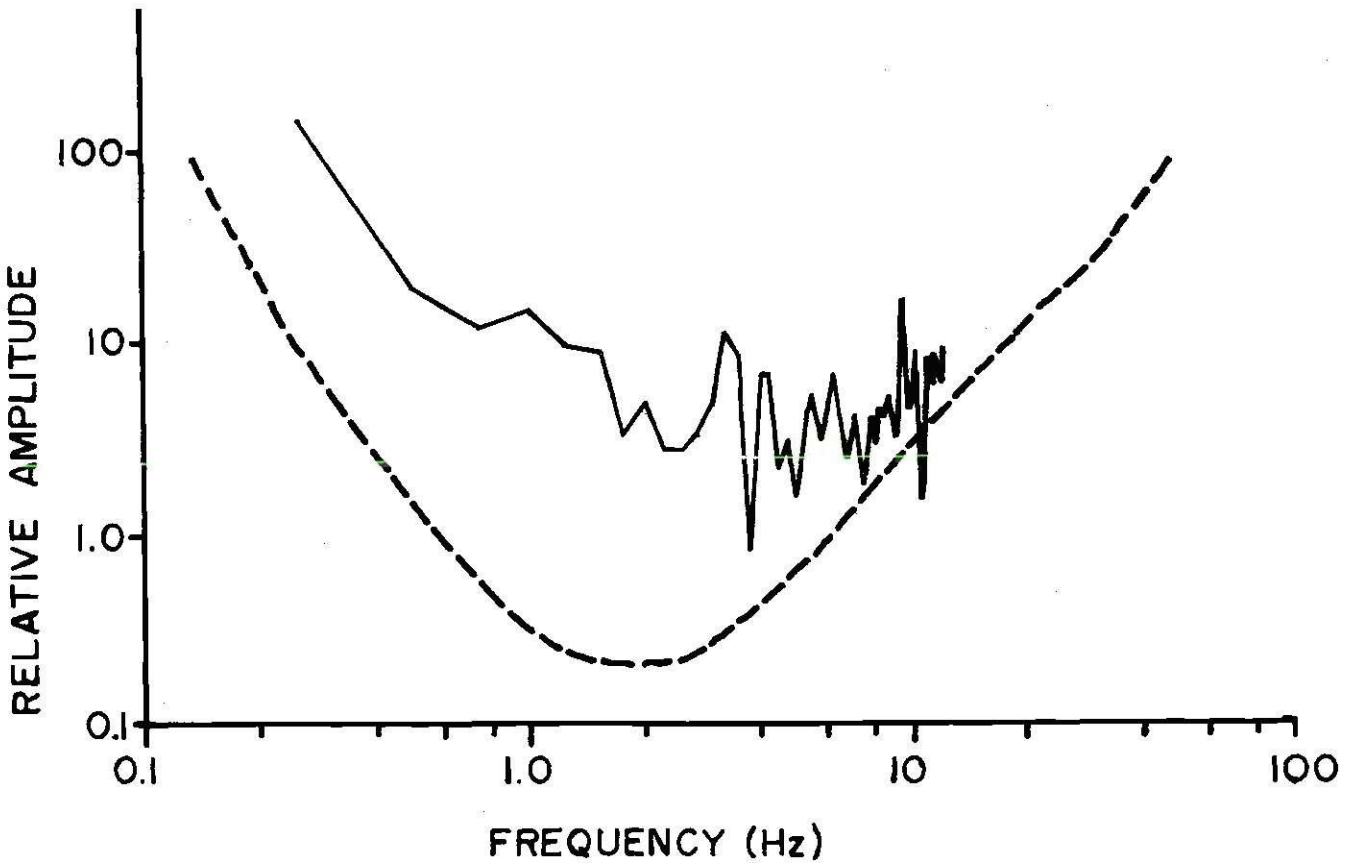


Figure 13. Compressional Wave Displacement Spectrum of the August 2, 1974 Event Recorded at AMG. Dashed Line is the Inverse of the Displacement Response of Station AMG.

and reevaluate the stress drop of the August 2, 1974 event. For $M_L$ = 4.8 and r = 0.93 km, we obtain a stress drop of about 12 bars. This is extremely high, since the normal stress drop for an event of this magnitude is 0.74 bars (Gibowicz, 1973).

If we assume that the fault ruptured at a velocity as high as the compressional wave velocity (i.e., $\beta$ = 6.0 km/sec) rather than the shear wave velocity ($\beta$ = 3.5 km/sec), we may reevaluate the characteristic fault radius. This assumption gives a fault radius of 1.60 km and, hence, (Randall, 1973) a stress drop of 4.0 bars. This is still anomalously high.

By assuming a rupture at the compressional wave velocity (6.0 km/sec), we obtained a characteristic fault radius of 1.60 km. This is virtually the same as the fault radius estimated from the aftershock zone (1.54 km), indicating that the rupture velocity of the August 2, 1974 event could possibly have been at or near the compressional wave velocity of 6.0 km/sec.

## Aftershock Spectral Analysis

Displacement spectra were obtained for several of the aftershocks. Appendix IV gives the details of these calculations. The aftershock spectrum for an event occurring September 18, 1974 at 20:15 GMT is typical of these events (see Figure 14). It shows a corner frequency at 76 hertz, which is apparently quite high; however, in order to evaluate just how high this corner frequency really is (in terms of stress drop), we must first determine the magnitude of the aftershock.

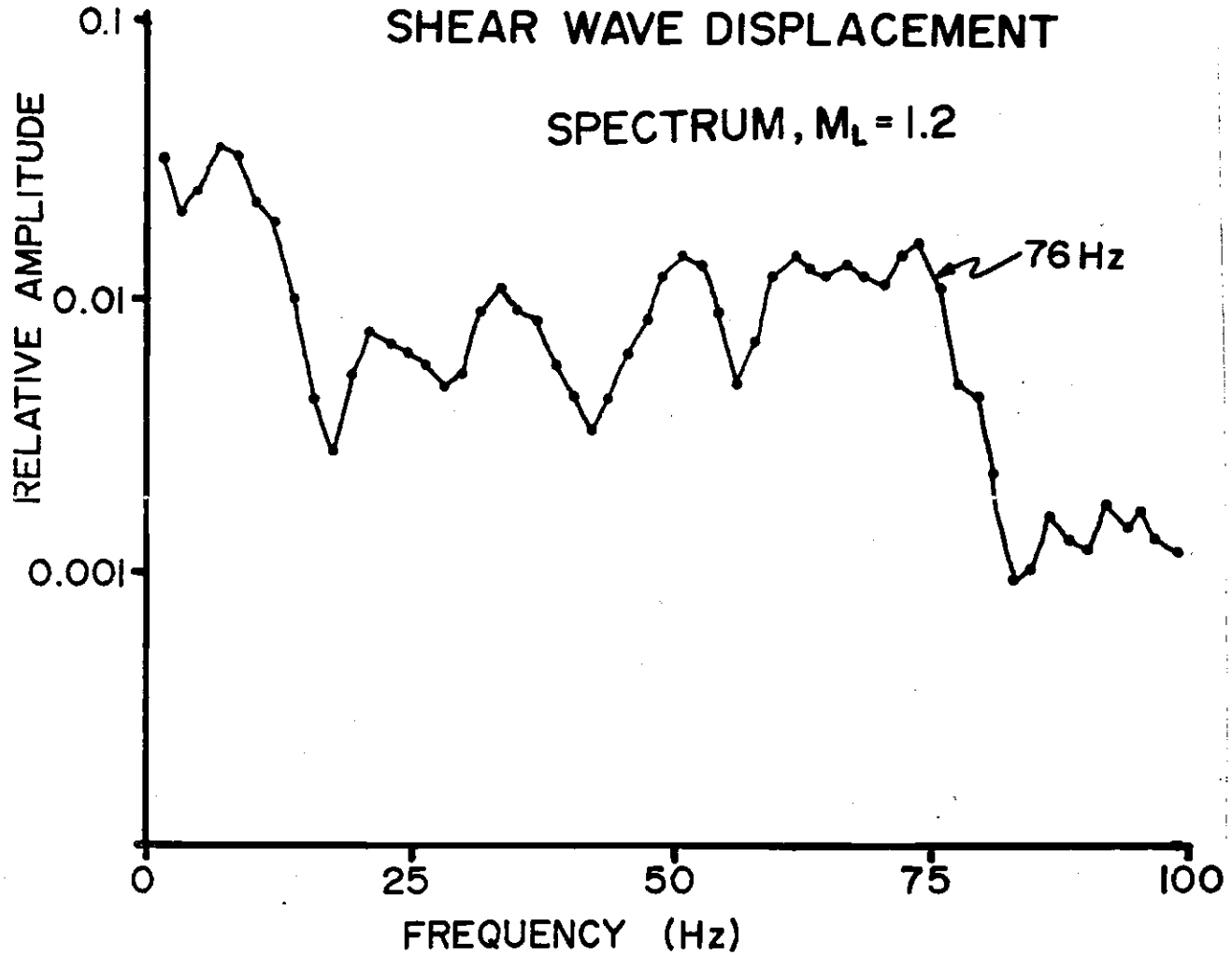


Figure 14. Shear Wave Displacement Spectrum of a Microearthquake that Occurred September 18, 1974 at 20:15 GMT. This Event Was Recorded on the Honeywell Tape Recording System.

## Evaluation of Aftershock Magnitude

In order to obtain an estimate of magnitude, all events for the period 20:11 GMT, September 18, 1974 through 20:00 GMT, September 19 recorded on an MEQ-800 smoked paper seismograph were cataloged according to amplitude. Since more than five hundred events were cataloged for this period, the effect of hypocentral distances (which ranged from 1.0 to 3.0 km) on trace amplitude was considered statistically random and was, therefore, ignored. These data were then divided into five amplitude divisions and normalized by dividing the number of events in each division by the division's width (i.e., the number of events in the amplitude division of two to four millimeters was divided by two, whereas the number of events in the division of eight to twelve millimeters was divided by four). They were then plotted (Figure 15) as log $N_c$ (cumulative number) versus log A (amplitude). Since the magnitude is generally defined to be proportional to the log of trace amplitude, the resulting plot is essentially a plot of recurrence rate. As will be shown later, if the actual "a" and "b" values from equation (1) were known, then a relationship could be established between trace amplitude and magnitude. A relationship of this type is derived for this study.

## A Magnitude Relation For Station TDS

In order to determine values for "a" and "b" in equation (1), it was first necessary to establish a relationship between local magnitude and microearthquake trace amplitude. For this purpose, smoked paper seismograms recorded at station TDS were available. These

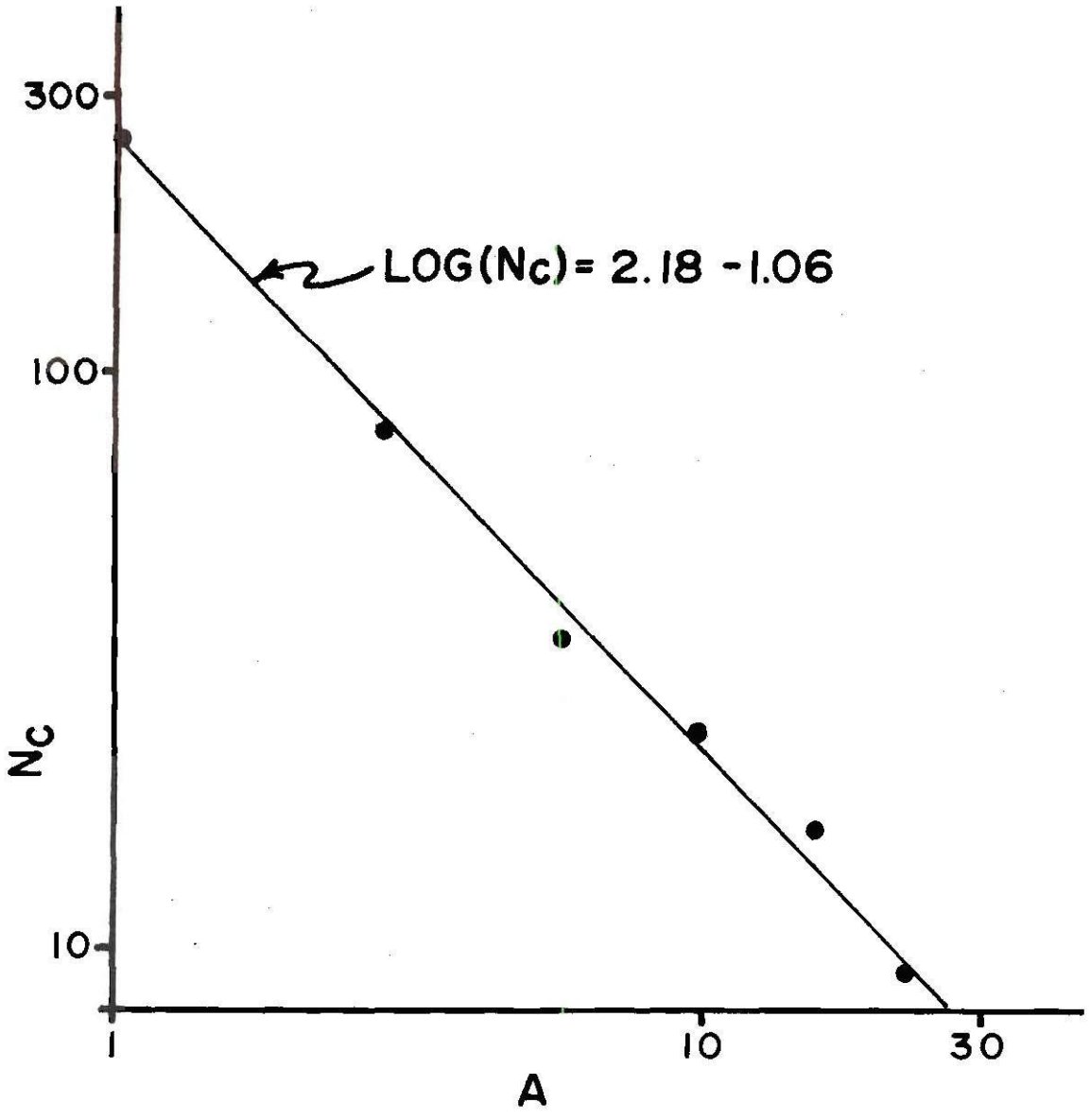


Figure 15. Cumulative Number of Events ($N_c$) of Amplitude A or Greater Versus Zero to Peak Amplitude (A) in Millimeters at Station SUM.

covered the period September 24, 1974 through January 21, 1975. Using these data, we may establish the time varying character of the "a" and "b" values, and estimate their values for September 18, 1974.

Twelve shocks with a magnitude range of 1.8 to 3.3 magnitude units were recorded at both stations, ATL and TDS. The local magnitude at station ATL was calculated and plotted as a function of the log of shear wave trace amplitude at station TDS. The resulting graph (Figure 16) demonstrates a strong linear relationship between local magnitude which can be described by the following equation

$$M_L = 1.77 + 1.32\log_{10}(A) \qquad (10)$$

where A is the maximum shear wave zero to peak trace amplitude in millimeters.

Recurrence Rates For Data From Station TDS

Using this relation, the events recorded at TDS were cataloged by trace amplitude and local magnitudes were calculated (Table 2). The magnitudes were than plotted as a function of the log of the cumulative number of events (Figure 17) with the values for "a" normalized to a one month period. Then the values for "a" and "b" were plotted as a function of time (Figure 18). Using these graphs, the approximate "a" and "b" values for September 18 were obtained as follows

$$\log_{10}(N_c) = 4.2 - 1.5M_L . \qquad (11)$$

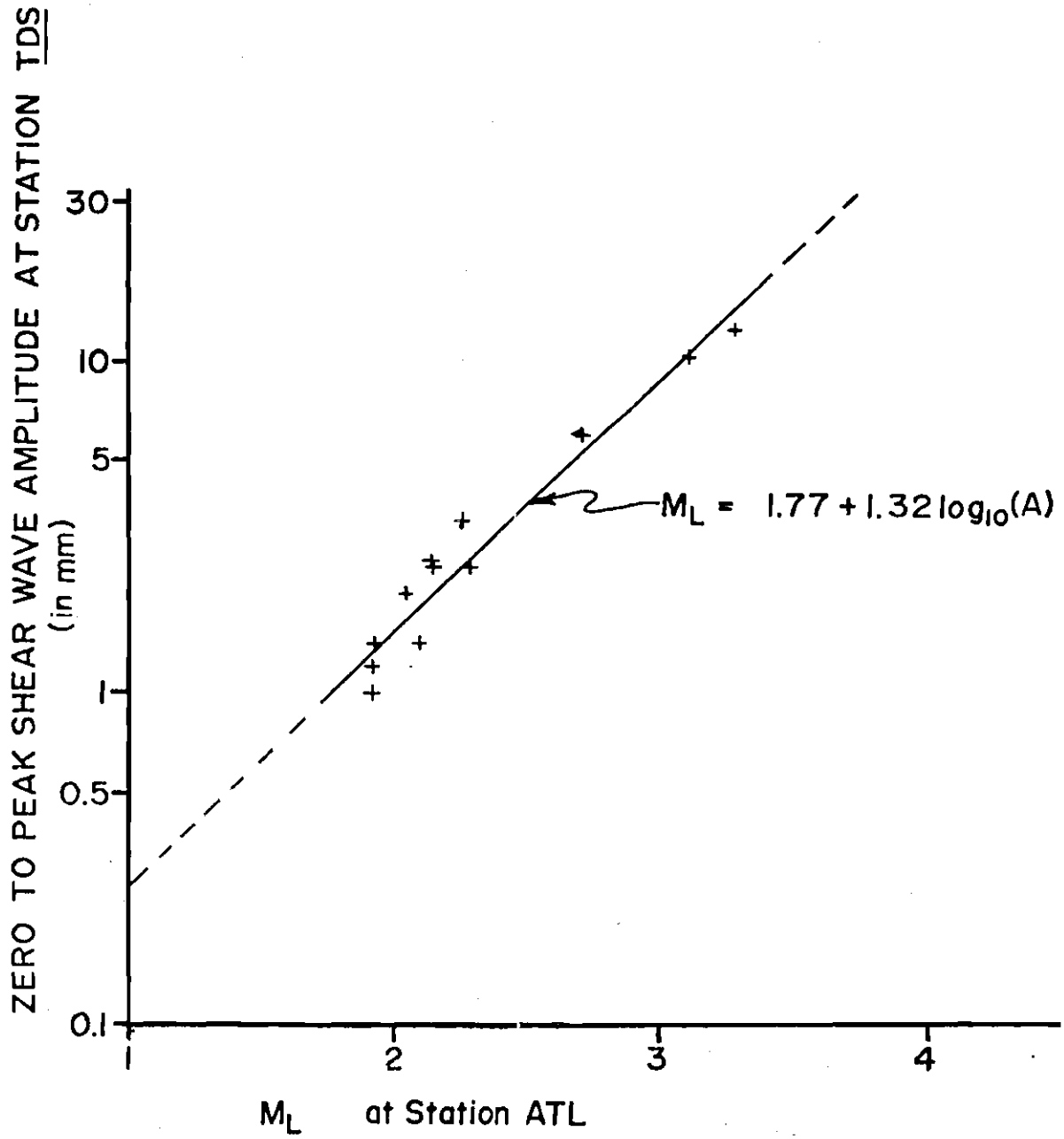


Figure 16. Trace Amplitude Versus Magnitude, Station TDS.

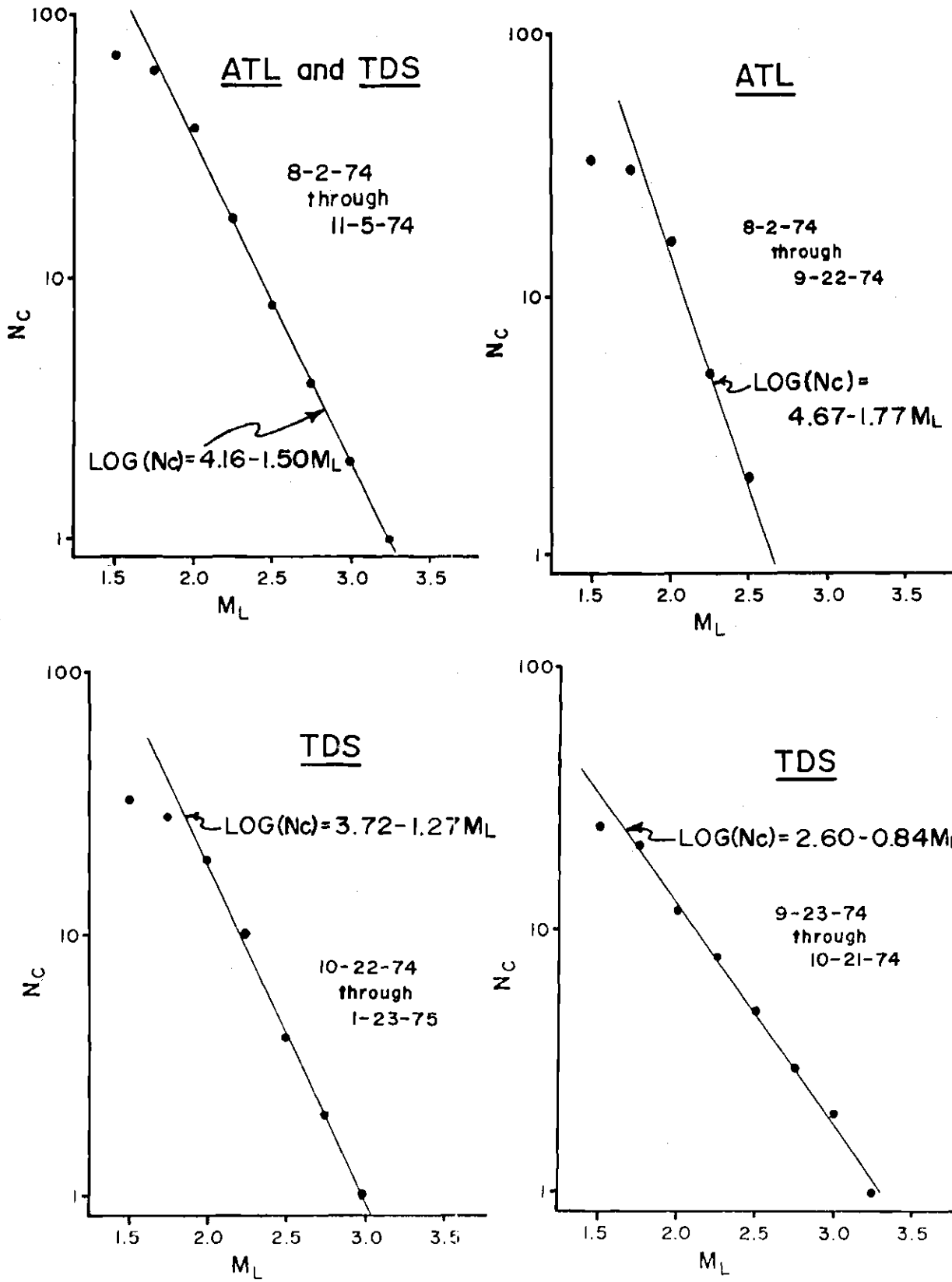


Figure 17. Recurrence Relations for the Aftershocks of the August 2, 1974 Event.

# VARIATIONS IN RECURRENCE RATES WITH TIME

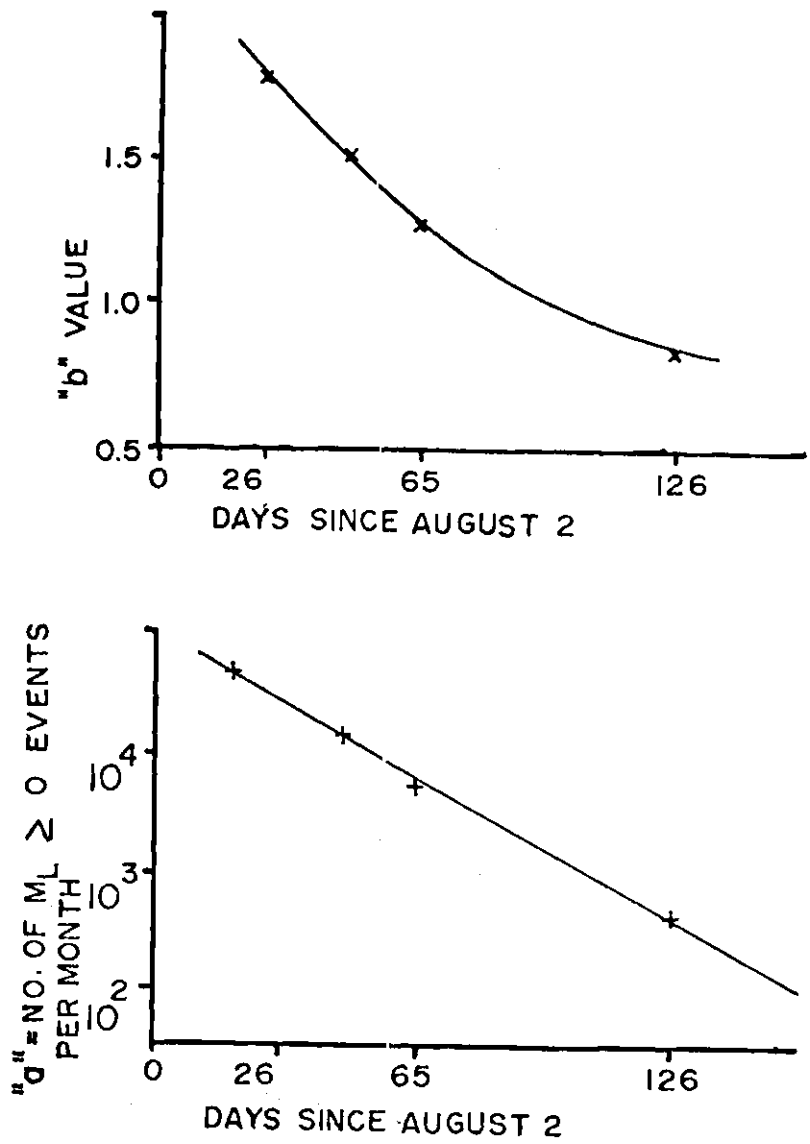


Figure 18. Time Variance of "a' and "b" Values.

## Evaluation of Magnitude From Trace Amplitude, Station SUM

In order to determine the relationship between local magnitude and trace amplitude at station SUM, we assume a dependence of magnitude on trace amplitude of the form (Richter, 1958)

$$M_L = C + D\left[\log_{10}(A)\right] \tag{12}$$

where C and D are constants, and further assume, for the particular "a" and "b" values obtained for September 18

$$\log_{10}(N_c) = a - bM_L = E - F\left[\log_{10}(A)\right] \tag{13}$$

where A is the zero to peak shear wave trace amplitude at SUM for events recorded on September 18 and E and F are constants (from Figure 15, E = 2.18 and F = 1.06). By taking derivatives of equations (12) and (13), we obtain

$$\frac{dM_L}{d\left[\log_{10}(A)\right]} = D = \frac{F}{b}. \tag{14}$$

We need now only determine the value of C. For a magnitude zero event, we have

$$C = -D\left[\log_{10}(A_o)\right] \tag{15}$$

where $A_o$ is the trace amplitude of a magnitude zero event, and

$$\log_{10}(N_c) = a = E - F\left[\log_{10}(A_o)\right] . \qquad (16)$$

hence, when the right half of equation (16) is satisfied, we may read $A_o$ from the graph (Figure 15) and C may be evaluated using equation (15). We finally obtain

$$M_L = 0.20 + 0.71\left[\log_{10}(A)\right] \qquad (17)$$

which is the approximate magnitude relation for station SUM.

## Evaluation of Aftershock Stress Drop

Using equation (17) the stress drop of the aftershock whose spectrum is shown in Figure 14 may now be evaluated. Using this equation and the microearthquake's recorded trace amplitude of 24.0 millimeters recorded at station SUM, a magnitude of 1.2 is obtained for the event. Assuming the circular dislocation model of Brune (1970) and using the measured corner frequency of 75 hertz, equation (9) gives a characteristic fault radius of 17 meters for a rupture at the shear wave velocity ($\beta$ = 3.5 km/sec) and a characteristic fault radius of 29 meters for a rupture at the compressional wave velocity ($\beta$ = 6.0 km/sec). Applying these values to Randall's (1973) theoretical curves (Figure 12), a stress drop of 100 bars for $\beta$ = 3.5 km/sec and a stress drop of 30 bars for $\beta$ = 6.0 km/sec were obtained. These stress drops are extremely high for a magnitude 1.2 event; normal stress drop for

an event this size according to Gibowicz (1973, equation (3)) is 0.07 bars.

# CHAPTER V

# DISCUSSION

## Significance of the Stress Drop Calculations

The definition of "normal" stress drop given by Gibowicz in equation (3) was based on statistical studies of well-developed fault zones (the San Andreas Fault of California and the Kermadec and Tonga trenches and associated fracture zones of New Zealand). The faulting usually occurs in shear zones in which the rocks have been reduced to a mylonitic texture. The fractured zones in these rocks would certainly not be expected to withstand the accumulation of very large amounts of shear stress. Large magnitude earthquakes are commonly produced by relatively low levels of shear stress acting on very large fault zones.

In contrast, all available evidence indicates that the Clark Hill epicentral zone is characterized by relatively fresh rock and the absence of large and well-developed fault zones. Surface faults with measurable recent movements have not been observed in the area. Consequently, it seems reasonable that large shear stresses must accumulate before faulting can take place, resulting in earthquakes whose magnitudes are large relative to their source dimensions. Due to the ability of the relatively crystalline rocks of the Clark Hill area to support substantial shear stresses before structural failure occurs, an earthquake having a characteristic fault radius of 17 meters (see

previous section) produced a local magnitude 1.2 event in the Clark Hill epicentral zone. By contrast, an earthquake having the same source dimensions but occurring in the highly sheared rock of California would probably have a local magnitude of -1 or less (see Figure 12).

Because the source dimensions of the Clark Hill events are small, more seismic energy is released in higher frequencies, or equivalently, the spectral corner frequencies of these microearthquakes are higher. It should be noted that in comparison to most aftershock investigations the upper limit of frequency response for the instrumentation used during this study is uncommonly high (greater than 200 hertz). Most aftershock instrumentation is designed to attenuate energy above a few tens of hertz at most, since the observation of seismic energy in frequencies above about ten hertz is unusual at common hypocentral recording distance of about 25 km.

If we assume the fault rupture propagated at the shear wave velocity, the direct method of Randall (1973) gives an estimate for stress drop for the August 2, 1974 event which is about twice as large as is predicted by the statistical methods of Gibowicz (Table 4). However, it must be again emphasized that Gibowicz's empirical relations were developed on the basis of data from well-established fault zones, which is not believed to be the case in the Clark Hill epicentral zone.

Two of the three empirical relations given by Gibowicz use "b" value as a variable in the calculation of stress drop. The "b" values of the aftershock sequences Gibowicz studied ranged from 0.51 to 1.09

Table 4. Stress Drop Estimates for the August 2, 1974 Earthquake. Normal Stress Drop for an Event of the Same Magnitude is (Gibowicz, 1973) 0.74 bars.

| Stress Drop Estimate (bars) | Method |
|---|---|
| 12. | Theoretical - Fault Area Estimated from Spectrum Rupture Velocity = 3.5 km/sec |
| 4.0 | Theoretical - Fault Area Estimated from Spectrum Rupture Velocity = 6.0 km/sec |
| 5.0 | Theoretical - Fault Area Estimated from Aftershock Zone |
| 6.3 | Empirical - Based on "b" Value |
| 5.0 | Empirical - Based on "b" Value and $M_L$-$M_1$ |
| 1.2 | Empirical - Based on Aftershock Duration |

with a mean of 0.83 and a standard deviation of 0.16. Since the "b" value for the six weeks following the August 2, 1974 event was 1.77, almost six standard deviations from the mean "b" value of Gibowicz's study, the application of Gibowicz's empirical relations to this study is questionable. However, the results obtained by two of Gibowicz's methods are surprisingly close to the results of Randall's method when we assume a rupture velocity of 6.0 km/sec, the compressional wave velocity (Table 4). Since the stresses in this area are considerably higher than most earthquake zones, the rupture of the fault may have progressed with the first arrival of seismic energy, i.e., the compressional wave. If this is true, two of Gibowicz's methods may have given fair estimates of the stress drop.

The direct method of Randall (1973) indicated stress drops of 30 bars at a rupture velocity of 6.0 km/sec and 100 bars at a rupture velocity of 3.5 km/sec for the September 18, 1974 20:15 GMT event. Although 30 and 100 bars are remarkably high stress drop values for this event, they are possible values since shear strengths of hard rocks are on the order of one to two kilobars for depths of zero to two kilometers (Hadley, 1973).

## Intensities

In the immediate epicentral area, events as small as $M_L = 1.0$ could easily be both felt and heard (Modified Mercalli Intensity of II to III); events as small as $M_L = 0.5$ could be heard but not generally felt. Usually events of this low a magnitude are not sensed. However, these events were unusually shallow (generally less than one

kilometer), and consequently hypocentral distances were unusually short. How much of the high intensity character of these events is due to the shallow depth of the activity or the competence of the country rock is not known.

Since the immediate epicentral area is unpopulated woodlands, the maximum Modified Mercalli intensity (V) shown on the August 2, 1974 earthquake intensity map (Figure 1) may be misleadingly low. There was at least one verified instance of cracked cinder block construction. In this case, fresh chips of paint and plaster were scattered below the cracks. However, the resident had built the dwelling and store himself and the construction would probably be classified as Masonry C (Richter, 1958). This site was located north of Bobby Brown State Park, ten kilometers northwest of the epicentral area. In view of the extent of damage, relatively large hypocentral distance (ten km) and undeveloped state of the epicentral area, it is believed that the intensity of the August 2, 1974 event would have been as high as VI if it had occurred in a populated area. An intensity of VI would normally be expected for an $M_L = 4.8$ event (Richter, 1958).

Possible Source Mechanisms for the Seismic Activity

Since the earthquake activity (1) has not been found to be associated with geologically observable fault zones in the field, (2) has demonstrated some planar trends in hypocenter plots (Appendix V) indicating the possible existance of two or three different planes of faulting, and (3) has a high stress drop character, it is interesting to speculate about the cause of the faulting. Bollinger (1973) and

Long (1975) have suggested that such faulting is a result of the crust in the southeastern United States undergoing a gentle warping. If this were the case, we might expect areas of particularly brittle rocks to accumulate high levels of stress and eventually fracture (ductile rocks would be deformed by these tectonic forces and elastic rocks would be bent). Fracture in brittle areas where stress is amplified should typically produce high stress drop earthquakes.

A second possibility is a thermal mechanism for the strain accumulation and resulting seismic activity of the Clark Hill Reservoir. In Chapter I, it was noted that many of the surface rocks of the epicentral area are fractured. Cold water from the reservoir, surrounding creeks and ground water may seep down into these cracks and cool the warmer rocks a kilometer or so beneath the surface. As these rocks were cooled, they would contract; this contraction could be the source of the stress which eventually results in faulting (Lister, 1974). In addition, as more faulting occurred, more cracks would open and more cooling water would be introduced; in this manner the activity could be sustained for a long period of time because of the large time factors required for heat conduction in rocks. In addition, one might expect high stress drop events if the cracking were not too extensive and the rocks were generally well consolidated. This type of mechanism might also be feasible for other lake- and reservoir-associated aftershocks and earthquake swarms, such as the Lake Hopatcong, New Jersey sequence of August through September, 1969 (Sbar et al., 1970).

# CHAPTER VI

## CONCLUSIONS

Based on the evidence presented in this thesis, the following may be concluded:

1. The August 2, 1974 Clark Hill earthquake and its aftershocks are unusually high stress drop events. This indicates faulting in relatively unfractured rock.

2. High stress conditions continued in the epicentral area after the August 2, 1974 event and throughout much of the aftershock period.

3. The aftershock activity of the August 2, 1974 event was generally confined to the upper two kilometers of the surface.

4. The aftershock activity probably occurred along two or more fault planes.

5. The intensities of the aftershocks were high relative to their magnitudes. This may be partially or wholly due to their short hypocentral distances.

# CHAPTER VII

## RECOMMENDATIONS

The primary direction of this study has been the investigation of the stress drop of the aftershock activity of the August 2, 1974 event. A great deal more information than has been used in this investigation is contained in the data obtained during this study. Numerous other aspects of this earthquake sequence should be studied. These other aspects include focal mechanism solutions from first motions and short term variations of "a" and "b" values for use in predicting larger aftershocks and relationships between coda lengths and magnitudes. In addition to studies of already existing data, geologic (including detailed mapping of the epicentral area with field checks on possible fault traces described in Appendix V), geophysical (gravity, magnetics, focal plane studies and reflection seismology) and engineering (including core drilling and tests of rock shear and compressive strengths) studies could provide valuable information on the cause and nature of the faulting.

It is also recommended that, if possible, a detailed seismic reflection line be shot across the epicentral area. This should be done as soon as possible because the continued aftershock activity rate indicates the continued existence of large stresses acting within this area. Such stresses may perturb the velocity. If the ambient stress field changes and most of the stresses are relieved the

velocities may change. At this time, the seismic line should be shot again. Time variation of velocities along this line could provide data for measurement of stress conditions in the earth. Variations in the arrival times of seismic waves reflected from subsurface structures could be used to estimate the percentage dilatancy as well as to define a dilatant volume. Such studies would be helpful to current research on earthquake prediction; if such a study were successful, it would be the first example of a truly accurate determination of the dimensions of a dilatant volume. This would be especially meaningful, since there is currently controversy over whether dilatant volumes are characterized by small percentage (1-2%) velocity changes of regional extent or large percentage (8-10%) velocity changes over a smaller volume (a few cubic kilometers). The magnitude of the volume effect is difficult to establish with current refraction methods. However, a reflection seismic study is very possible for this area due to the unusually shallow nature of the aftershock activity and the probable existence of a reflector at about ten km.

If a reflection seismic survey were not possible, the existence of dilatancy might be proved or disproved by a regional refraction seismic line which sampled the hypocentral volume. This study would also involve shooting the line again after the cessation of seismic activity (hopefully corresponding to the relief of stress).

With regard to the two proposed tectonic models for faulting (Chapter V), the following recommendations are made. The possibility of a thermal source for the activity could be investigated using finite

difference heat flow models (Lister, 1974) such as have been used in a study of thermal springs in the Southeast (Lowell, 1975). Using such a model, the actual contraction of the rocks at depth might be estimated and its significance be evaluated. The brittle rock-crustal warping theory would be more difficult to directly assess; however, since high stress drop might be expected for shocks of this type, a study of the spectral corner frequencies of well-recorded southeastern United States earthquakes is recommended. Such studies may be used to estimate the dimensions of the fault planes, hence allowing the stress drops to be evaluated by the method of Randall (1973). This study would be relatively straight forward and could provide substantial insight into the currently active tectonic forces as well as the nature of faulting in the Southeast.

# APPENDIX I

## SEISMIC RECORDING SYSTEMS

The seismic recording system used in the microearthquake reconnaissance surveys included four systems with smoked paper recorders and two systems with magnetic tape recorders. Detailed information of the make-up of these systems is given in Tables 5 and 6. Except with the Sony tape system, seismometers used were generally Hall-Sears HS10-1A one hertz vertical or horizontal geophones. In a few instances a pair of 15 hertz exploration geophones was used. Typically the smoked paper systems operated with voltage gains of 1,000 to 16,000, and displacement gains at 10 hertz of 2,000 to 32,000. Typical acceleration response curves and particle velocity response curves for smoked paper systems are plotted in Figure 19.

The Honeywell FM tape system had a response which was essentially flat from 0 to 600 hertz for recordings made at 1 7/8 ips; however, the amplifier and geophone limited this system's response to 0.5 to 100 hertz. Figure 20 gives the particle velocity response curve for this system.

The Sony AM tape recorder's response ranged from 20 to 4,000 hertz at a tape speed of 15/16 ips to 20 to 18,000 hertz at 7 1/2 ips. Seismic recordings were made at 15/16 ips and 1 7/8 ips; only those events recorded at 1 7/8 ips were used for spectral analysis. These events were played back at 15/16 ips to extend the upper frequency

response limit of the strip chart recorder. Using this method, resolution of frequencies as high as 400 hertz was possible. Figure 21 shows the particle velocity response of the Sony tape recorder-Hewlett Packard Strip Chart Recorder system. The lower end of the frequency response is limited by the Sony tape recorder; the higher end of the frequency response is limited by the Hewlett Packard Strip Chart recorder. Corrections for this response were made to the spectra obtained for microearthquakes recorded by this system.

Figures 22 and 23 give the displacement responses for stations ATL and AMG (Americus, Georgia) respectively. Corrections for the response at AMG were made in the spectral calculations for the August 2, 1974 event.

Table 5. Smoked Paper Seismograph Component Information

| Instrument Designation | Sniper Case | Yellow Box | MEQ-800 | LTL Special |
|---|---|---|---|---|
| Amplifier System | Teledyne-Geotech AS-330 Gain 58 to 112 dB in 6 dB Steps | Homebuilt Amplifier, Gain 60 to 95 dB in Approximately 6 dB Steps | Sprengnether AS-110, Gain 60 to 120 dB in 6 dB Steps | Teledyne-Geotech AS-330, Gain 58 to 112 dB in 6 dB Steps |
| Timing System | Sprengnether TS-300-1 Crystal Oscillator | Sprengnether TS-300-1 Crystal Oscillator | Sprengnether TS-300-10 Crystal Oscillator | Sprengnether TS-300-1 Crystal Oscillator |
| Recorder System | Sprengnether Model R-6034 3" Diameter Drum Recorder | Sprengnether Model R-6034 3" Diameter Drum Recorder | Sprengnether Model R-6040 13.5" Diameter Drum Recorder | Homebuilt 6" Diameter Drum Recorder |

Table 6. Magnetic Tape Seismograph Component Information

| Instrument Designation | Sony | Honeywell |
|---|---|---|
| Model Number | TC-800B | 8100 |
| Record Mode | AM | FM |
| Frequency Response @ 1 7/8 ips | 20-8000 Hz | 0 to 600 Hz |
| Tape Reel Diameter | 5" | 10 1/2" |
| Tape Width | 1/4" | 1/2" |
| Power | 12 Volt DC or 110 Volt AC | 12 Volt DC or 110 Volt AC |
| Maximum Recording Time | 8.5 Hours | 8 Hours |
| Weight | 11 Pounds | 100 to 150 Pounds |
| External Amplifier | 1 K Voltage Gain Amp Built Into Geophone | 1 K to 100 K Voltage Gain (Home Built Amp) |
| Internal Amplifier | 0.1 to 40 Times Record Volume Gain | None |
| Geophone | 15 Hertz Exploration | Hall-Sears HS-10-1 Vertical or Horizontal |

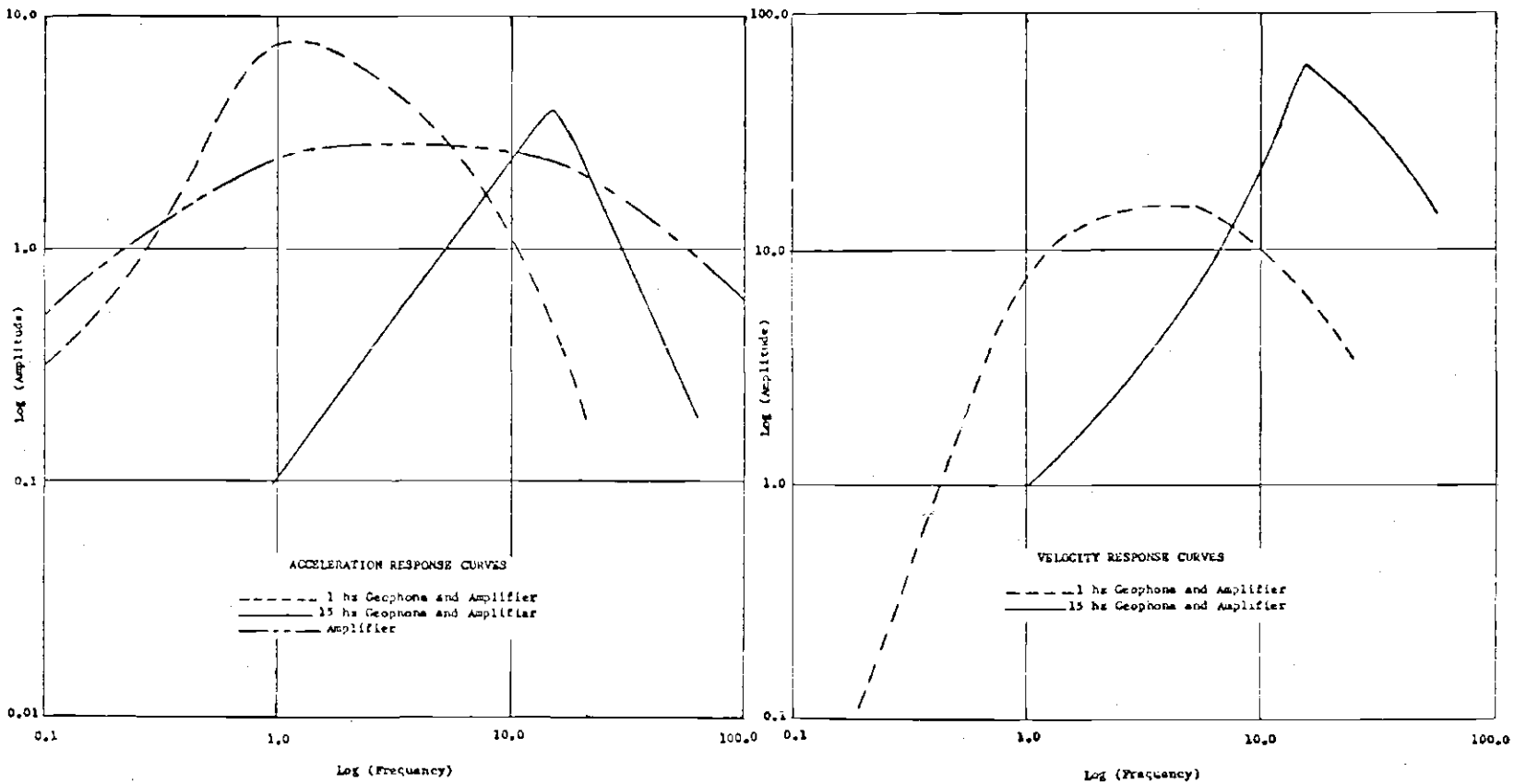


Figure 19. Typical Acceleration and Particle Velocity Response Curves for Smoked Paper Systems.

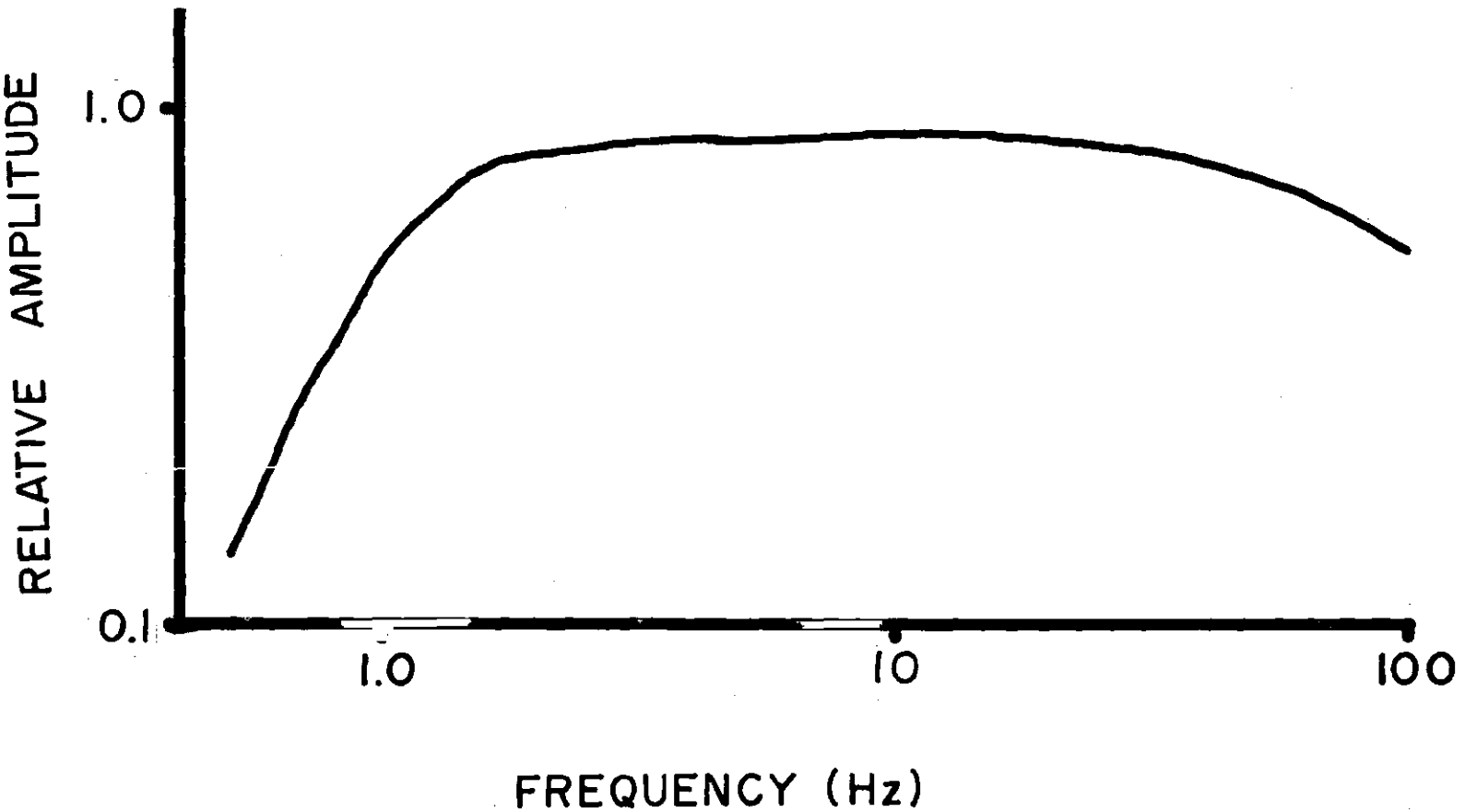


Figure 20. Particle Velocity Response Curve for the Honeywell-Amplifier System.

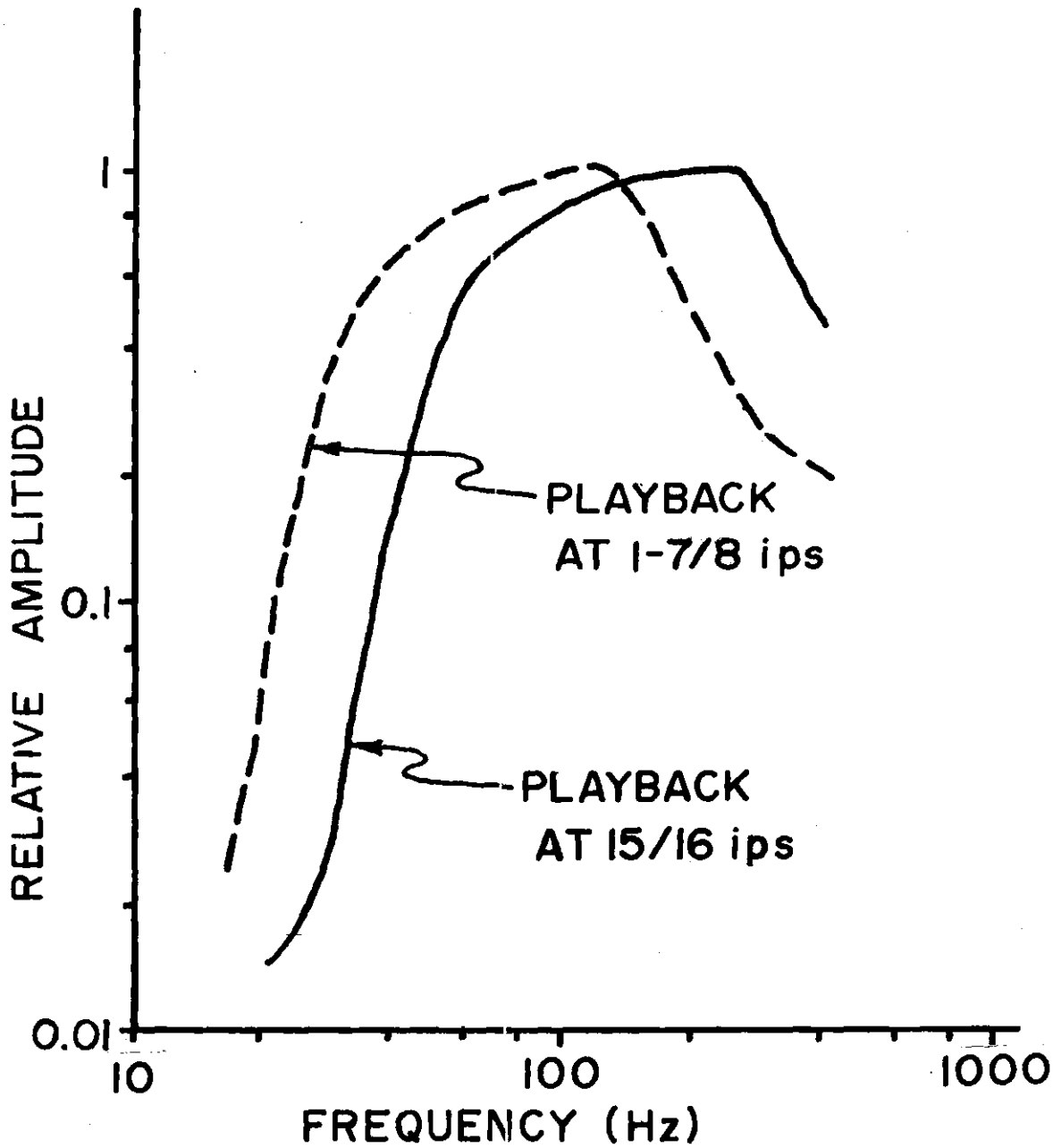


Figure 21. Particle Velocity Response Curve for the Sony Tape Recorder-Hewlett Packard Strip Chart Recorder System. Recording Speed 1 7/8 ips.

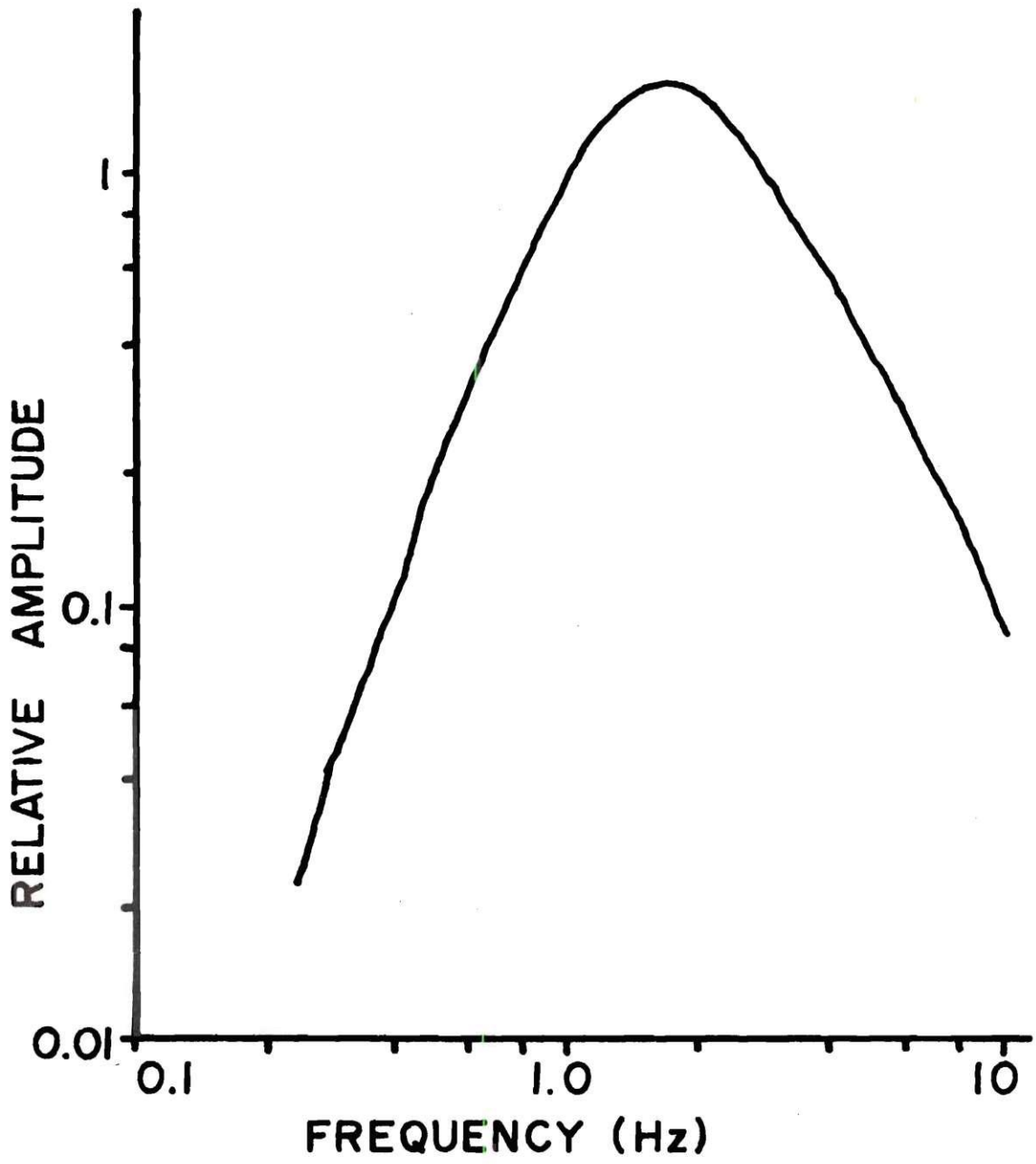


Figure 22. ATL Worldwide Standard Seismograph Station Short Period Seismometer Displacement Response.

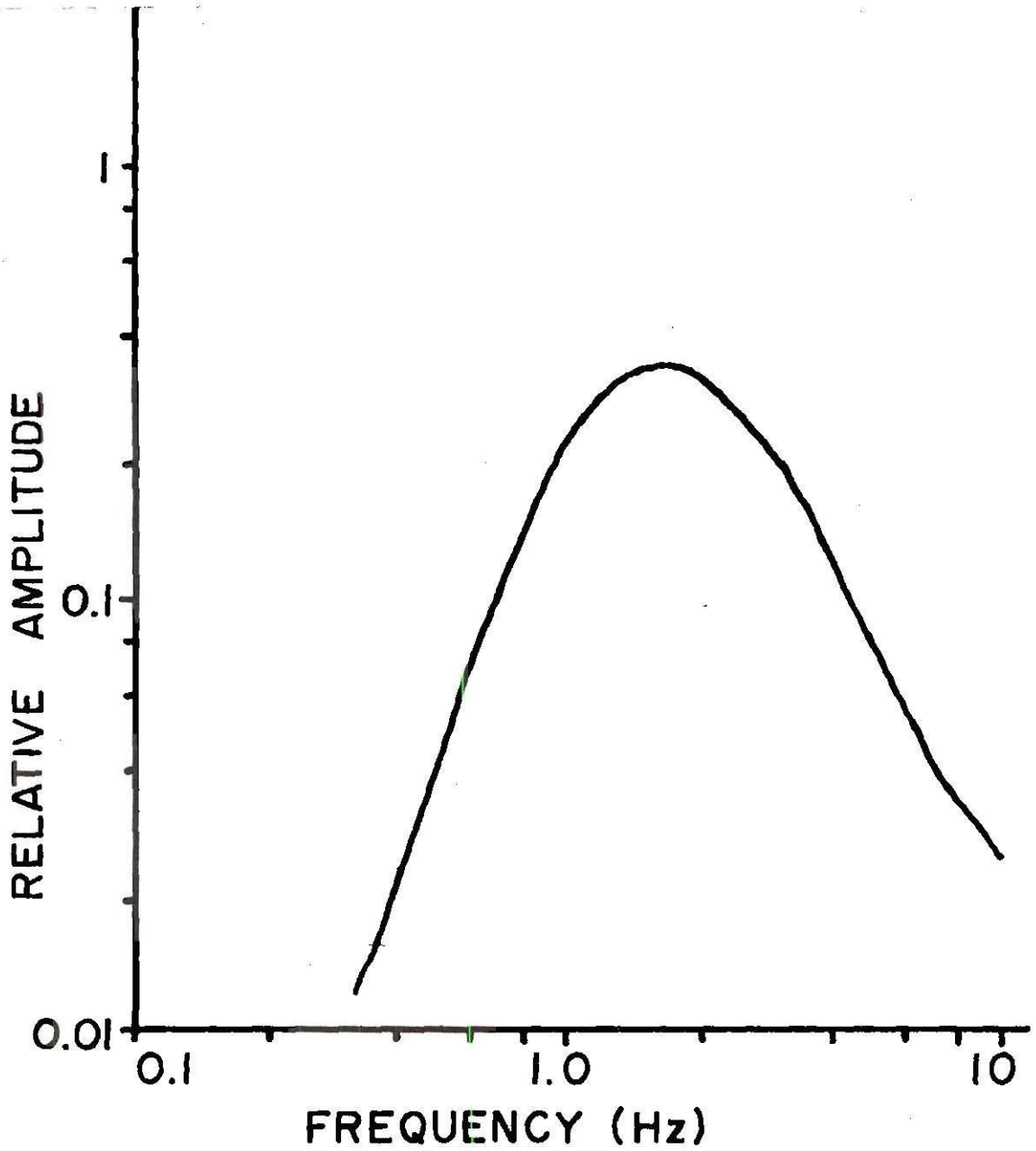


Figure 23. AMG Short Period Vertical Seismometer Displacement Response.

# APPENDIX II

## DETAILS OF FIELD TRIPS AND SEISMIC RECORDING STATION DATA

The data presented in this thesis involved many weeks of field microearthquake reconnaissance study. A summary of these data are given in Table 7. Table 8 presents locations of temporary field seismic recording stations occupied during this study.

Table 7. Summary of Dates of Station Occupation*

| Date | | Instrument | | | | | |
|---|---|---|---|---|---|---|---|
| | | Sniper Case | Yellow Box | LTL Special | MEQ-800 | Honeywell | Sony |
| 1974 | | | | | | | |
| August | 3 | TIG | | | | AMT | |
| | 4 | TIG | SCL | | | AMT | |
| | 5 | DBG | BBP | | | AMT | |
| | 6 | DBG | BBP | | | | |
| | 7 | DBG | SCL | | | SCL | |
| | 8 | DBG | CRK | | | SCL | |
| | 9 | DBG | BBR | | | | |
| | 10-19 | | | | | | |
| | 20 | HFR | | CEB | CRP | | |
| | 21 | HFR | | CEB | CRP | FRT | |
| | 22 | HFR | | CEB | CRP | FRT | |
| | 23 | HFR | | HUL | CRP | FRT | |
| | 24 | CPK | | HUL | HES | FRT | |
| | 25 | CPK | | HUL | HES | FRT | |
| | 26 | CPK | | HUL | HES | | |
| | 27 | CPK | | HUL | HES | | |
| | 28 | CPK | | HUL | HES | | |
| | 29 | CPK | | HUL | HES | | |
| | 30 | CPK | | HUL | HES | | |
| | 31 | CPK | | HUL | HES | | |

*Three letter codes indicate station location

Table 7. Summary of Dates of Station Occupation (Continued)

| Date | | Instrument | | | | | |
|---|---|---|---|---|---|---|---|
| | | Sniper Case | Yellow Box | LTL Special | MEQ-800 | Honeywell | Sony |
| September | 1 | CPK | | HUL | HES | | |
| | 2 | CPK | | HUL | HES | | |
| | 3 | CPK | | HUL | HES | | |
| | 4 | CPK | | HUL | HES | | |
| | 5 | CPK | | HUL | HES | | |
| | 6-15 | | | | | | |
| | 16 | CEB | | CRP | HST | | |
| | 17 | NAT | | CRP | HST | FRT | |
| | 18 | NAT | | CRP | HST | FRT | |
| | 19 | KAT | | CRP | SUM | FRT | |
| | 20 | KAT | | CRP | SUM | FRT | |
| | 21 | KAT | | CRP | SUM | FRT | |
| | 22 | KAT | | CRP | SUM | FRT | |
| | 23-30 | | | | TDS | | |
| October | 1-25 | | | | TDS | | |
| Nov. 3-Dec. 2 | | | | | TDS | | |
| Dec. 11-Dec. 31 | | | | | TDS | | |
| 1975 | | | | | | | |
| Jan. 1-Jan. 23 | | | | | TDS | | |
| January | 24 | HES | BOB | | | | |
| | 25 | FRT | BBN | | HUL | | |
| | 26 | FRT | BBN | | HUL | | |

Table 7. Summary of Dates of Station Occupation (Continued)

| Date | | Instrument | | | | | |
|---|---|---|---|---|---|---|---|
| | | Sniper Case | Yellow Box | LTL Special | MEQ-800 | Honey-well | Sony |
| Jan. 27-Feb. | 20 | | BBN | | | | |
| February | 21 | NAT | BBN | | SUM | | |
| | 22 | NAT | BBN | SNT | SUM | | |
| | 23 | NAT | BBN | SNT | SUM | | |
| | 24 | NAT | BBN | SNT | SUM | | |
| Feb. 25-March | 19 | | BBN | | | | |
| March | 20 | NAT | KPG | SNT | SUM | | |
| | 21 | NAT | KPG | SNT | SUM | | |
| | 22 | NAT | KPG | SNT | SUM | | |
| | 23 | NAT | KPG | SNT | SUM | | SUM |
| | 24 | NAT | KPG | | SUM | | GNT |
| April | 23 | DKE | JAM | | HUL | | HHH |
| | 24 | DKE | JAM | | HAL | | HHH |
| | 25 | DKE | JAM | | HAL | | HHH |
| | 26 | DKE | JAM | | HAL | | HHH |
| May | 22 | DKE | JAM | | HUL | | CKF |
| | 23 | DKE | JAM | | HUL | | CKF |
| | 24 | DKE | JAM | | HUL | | CKF |
| | 25 | DKE | JAM | | HUL | | CKF |
| July | 19 | | | | HUL | | CKF |
| | 20 | | | | HUL | | CKF |
| | 21 | | | | HUL | | CKF |

Table 8. Field Seismic Recording Station Location Data

| Station # | Latitude | Longitude | Elevation (in km) | Station Designation |
|---|---|---|---|---|
| 1 | 33°55.60' | 82°32.70' | .1228 | HES |
| 2 | 33°55.42' | 82°32.28' | .1036 | HST |
| 3 | 33°56.22' | 82°31.99' | .1036 | HTR |
| 4 | 33°56.17' | 82°32.41' | .1219 | HFR |
| 5 | 33°55.79' | 82°32.06' | .1021 | KAT |
| 6 | 33°54.73' | 82°30.93' | .1371 | FRT |
| 7 | 33°55.40' | 82°30.65' | .1051 | CRP |
| 8 | 33°53.13' | 82°28.27' | .1067 | CPK |
| 9 | 33°53.21' | 82°28.03' | .1067 | CRK |
| 10 | 33°57.05' | 82°31.43' | .1067 | NAT |
| 11 | 33°57.19' | 82°30.38' | .1036 | SUM |
| 12 | 33°57.00' | 82°31.76' | .1067 | HTL |
| 13 | 33°57.74' | 82°30.23' | .1402 | HUL |
| 14 | 33°56.71' | 82°33.85' | .1188 | CEB |
| 15 | 33°58.11' | 82°34.69' | .1173 | BOB |
| 16 | 33°58.29' | 82°35.21' | .1124 | BBN |
| 17 | 33°56.23' | 82°30.14' | .1158 | SNT |
| 18 | 33°57.76' | 82°30.25' | .1408 | HAL |
| 19 | 33°56.82' | 82°30.52' | .1280 | JAM |
| 20 | 33°56.75' | 82°29.41' | .1646 | DKE |
| 21 | 33°58.75' | 82°28.65' | .1372 | HHH |

# APPENDIX III

## AFTERSHOCK LOCATION PROCEDURE

### Data Preparation

Smoked paper seismograms were compared until events were found which were recorded clearly on three or more stations. Compressional (P) and shear (S) wave arrival times were then read to ± 0.05 seconds with the aid of a low power microscope and a slide etched with a millimeter scale. When accurate absolute time control was not possible, S-P times were read instead.

Events which were also recorded on magnetic tape were played back on a strip chart recorder at 125 mm/sec. S-P times for these events were read to ± 0.01 second or better.

### Hypocenter Location

A Fortran program, "DOALL," which was developed by Dr. L. T. Long to compute the location of Southeastern earthquakes, was modified for the Clark Hill epicentral area. The velocity model used was a semi-infinite medium with a compressional wave velocity of 6.0 km/sec and a shear wave velocity of 3.5 km/sec. The program "DOALL" is listed at the end of this Appendix.

The program "DOALL" employs the method of Wiggins (1972) to find an origin time and hypocenter corresponding to the least mean squares fit of the observed travel times to theoretical travel times.

This method requires an initial guess with a small error. Therefore, hypocenters were first estimated using graphical techniques; this estimate was then used as the initial guess. If the seismic wave arrival times were accurately determined, the program rapidly converged to a solution. The hypocenters listed in this Appendix (Table 9) are accurate to better than ± 0.3 km in latitude and longitude (± 0.2 minutes) and ± 0.4 km in depth.

Table 9. Aftershock Hypocenters

| Event # | Date | Origin Time (GMT) | North Latitude | West Longitude | Depth (km) | Precision E = ±0.1 km G = ±0.2 km F = ±0.4 km |
|---|---|---|---|---|---|---|
| 1 | 1-26-75 | 04:04:34.25 | 33°56.94' | 82°30.12' | 0.9 | G |
| 2 | 1-26-75 | 04:24:51.95 | 33°57.84' | 82°29.52' | 0.8 | F |
| 3 | 1-26-75 | 04:26:15.65 | 33°57.96' | 82°29.88' | 1.0 | F |
| 4 | 2-22-75 | 04:09:19.08 | 33°57.61' | 82°29.47' | 1.0 | F |
| 5 | 2-22-75 | 17:37:55.77 | 33°57.67' | 82°29.15' | 1.0 | F |
| 6 | 2-22-75 | 17:38:21.53 | 33°57.85' | 82°29.13' | 1.0 | F |
| 7 | 2-22-75 | 18:11:33.39 | 33°55.93' | 82°29.93' | 0.28 | F |
| 8 | 2-22-75 | 18:31:02.35 | 33°58.37' | 82°29.12' | 0.27 | F |
| 9 | 2-22-75 | 20:25:52.66 | 33°57.95' | 82°29.36' | 1.0 | F |
| 10 | 2-22-75 | 23:35:01.74 | 33°58.06' | 82°29.56' | 1.0 | F |
| 11 | 2-23-75 | 00:45:24.31 | 33°58.16' | 82°29.65' | 1.0 | F |
| 12 | 2-23-75 | 23:55:58.15 | 33°56.99' | 82°29.15' | 0.94 | G |
| 13 | 2-24-75 | 02:08:16.18 | 33°57.78 | 82°29.69' | 1.1 | F |

Table 9. Aftershock Hypocenters (Continued)

| Event # | Date | Origin Time (GMT) | North Latitude | West Longitude | Depth (km) | Precision E = ±0.1 km G = ±0.2 km F = ±0.4 km |
|---|---|---|---|---|---|---|
| 14 | 4-24-75 | 04:04:56.00 | 33°57.66' | 82°29.77' | 0.91 | G |
| 15 | 4-24-75 | 05:50:17.49 | 33°57.52' | 82°29.66' | 0.97 | G |
| 16 | 4-24-75 | 05:52:22.36 | 33°57.48' | 82°29.46' | 0.89 | G |
| 17 | 4-24-75 | 05:53:36.12 | 33°57.47' | 82°29.42' | 0.86 | G |
| 18 | 4-24-75 | 06:27:59.36 | 33°57.56' | 82°29.52' | 0.93 | G |
| 19 | 4-24-75 | 06:28:54.18 | 33°57.52' | 82°29.73' | 0.97 | G |
| 20 | 4-24-75 | 15:33:00.38 | 33°57.51' | 82°29.14' | 0.48 | G |
| 21 | 4-24-75 | 17:31:52.61 | 33°57.54' | 82°29.69' | 0.96 | E |
| 22 | 4-24-75 | 18:50:27.54 | 33°57.60' | 82°29.59' | 0.92 | G |
| 23 | 4-25-75 | 00:55:24.32 | 33°57.39' | 82°29.64' | 0.91 | G |
| 24 | 4-25-75 | 04:59:20.16 | 33°57.47' | 82°29.65' | 0.99 | G |
| 25 | 4-25-75 | 05:01:07.75 | 33°57.04' | 82°30.21' | 0.95 | G |
| 26 | 4-25-75 | 05:46:56.91 | 33°57.44' | 82°29.52' | 0.47 | G |

Table 9. Aftershock Hypocenters (Continued)

| Event # | Date | Origin Time (GMT) | North Latitude | West Longitude | Depth (km) | Precision E = ±0.1 km G = ±0.2 km F = ±0.4 km |
|---|---|---|---|---|---|---|
| 27 | 4-25-75 | 17:50:49.80 | 33°57.78' | 82°30.44' | 1.01 | G |
| 28 | 4-25-75 | 18:10:01.24 | 33°57.59' | 82°30.00' | 1.19 | G |
| 29 | 4-25-75 | 18:12:14.96 | 33°57.46' | 82°30.24' | 0.66 | G |
| 30 | 4-25-75 | 18:20:43.59 | 33°57.55' | 82°29.66' | 0.96 | E |
| 31 | 4-26-75 | 00:25:34.22 | 33°57.65' | 82°29.67' | 0.79 | F |
| 32 | 4-26-75 | 00:36:55.95 | 33°57.64' | 82°29.50' | 0.00 | G |
| 33 | 4-26-75 | 05:34:22.12 | 33°57.65' | 82°29.80' | 0.98 | G |
| 34 | 4-26-75 | 06:54:57.92 | 33°57.61' | 82°29.74' | 0.96 | E |
| 35 | 4-26-75 | 06:56:28.53 | 33°57.58' | 82°30.10' | 1.43 | G |
| 36 | 4-26-75 | 07:24:31.39 | 33°57.49' | 82°29.71' | 0.98 | E |
| 37 | 4-26-75 | 07:25:12.01 | 33°57.72' | 82°29.46' | 0.31 | E |
| 38 | 4-26-75 | 07:36:39.78 | 33°57.57' | 82°29.74' | 0.82 | G |
| 39 | 4-26-75 | 08:17:13.28 | 33°57.64' | 82°29.25' | 0.28 | F |

Table 9. Aftershock Hypocenters (Continued)

| Event # | Date | Origin Time (GMT) | North Latitude | West Longitude | Depth (km) | Precision E = ±0.1 km G = ±0.2 km F = ±0.4 km |
|---|---|---|---|---|---|---|
| 40 | 4-26-75 | 08:25:10.59 | 33°57.55' | 82°29.43' | 0.02 | E |
| 41 | 4-26-75 | 08:40:30.37 | 33°57.49' | 82°29.52' | 0.66 | E |
| 42 | 4-26-75 | 17:36:06.14 | 33°57.04' | 82°29.86' | 0.47 | E |
| 43 | 4-26-75 | 18:12:31.88 | 33°57.09' | 82°29.79' | 0.12 | E |
| 44 | 4-26-75 | 19:03:00.34 | 33°58.41' | 82°30.17' | 0.50 | G |

PRINTOUT OF DOALL

```
001   @FOR,IS MAIN
002   C****PROGRAM DO-ALL---ITERATIVE-WEIGHTED-LEAST SQUARES EPICENTER LOCATION
003   C
004   C
005         DIMENSION PHAS(30),LABEL(8),C(5),IPH(50),Q(50),SI(50),ID(50),
006        2DC(50),S(50),A(50,4),W(4),DP(4),FDP(4),SPD(50)
007         COMMON STAT(200),SLAT(200),SLONG(200),ELEV(200)
009   C
009   C*****READ STATIONS TO BE USED**********
010     201 READ(5,109)ISTA,STAT(ISTA),SLAT(ISTA),SLONG(ISTA),ELEV(ISTA)
011     109 FORMAT(I5,5X,A3,7X,3F10.4)
012         IF (ISTA.EQ.200)GO TO 70
013         WRITE(6,110) ISTA,STAT(ISTA),SLAT(ISTA),SLONG(ISTA),ELEV(ISTA)
014     110 FORMAT(1X,I5,2X,A3,3F15.4)
015         GO TO 201
016      70 CONTINUE
017   C*****READ PARAMETERS FOR TRAVEL-TIME COMPUTATION**********
018         CALL TTIME(PHAS)
019   C*****READ BASIC EQ DATA CARD CONTAINING ESTIMATES OF EPICENTER********
020   C       THIS CARD SHOULD BE IN FORMAT OF CARD FILE OF EARTHQUAKES
021     200 READ(5,100,END=99)IYR,MO,IDA,IHR,MIN,SEC,ELAT,ELONG,EZ,
022        2IST,TQ,SP,(LABEL(JR),JR=1,8)
023         IF (IYR.EQ.0) GO TO 99
024     100 FORMAT(I4,4I2,F3.1,2F7.3,F4.1,   2I1,A4,8A5)
025         WRITE(6,105)MO,IDA,IYR,IHR,MIN,SEC,ELAT,ELONG,(LABEL(J8),J8=1,8)
026     105 FORMAT(2H1,I2,1H/,I2,1H/,I4,4H H=,I2,2X,I2,2X,F4.1,6H LAT=,
027        2F7.3/,7H LONG=,F7.3/,2X,A4,8A5//)
028   C*****READ WEIGHTS TO BE ASSIGNED IN COMPUTATION OF X,Y,T & Z
029   C       CAN ELIMINATE Z OR Z AND T BY SETTING TO ZERO EITHER WZ OR WZ & WT
030         READ(5,101) WX,WY,WT,WZ,EZ,CDIST,NITER,SECERR,SMINER
031     101 FORMAT(2X,6F8.3,I5,2F5.1)
032         WRITE(6,101) WX,WY,WT,WZ,EZ,CDIST,NITER,SECERR,,SMINER
033         XCDIST=CDIST/2.
034         IF(WZ.LT.0.0001)GO TO 22
035         M=4
036         GO TO 23
037      22 IF(WT.LT.0.0001) GO TO 24
038         M=3
039         GO TO 23
040      24 M=2
041      23 TO=IHR*3600.+MIN*60.+SEC
042         WRITE(6,120) IHR,MIN,SEC,TO,M
043     120 FORMAT(1H ,2I5,2E20.6,I5)
044         N=1
045         W(1)=SQRT(WX)
046         W(2)=SQRT(WY)
047         W(3)=SQRT(WT)
048         W(4)=SQRT(WZ)
049         XW4=W(4)
050         W(4)=0.0
051         M=3
052   C*****READ STATION,PHASE,ARRIVAL TIME DATA
053         N=0
054       6 N=N+1
```

PRINTOUT OF DOALL (Continued)

```
055         READ(5,102,END=5) IPH(N),ID(N),IH,IM,SEC,SI(N)
056       102 FORMAT(I5,5X,I5,5X,2I3,F7.3,F10.3)
057         Q(N)=IH*3600.0+IM*60.0+SEC
058         IF (ID(N).LT.1) GO TO 5
059         GO TO 6
060       5 CONTINUE
061         N=N-1
062       7 CONTINUE
063       C  CALCULATE DISTANCES BASED ON S-P
064         NB=N/2
065         NB=NB*2
066         DO 38 I=2,NB,2
067         SPD(I)  =(Q(I)-Q(I-1))*1.37*6.0
068         SPD(I-1)=SPD(I)
069       38 CONTINUE
070         KL=0
071       39 CONTINUE
072         DO 8 IN=1,N
073         CALL ATIME (IPH(IN),TO,ID(IN),ELAT,ELONG,EZ,C,R)
074         DC(IN)=Q(IN)-C(1)
075         A(IN,1)=C(3)
076         A(IN,2)=C(4)
077         A(IN,3)=C(2)
078         A(IN,4)=C(5)
079         S(IN)=1.0/SQRT(SI(IN))
080       8 CONTINUE
081         CALL MAMAN(A,DC,S,W,N,DP,M)
082         DO 14 I6=1,4
083       14 FDP(I6)=DP(I6)*W(I6)
084         TO=TO+FDP(3)
085         ELAT=ELAT+FDP(2)/111.11
086         ELONG=ELONG+FDP(1)/(111.11*COS(ELAT*0.01745))
087         EZ=EZ+FDP(4)
088         IHTO=TO/3600
089         IMTO=(TO-IHTO*3600)/60
090         TSEC=TO-IHTO*3600-IMTO*60
091         ELOMN=(ELONG-IFIX(ELONG))*60.
092         ELAMN=(ELAT-IFIX(ELAT))*60.
093         WRITE(6,108) IHTO,IMTO,TSEC,ELAT,ELAMN,ELONG,ELOMN,EZ
094       108 FORMAT(1H1,'THE RECOMPUTED EPICENTER IS'/2X,2I4,F7.2,/2X,
095          1'LATITUDE',F10.4,'  33  ',F6.2/2X,'LONGITUDE',F10.4,'  82  ',F6.2/
096          22X,'DEPTH',3X,F7.2/2X)
097         WRITE(6,106)
098       106 FORMAT(1H ,'STATION PHASE HR MIN SEC       C1      C2      C3       C4
099          *      C5      DIST  OBS-THE +OR-(SEC)    R(LOC)   R(S-P)')
100         DO 18 IN=1,N
101         IID=ID(IN)
102         IIPH=IPH(IN)
103         CALL CXY(SLAT(IID),SLONG(IID),ELAT,ELONG,X,Y)
104         R=(X*X+Y*Y)**0.5
105         RR=(R*R+EZ*EZ)**0.5
106         IH=Q(IN)/3600.
107         IM=(Q(IN)-IH*3600.)/60.
108         SEC=Q(IN)-IH*3600.-IM*60.
109         WRITE(6,107) STAT(IID),PHAS(IIPH),IH,IM,SEC,
110          C(C(I),I=1,5),R,DC(IN),SI(IN),RR,SPD(IN)
111       107 FORMAT(3X,A3,3X,A3,2X,I2,1X,I2,1X,F5.2,F10.1,4F7.3,F8.2,2F7.2,5X,2
```

PRINTOUT OF DOALL (Continued)

```
112         *F9.2)
113       18 CONTINUE
114          TESTC=SQRT(FDP(1)*FDP(1)+FDP(2)*FDP(2))
115          IF(TESTC.LT.CDIST)M=4
116          IF(TESTC.LT.CDIST)W(4)=XW4
117          IF(KL.EQ.1)KL=5
118          IF(TESTC.LT.CDIST)KL=KL+1
119          IF(KL.EQ.1)GO TO 39
120          IF(TESTC.LT.XCDIST)GO TO 200
121          IF(NITER.LT.0) GO TO 200
122          NITER=NITER-1
123          IF (SECERR.LT.SIMNER) GO TO 39
124          NRED=0
125          DO 9 I=1,N
126       92 DCS=ABS(DC(I+NRED)/S(I+NRED))
127          IF (DCS.LT.SECERR) GO TO 9
128          NRED=NRED+1
129          JEND=N-NRED
130          IF (JEND.LT.I) GO TO 91
131          DO 10 J=I,JEND
132          Q(J)=Q(J+1)
133          ID(J)=ID(J+1)
134          IPH(J)=IPH(J+1)
135       10 SI(J)=SI(J+1)
136          GO TO 92
137        9 CONTINUE
138          SECERR=SECERR/2.0
139          N=N-NRED
140          GO TO 39
141       91 N=N-NRED+1
142          IF (N.LE.M) GO TO 200
143          GO TO 39
144       99 STOP
145          END
146     @FOR,I TTIME
147          SUBROUTINE TTIME(PHAS)
148          DIMENSION C(5),A(20),PHAS(30)
149          COMMON STAT(200),SLAT(200),SLONG(200),ELEV(200)
150     C*********
151     C  DESIGNED FOR A CONSTANT VELOCITY SEMI INFINITE HALF SPACE.
152     C    DEPTH CONSTRAINED TO 0.5 KM ABOVE OR BELOW SEA LEVEL.
153     C     READ CRUSTAL MODEL ... IPHA=20. FOR LAST CARD.
154     C**********
155       49 READ(5,50)IPHA,A(IPHA),PHAS(IPHA)
156          IF(IPHA.EQ.20)RETURN
157          WRITE(6,50) IPHA,A(IPHA),PHAS(IPHA)
158          GO TO 49
159       50 FORMAT(I5,F10.4,A6)
160          ENTRY ATIME(IPH,TO,ID,ELAT,ELONG,EZ,C,R)
161          IF(EZ.LT.-0.5)EZ=-0.5
162          CALL CXY(SLAT(ID),SLONG(ID),ELAT,ELONG,X,Y)
163          R=SQRT(X*X+Y*Y)
164          D= SQRT(R*R+(ELEV(ID)+EZ)**2.)
165          C(1)=TO+A(IPH)*D
166          C(2)=1.
167          C(3)=A(IPH)*X/D
168          C(4)=A(IPH)*Y/D
```

PRINTOUT OF DOALL (Continued)

```
      C(5)=A(IPH)*(ELEV(ID)+EZ)/D
      RETURN
      END
@FOR,I CXY
C
C
      SUBROUTINE CXY(YO,XO,ALAT,ALONG,X,Y)
C****(YO,XO) IS ORIGIN IN DEGREES<500KMFROM DATA FOR < 1KM ERROR
C****(ALAT,ALONG) LATITUDE AND LONGITUDE OF DATA POINTS
C****FROM RICHTER-ELEM SEIS-USING CLARKE SPHEROID
C****LONGITUDE IS NEGATIVE FOR WEST,X IS POSITIVE EAST, Y IS POSITIVE
C     NORTH, (X,Y) IS DISTANCE TO (ALAT,ALONG) FROM ORIGIN (XO,YO)
      DIMENSION B(90),AC(90)
      DATA(B(I),I=20,45)/1.844998,1.845213,1.845437,1.845668,1.845907,
     C1.846153,1.846408,1.846670,1.846938,1.847213,1.847495,1.847781,
     C1.848073,1.848372,1.848673,1.848980,1.84929,1.849605,1.849922,
     C1.850242,1.850565,1.850890,1.851217,1.851543,1.851873,1.852202/
      DATA(AC(I),I=20,45)/1.856100,1.856173,1.856248,1.856325,1.856404,
     C1.846153,1.846408,1.846670,1.846938,1.847213,1.847495,1.847781,
     C1.857132,1.857231,1.857331,1.857435,1.857538,1.857643,1.857750,
     C1.857858,1.857964,1.858074,1.858184,1.858294,1.858403,1.858512/
      DLAT=ALAT-YO
      DLONG=ALONG-XO
      IA=(YO+ALAT)/2.0
      AA=(AC(IA)+(AC(IA+1)-AC(IA))*((YO+ALAT)/2.0-IA))
      AA=AA*60.0* COS(0.0174532D*ALAT)
      X=AA*DLONG
      BB=(B(IA)+(B(IA+1)-B(IA))*((YO+ALAT)/2.0-IA))*60.0
      Y=BB*DLAT
      RETURN
      END
@FOR,I MAMAN
C
C
      SUBROUTINE MAMAN(A,DC,S,W,N,DP,M)
      DIMENSION A(50,4),DC(50),S(50),W(4),AN(50,4),ATA(4,4),AVRT(5,5),
     CATDC(4),DP(4)
      DO 7 I=1,N
      DC(I)=S(I)*DC(I)
      DO 7 J=1,M
    7 AN(I,J)=S(I)*A(I,J)*W(J)
      DO 20 IA=1,N
   20 WRITE(6,201)(AN(IA,JA),JA=1,M)
  201 FORMAT(1X,4F12.4)
      DO 8 L=1,4
      DO 8 LL=1,4
    8 ATA(L,LL)=0
      DO 9 I1=1,M
      DO 9 J1=1,M
      DO 9 K1=1,N
    9 ATA(I1,J1)=AN(K1,I1)*AN(K1,J1) +ATA(I1,J1)
      WRITE(6,202)  ((ATA(IB,JB),IB=1,4),JB=1,4)
  202 FORMAT(1X//,(4(1X,F12.2)))
      M1=M+1
      CALL MINVRT(AVRT,ATA,M,M1)
      WRITE(6,203) ((AVRT(IC,JC),IC=1,4),JC=1,4)
  203 FORMAT(2X//,(4(1X,F12.2)))
```

PRINTOUT OF DOALL (Continued)

```
226         DO 10 I2=1,4
227      10 ATDC(I2)=0
228         DO 11 I3=1,M
229         DO 11 K3=1,N
230      11 ATDC(I3)=AN(K3,I3)*DC(K3)+ATDC(I3)
231         WRITE(6,203) (ATDC(IE),IE=1,4)
232         DO 12 I4=1,4
233      12 DP(I4)=0
234         DO 13 I5=1,M
235         DO 13 J5=1,M
236      13 DP(I5)=AVRT(I5,J5)*ATDC(J5)+DP(I5)
237         WRITE(6,203)(DP(IG),IG=1,4)
238         RETURN
239         END
240   @FOR,I MINVRT
241         SUBROUTINE MINVRT(A,X,NN,MM)
242         DIMENSION A(5,5),X(4,4)
243   C     MATRIX INVERSION SUBROUTINE, A IS THE INPUT MATRIX,
244   C     X IS THE OUTPUT
245       8 DO 9 I=1,NN
246         DO 9 J=1,NN
247       9 A(I,J)=X(I,J)
248         DO 16 N=1,NN
249         A(1,MM)=1.
250         DO 10 I=2,MM
251      10 A(I,MM)=0.
252         DO 11 J=1,NN
253      11 A(MM,J)=A(1,J+1)/A(1,1)
254         DO 12 I=2,NN
255         XX=A(I,1)
256         DO 12 J=1,NN
257      12 A(I-1,J)=A(I,J+1)-XX*A(MM,J)
258         DO 16 J=1,NN
259      16 A(NN,J)=A(MM,J)
260         RETURN
261         END
262   @XQT
263
264        1      HES        33.9266   82.5449   .1128
265        2      HST        33.9237   82.5381   .1036
266        3      HTR        33.9370   82.5332   .1036
267        4      HFR        33.9362   82.5402   .1219
268        5      KAT        33.9298   82.5343   .1021
269        6      FRT        33.9121   82.5154   .1371
270        7      CRP        33.9233   82.5109   .1051
271        8      CPK        33.8854   82.4711   .1067
272        9      CRK        33.8868   82.4672   .1067
273       10      NAT        33.9508   82.5238   .1067
274       11      SUM        33.9532   82.5063   .1036
275       12      HTL        33.9500   82.5293   .1067
276       13      HUL        33.9623   82.5038   .1402
277       14      CEB        33.9452   82.5642   .1188
278       15      BOB        33.9685   82.5782   .1173
279       16      BBN        33.9715   82.5868   .1124
280       17      SNT        33.9372   82.5023   .1158
281       18      HAL        33.9627   82.5042   .1408
282       19      JAM        33.9470   82.5087   .1280
```

PRINTOUT OF DOALL (Continued)

```
283     20      DKE             33.9458   82.4902   .1646
284     21      HHH             33.9792   82.4775   .1372
285    200
286      1  .1667   P
287      2 .2888    S
288      3 .1217    S-P
289     20
290 19750426181232.33.96  82.5
291          1.0      1.0      1.0  1.          1.0      .01    2^0  16.  0.1
292      1          18       18 1232.12   0.5
293      2          18       18 1232.30   0.5
294      1          19       18 1232.09   0.5
295      2          19       18 1232.24   0.5
296      3          20       18 1231.99   0.5
297
298 19750426190138.33.96  82.5
299          1.0      1.0      1.0  1.          1.0      .01    2^0  16.  0.1
300      1          19       19 0138.35   0.5
301      2          19       19 0138.69   0.5
302      1          18       19 0138.00   0.5
303      3          20       19 0138.23   0.5
304
```

# APPENDIX IV

## CALCULATION OF EARTHQUAKE SPECTRA

### Data Preparation

The aftershocks recorded on magnetic tape and selected for spectral analysis were played back at half speed (recorded at 1 7/8 ips, played back at 15/16 ips) on a two channel strip chart recorder at 125 mm/sec. These strip chart seismograms were then placed in a microfilm reader and projected onto a screen (magnification 14.8X). They were then traced onto a large fine lined sheet of graph paper. Digitization was performed at a 1.0 millisecond interval for the events recorded on the Honeywell system (giving a maximum resolvable frequency of 500 hertz) and a 0.5 millisecond interval for events recorded on the Sony system (giving a maximum resolvable frequency of 1000 hertz). Program SPEC1 was used to calculate the spectra of these events.

Due to the marginal quality of recording of the AMG seismogram of the August 2, 1974 event, this seismic trace was represented by measuring the times and heights of the peaks and troughs of the seismogram. Regular time interval digitization was then performed by fitting a cosine function to the peaks and troughs and interpolating between data points (see subroutine DIGI, program SPEC2).

### Theory of Spectral Analysis

The digitized time series representations of the compressional and shear waves of the earthquakes were transformed into the frequency

domain using a numerical Fourier Transform method (see subroutine SERTRA). The Fourier transform pair is as follows

$$Z(t_i) = \sum_{j=1}^{N} Z(f_j) e^{i2\pi f_j t_i} dt \tag{18}$$

and

$$Z(f_j) = \sum_{i=1}^{N} Z(t_i) e^{-i2f_j t_i} df \tag{19}$$

where $Z(t_i)$ is time domain representation of the wave form and $Z(f_j)$ is the frequency domain representation of the wave form. $Z(t_i)$ and $Z(f_j)$ are discrete functions of time and frequency respectively. $Z(f_j)$ is complex and takes the form

$$Z(f_j) = R(f_j) + iI(f_j) \tag{20}$$

where $R(f_j)$ is the real part of $Z(f_j)$ and $I(f_j)$ is the imaginary part of $Z(f_j)$. The modulus of the frequency-domain function $Z(f_j)$ is given by

$$[Z(f_j)] = (R(f_j)^2 + I(f_j)^2)^{\frac{1}{2}} \tag{21}$$

This is the quantity plotted in the spectral representations of the wave forms.

PRINTOUT OF SPEC1

```
001   @HDG,N X.M,66,0,0.
002   @FOR,I MAIN
003         DIMENSION A(5000),AFREQ(2500),PH(2500),LABEL(13),J(5000),SFREQ(250
004        *0)
005         PI=3.1415924536
006       1 READ(5,2,END=999)N,IP,T,(LABEL(I),I=1,13)
007       2 FORMAT(1X,2I3,F8.7,13A5)
008         READ(5,12)AMP60,PHI60
009      12 FORMAT(1X,2F10.5)
010     112 FORMAT(//17H DIRECT TRANSFORM,6H WO = ,2E17.7/10H   MODULUS,
011        110H AND PHASE/ (1X,E15.6,F10.2,E15.6,F10.2,E15.6,F10.2,E15.6,F10.2
012        2,E15.6,F10.2))
013       5 FORMAT(1H1//,40X,13A5///)
014       8 FORMAT(1X,10F10.1)
015       6 FORMAT(40X,'NUMBER OF DIGITIZED POINTS = ',I5,'   TIME INTERVAL ='
016        1,F10.8,' SEC'//)
017         READ(5,3)(J(I),I=1,N)
018       3 FORMAT(1X,19I4)
019         L=200-N
020         NN=N
021         N=200
022         DO 22 I=1,L
023      22 A(I)=0.0
024         DO 4 I=1,NN
025         IL=I+L
026       4 A(IL)=J(I)
027         WRITE(6,5)(LABEL(I),I=1,13)
028         WRITE(6,6)N,T
029         WRITE(6,8)(A(I),I=1,N)
030         WRITE(6,7)
031       7 FORMAT(1H1//,' PLOT OF AMPLITUDE VERSUS TIME--WITH 60 CYCLE NOISE
032        *'//)
033         DF=1.0/(N*T)
034         NW=N/2
035         CALL DRAW(N,1,A)
036         WRITE(6,23)
037      23 FORMAT(1H1//,' RAW SPECTRAL DATA WITH 60 CYCLE NOISE')
038         CALL SERTRA(0.0,N,NW,DF,AFREQ,PH,WO,A)
039         CALL TIC(NW,DF,AFREQ)
040         NW=NW-1
041         WRITE(6,18)
042      18 FORMAT(1X//,9X,'PLOT OF LOG10 SPECTRA VERSUS FREQUENCY(WITH 60 CYC
043        *LE NOISE)'//)
044         CALL DRAWML(NW,1,AFREQ,DF)
045         SFREQ(1)=AFREQ(1)
046         SFREQ(NW)=AFREQ(NW)
047         NL=NW-1
048         DO 14 I=2,NL
049         K=I+1
050         L=I-1
051      14 SFREQ(I)=(AFREQ(I)+AFREQ(L)*.5+AFREQ(K)*.5)/2.
052         WRITE(6,10)
053      10 FORMAT(1H1//,40X,'SMOOTHED SPECTRA'/)
054         WRITE(6,112)WO,DF,(SFREQ(I),PH(I),I=1,NW)
```

PRINTOUT OF SPEC1 (Continued)

```
055         WRITE(6,16)
056      16 FORMAT(1X///,30X,'PLOT OF LOG10 OF SMOOTHED SPECTRA VERSUS FREQUEN
057        *CY'//)
058         CALL DRAWML(NW,1,SFREQ,DF)
059         GOTO 1
060     999 STOP
061         END
062  @FOR,I SERTRA
063         SUBROUTINE SERTRA(DET,N,NW,DF,G,PH,WO,T)
064  C    DET = 0 TIME TO FREQ DOMAIN, NOT = 0 FREQ TO TIME, N=NUMBER OF TIME PO
065  C    NW=N/2 OR NO. OF FREQUENCY PTS. DF = FREQ INTERVAL = 1/T, T=N*DT
066         DIMENSION G(NW),PH(NW),T(N),CFN(500),SFN(500)
067         PI = 3.1415926536
068         CF = 0.0174532925
069         AN = N
070         DO 119 I = 1,N
071         A = I
072         ARG = (6.28318531*A)/AN
073     119 CFN(I) = COS(ARG)
074         SFN(I) = SIN(ARG)
075         IF (DET) 131,132,131
076     132 DO 133 I = 1,NW
077          G(I) = 0.0
078     133 PH(I) = 0.0
079          WO = 0.0
080          DO 139 J = 1,NW
081          X = 0.0
082          Y = 0.0
083          DO 140 I = 1,N
084          IJ = I*J - N*((I*J-1)/N)
085          X = X + T(I)*CFN(IJ)
086     140 Y = Y - T(I)*SFN(IJ)
087         PH(J)=(ATAN2(-Y,-X))/CF +180.
088     139 G(J) = (1.0/(AN*DF*6.28318531))*SQRT(X*X + Y*Y)
089          DO 134 I = 1,N
090     134 WO = WO +T(I)
091          WO = (1.0/(AN*DF*6.28318531))*WO
092         WRITE(6,112) WO,DF, (G(I),PH(I), I = 1,NW)
093     112 FORMAT(//17H DIRECT TRANSFORM,6H WO = ,2E17.7/10H   MODULUS,
094        110H AND PHASE/ (1X,E15.6,F10.2,E15.6,F10.2,E15.6,F10.2,E15.6,F10.2
095        2,E15.6,F10.2))
096          RETURN
097     131 DO 142 I = 1,N
098     142  T(I) = WO/2.0
099          DO 143  J = 1,NW
100          NSG = (PH(J)/360.)*AN
101          DO 143 I = 1,N
102          IJ = I*J + NSG -N*((I*J + NSG - 1)/N)
103     143 T(I) =T(I) + G(J)*CFN(IJ)
104          DO 144 I = 1,N
105     144 T(I) = 12.5663706*DF*T(I)
106         DT = (1.0)/(AN*DF)
107          RETURN
108          END
109  @FOR,I DRAW
110         SUBROUTINE DRAW (NTOT, INC, F)
111  C    NTOT=TOTAL NUMBER OF POINTS IN F.  F IS THE DATA (ONE DIMENSIONAL)
```

PRINTOUT OF SPEC1 (Continued)

```
C    TO BE PLOTTED. INC IS THE SAMPLE INTERVAL FOR PLOTTING F.
C    SCALE IS THE AMPLITUDE OF ONE FULL SCALE DEFLECTION
       DIMENSION   F(NTOT)
       DATA AA1/1H /,AA2/1H*/,AA3/1H+
       SCALE=0.
       DO 1 I=1,NTOT
       IF(SCALE.GT.ABS(F(I)))GOTO 1
       SCALE=ABS(F(I)+0.1*F(I))
     1 CONTINUE
       WRITE(6,1011) (I,I=-9,10) , (AA2,M=1,21)
  1011 FORMAT(3X,2015/2X,22A5)
  10   DO 1501 K = 1, NTOT, INC
       FK = 50.0*((F(K)/SCALE)+0.0001)
       KI = FK/50.
       KK = FK-KI*50.+50.495
   511 FORMAT (1X,110A1)
       WRITE (6,511) AA2, (AA1,I=1,KK),AA2
  1501 CONTINUE
       RETURN
       END
@FOR,I DRAWML
       SUBROUTINE DRAWML (NTOT,INC,F,DF)
C    NTOT=TOTAL NUMBER OF POINTS IN F.  F IS THE DATA (ONE DIMENSIONAL)
C    TO BE PLOTTED. INC IS THE SAMPLE INTERVAL FOR PLOTTING F.
C SCALE IS THE # OF LOG CYCLES
C  AMAXL IS MAX VALUE OF G(I)
        DIMENSION  F(NTOT)
        DATA AA1/1H /,AA2/1H*/,AA3/1H+
       AMNL=F(1)
       AMAXL=0.
       DO 2 I=1,NTOT
       IF(AMAXL.GT.F(I))GOTO 1
       AMAXL=F(I)
     1 IF(AMNL.LT.F(I))GOTO 2
       AMNL=F(I)
     2 CONTINUE
       SCALE= IFIX(ALOG10(AMAXL)-ALOG10(AMNL)+1.5)
        J1=100./SCALE-1
        I2=SCALE
        WRITE(6,1010) AA2,(((AA3,J=1,J1),AA2),I=1,I2)
 1010 FORMAT(11X,115A1)
        ALMAX=ALOG10(AMAXL)
       MAXF=ALMAX
        SCAL=FLOAT(MAXF)+0.5+SIGN(0.5,ALMAX)
       DO 1501 K=1,NTOT,INC
        FK=100.0*(ALOG10(F(K))-SCAL)/SCALE
       KI=FK/100.
       KI=-KI+(1.0-SIGN(1.0,FK))/2.0
       KK= FK+100.*KI
        DDF=DF*K
        WRITE(6,511)DDF,AA2,(AA1,I=1,KK),AA2
   511 FORMAT(1X,F10.2,110A1)
  1501 CONTINUE
       RETURN
       END
@FOR,SI TIC
       SUBROUTINE TIC (NW,DF,G)
```

PRINTOUT OF SPEC1 (Continued)

```
C GT TAPE CORRECTION FROM ABP AND HALL-SEARS FREQ CURVES
      DIMENSION GSOR(23),FRES(23),G(NW)
      DATA FRES/.5,.75,1.0,1.25,1.5,1.75,2.0,2.5,3.0,4.0,5.0,
     *7.5,10.0,15.0,20.,30.,40.,50.,60.,70.,80.,90.,100./
      DATA GSOR/6.6,23.6,50.9,78.3,111.2,135.2,161.0,204.6,
     *253.,343.,435.,655.,871.,1306.,1689.,2454.,3061.,
     *3695.,4117.,4433.,4750.,5106.,5278./
      FMIN=0.50
      FMAX=100.0
      IF(DF.LT.0.50) GO TO 7
      FMIN=DF
    7 IF(NW*DF.GT.FMAX) GO TO 8
      FMAX=NW*DF
    8 ISTART=FMIN/DF +0.00001
      ISTOP=FMAX/DF
      J=1
      DO 18 I=ISTART,ISTOP
      FQ=I*DF
   40 IF(FQ.LT.FRES(J)) GO TO 42
      J=J+1
      GO TO 40
   42 VAL=GSOR(J-1)+(GSOR(J)-GSOR(J-1))*(FQ-FRES(J-1))/
     *(FRES(J)-FRES(J-1))
   18 G(I)=G(I)/VAL
      RETURN
      END
@XQT
   71  0.0006873 S WAVE DATA,TPR,TAPE 2,SIDE 2 AT 1778, MARCH 23,1975

    10  27  53 120 145 152 110  15 -80-155-198-190-108 -73 -72 -68 -10  90
   180 193 177 115  55 -31 -61 -62 -67 -68 -15  35  57  53  55  55  33 -30
   -86 -65 -54 -56 -57 -53 -38 -12  30  63  58  36  28  20   0   1  51  95
    70  20 -20 -38 -76 -79 -65 -37 -27 -15  24  25  10 -40
```

PRINTOUT OF SPEC2

```
001   @ASG,T 41,D
002   @USE 41.,TPF$.
003   @FOR,SI MAIN
004   C NDT (NO.OF INTERVALS),TTIME(LENGTH OF TIME) DT*NDT
005   C HEIGHT SCALE FACTOR MM/MM,LAB  2I5,4F10.3,4A6,I1
006   C DATA ( )H(I),T(I),I(1,N)  (10F7.1)
007   C HEIGHT SCALE FACTOR MM/MM,LAB  2I5,4F10.3,5A6
008   C DATA  0-193 MM TIME SCALE
009         DIMENSION G(500),PH(500),T(1000),H(1000),F(2000),LAB(4),FN(2000)
010         DIMENSION IBUFF(5000)
011         CALL PLOTS(IBUFF(1),5000,41)
012         PI2 =   6.2831853072
013         NI=1
014         NTOT=100
015         IND=1
016         READ(5,101,END=999) N,NDT,DT,TI,TCAL,HCAL,LAB,IV
017    101  FORMAT (2I5,4F10.3,4A6,2X,I1)
018         IF(N.EQ.0) GO TO 999
019         WRITE (6,103) N,NDT,DT,TI,TCAL,HCAL,LAB,IV
020    103  FORMAT(1H1,I5,44H  PAIRS OF POINTS ARE TO BE INTERPOLATED AT ,I5
021        *,7H POINTS,F10.2,14H SECONDS APART,//13H BEGINNING AT, F10.3/
022        *15H TCAL UNITS/SEC,1F10.3,15H HCAL UNITS/MM,1F10.3,//4A6,
023        *5X,15HTYPE CORRECTION,I1)
024         TTIME = DT*NDT
025         NW = NDT / 2
026         DF = 1.0 / TTIME
027     47  READ(5,102)  (T(I),H(I),I=1,N)
028    102  FORMAT(10F7.0)
029         WRITE(6,104) (H(I),T(I),I=1,N)
030    104  FORMAT(1X, 10F10.3)
031         DO 20 I=1,N
032     21  H(I)=H(I)*HCAL
033     20  T(I)=T(I)/TCAL
034         WRITE(6,180)
035    180  FORMAT(1H1, 'VALUES OF H AND T CORRECTED TO MM AND SEC',/)
036         WRITE(6,105) (H(I),T(I),I=1,N)
037    105  FORMAT(1X,10F10.3)
038         CALL DIGI( H, T, N, TI, NDT, DT, F)
039    600  CONTINUE
040     48  DO 10 I=1,NDT
041         F(I)=-F(I)
042     10  FN(I)=I*DT
043         CALL CALFT (FN,F,IBUFF,NDT,LAB)
044         CALL STLNFT(FN,F,N,A,B,SGA,SGB)
045    601  CONTINUE
046         DO 11 I=1,NDT
047     11  F(I)=F(I)-A*I*DT-B
048         CALL SERTRA(0.0,NDT,NW,DF,G,PH,W0,F)
049    221  CONTINUE
050         GO TO (60,61,62), IV
051     60  CONTINUE
052         CALL WWSSC(NW,DF,G,PH)
053          GO TO 602
054     61  CONTINUE
```

PRINTOUT OF SPEC2 (Continued)

```
055         CALL SCSPC (NW,DF,G,PH)
056          GO TO 602
057      62 CONTINUE
058         CALL TIC (NW,DF,G,PH)
059     602 CONTINUE
060         WRITE(6,112) WO,DF,IV,(G(I),PH(I), I=1,NW)
061     112 FORMAT(//17H DIRECT TRANSFORM,6H WO = ,2E17.7/10H   MODULUS,
062        110H AND PHASE/,16H CORRECTION TYPE,I1,/1X,5(E15.6,F10.2))
063         DO 12 J=1,NW
064         FN(J)=LOG10(G(J))
065         FN(J)=-FN(J)
066      12 F(J)=LOG10(DF*FLOAT(J))
067         CALL SPLOT(FN,F,IBUFF,NW,LAB)
068     999 STOP
069         END
070   @FOR,SI ,CALFT
071         SUBROUTINE CALFT (FN,F,IBUFF,NDT,LAB)
072         DIMENSION IBUFF(5000),FN(500),F(500),LAB(5)
073         CALL PLOT(5.0,-10.0,-3)
074         CALL PLOT(0.0,+3.0,-3)
075         CALL SYMBOL (-1.5,0.0,0.14,LAB,90.,30)
076         CALL SCALE (FN(1),5.0,NDT,+1)
077         CALL SCALE (F(1),2.0,NDT,+1)
078         CALL LINE(F(1),FN(1),NDT,+1,40,3)
079         CALL AXIS(0.0,0.0,7HSECONDS,-7,5.0,90.,FN(NDT+1),FN(NDT+2))
080         RETURN
081         END
082   @FOR,SI ,STLNFT
083         SUBROUTINE STLNFT(X,Y,N,A,B,SGA,SGB)
084         DIMENSION X(N), Y(N)
085         SX =0.0
086         SXX =0.0
087         SY =0.0
088         SYY =0.0
089         SXY =0.0
090         DO 325 I=1,N
091         SX = SX + X(I)
092         SXX = SXX + X(I)*X(I)
093         SY = SY + Y(I)
094         SYY =SYY +Y(I)*Y(I)
095      325 SXY = SXY +X(I)*Y(I)
096         AN = N
097         DNOM = AN*SXX -SX*SX
098         A = (AN*SXY -SX*SY)/DNOM
099         B = (SY*SXX - SX*SXY)/DNOM
100         D2 = SYY -A*SXY-B*SY
101         SGA = SQRT (AN*D2/(DNOM*(AN-2.)))
102         SGB = SQRT(SX*SX*D2/(DNOM*(AN-2.)))
103         D2=SQRT(D2/AN)
104         WRITE(6,326) A,SGA,B,SGB,D2
105      326 FORMAT ( 30H LEAST SQUARE FIT, Y = A*X + B/3H A=,E13.6,4H+OR-,
106        1E13.6,3H B=,E13.6,4H+OR-,E13.6,13HMIN DEVIATION,E15.6)
107         RETURN
108         END
109   @FOR,SI TIC
110         SUBROUTINE TIC (NW,DF,G,PH)
111   C GT TAPE CORRECTION FROM AMP AND HALL-SEARS FREQ CURVES
```

PRINTOUT OF SPEC2 (Continued)

```
      DIMENSION GTOR(23),FRET(23),G(NW),PH(NW)
      DATA FRET/.5,.75,1.0,1.25,1.5,1.75,2.0,2.5,3.0,4.0,5.0,
     *7.5,10.0,15.0,20.,30.,40.,50.,60.,70.,80.,90.,100./
      DATA GTOR/6.6,23.6,50.9,78.3,111.2,135.2,161.0,204.6,
     *253.,343.,435.,653.,871.,1306.,1689.,2454.,3061.,
     *3695.,4117.,4433.,4750.,5106.,5278./
      FMIN=0.50
      FMAX=100.0
      IF(DF.LT.0.50) GO TO 7
      FMIN=DF
    7 IF(NW*DF.GT.FMAX) GO TO 8
      FMAX=NW*DF
    8 ISTART=FMIN/DF +0.00001
      ISTOP=FMAX/DF
      J=1
      DO 18 I=ISTART,ISTOP
      FQ=I*DF
   40 IF(FQ.LT.FRET(J)) GO TO 42
      J=J+1
      GO TO 40
   42 VAL=GTOR(J-1)+(GTOR(J)-GTOR(J-1))*(FQ-FRET(J-1))/
     *(FRET(J)-FRET(J-1))
   18 G(I)=G(I)/VAL
      WRITE(6,1066) ISTART,ISTOP,DF
 1066 FORMAT(1H1,55HDATA CORRECTED FOR DISPLACEMENT RESPONSE BETWEEN IST
     *ART,I5,3H*DF,10HAND ISTOP ,I5,3H*DF,/6H DF = ,F8.3)
      RETURN
      END
@FOR,SI ,DIGI
      SUBROUTINE DIGI(H,T,N,TI,NDT,DT,F)
      DIMENSION H(I),T(I),F(NDT)
      PI=3.1415926536
      I=0
      DO 20 J=1,NDT
      TIME=TI + (J-1)*DT
   22 IF (T(I+1).GT.TIME) GO TO 20
      I=I+1
      GO TO 22
   20 F(J)=H(I)+(TIME-T(I))*(H(I+1)-H(I))/(T(I+1)-T(I))
      RETURN
      END
@FOR,SI ,SERTRA
      SUBROUTINE SERTRA(DET,N,NW,DF,G,PH,WO,T)
C     DET = 0 TIME TO FREQ DOMAIN, NOT = 0 FREQ TO TIME, N=NUMBER OF TIME
C     NW=N/2 OR NO. OF FREQUENCY PTS. OF = FREQ INTERVAL = 1/T, T=N*DT
      DIMENSION G(NW),PH(NW),T(N),CFN(500),SFN(500)
      PI = 3.1415926536
      CF = 0.0174532925
      AN = N
      DO 119 I = 1,N
      A = I
      ARG = (6.28318531*A)/AN
      SFN(I) = SIN(ARG)
  119 CFN(I) = COS(ARG)
      IF (DET) 131,132,131
  132 DO 133 I = 1,NW
       G(I) = 0.0
```

PRINTOUT OF SPEC2 (Continued)

```
      133 PH(I) = 0.0
          WO = 0.0
          DO 139 J = 1,NW
          X = 0.0
          Y = 0.0
          DO 140 I = 1,N
          IJ = I*J - N*((I*J-1)/N)
          X = X + T(I)*CFN(IJ)
      140 Y = Y - T(I)*SFN(IJ)
          PH(J)=(ATAN2(-Y,-X))/CF +180.
      139 G(J) = (1.0/(AN*DF*6.28318531))*SQRT(X*X + Y*Y)
          DO 134 I = 1,N
      134 WO = WO +T(I)
          WO = (1.0/(AN*DF*6.28318531))*WO
          WRITE(6,112) WO,DF, (G(I),PH(I), I = 1,NW)
      112 FORMAT(//17H DIRECT TRANSFORM,6H WO = ,2E17.7/10H   MODULUS,
         110H AND PHASE/ (1X,E15.6,F10.2,E15.6,F10.2,E15.6,F10.2,E15.6,F10.2
         2,E15.6,F10.2))
          RETURN
      131 DO 142 I = 1,N
      142  T(I) = WO/2.0
          DO 143  J = 1,NW
          NSG = (PH(J)/360.)*AN
          DO 143 I = 1,N
          IJ = I*J + NSG -N*((I*J + NSG - 1)/N)
      143 T(I) =T(I) + G(J)*CFN(IJ)
          DO 144 I = 1,N
      144 T(I) = 12.5663706*DF*T(I)
          DT = (1.0)/(AN*DF)
          RETURN
          END
@FOR,SI ,WWSSC
          SUBROUTINE WWSSC(NW,DF,G,PH)
C   WORLD WIDE SEISMIC SYS. CORRECTION FROM FREQ RESPONSE CURVE
C   WWSSC (NW,G,DF,ISTART,ISTOP)
C   NW=NO. OF PTS. IN SPECTRA; G=MODULUS OF SPECTRA
C   DF=FREQ INCREMENT  1/T   T=TOTTAL TIME
          DIMENSION GCOR(11),FREQ(11),G(NW),PH(NW)
          DATA GCOR/.65,300.0,400.0,540.0,580.0,610.0,590.0,480.0,
         *310.0,38.0,1.8/
          DATA FREQ/.1,.8,1.0,1.25,1.43,1.67,2.00,2.50,
         *3.33,10.0,50.0/
          FMIN=0.1
          FMAX=50.0
          IF(DF.LT.0.1) GO TO 7
          FMIN=DF
        7 IF(NW*DF.GT.FMAX) GO TO 8
          FMAX=NW*DF
        8 ISTART=FMIN/DF+0.00001
          ISTOP=FMAX/DF
          J=1
          DO 18 I=ISTART,ISTOP
          FQ=I*DF
       40 IF(FQ.LT.FREQ(J)) GO TO 42
          J=J+1
          GO TO 40
       42 VAL=GCOR(J-1)+(GCOR(J)-GCOR(J-1))*(FQ-FREQ(J-1))/
```

PRINTOUT OF SPEC2 (Continued)

```
      *(FREQ(J)-FREQ(J-1))
   18 G(I)=G(I)/VAL
      WRITE(6,1066) ISTART,ISTOP,DF
 1066 FORMAT(1H1,55HDATA CORRECTED FOR DISPLACEMENT RESPONSE BETWEEN IST
     *ART,I5,3H*DF,10HAND ISTOP ,I5,3H*DF,/6H DF = ,F8.3)
      RETURN
      END
@FOR,SI SCSPC
      SUBROUTINE SCSPC (NW,DF,G,PH)
C SGS,JKS CORRECTION, S.C.SEISMIC PROGRAM,FROM FREQ RESPONSE CURVE
      DIMENSION GSOR(18),FRES(18),G(NW),PH(NW)
      DATA FRES/.72,.8,.9,1.,1.2,2.0,3.,5.,7.,10.,12.,20.,
     *30.,40.,50.,60.,70.,80./
      DATA GSOR/20.,22.,30.,38.,72.,120.,180.,310.,420.,580.,
     *880.,1010.,1050.,1075.,1080.,1067.,1060.,1020./
      FMIN=0.72
      FMAX=80.0
      IF(DF.LT.0.72) GO TO 7
      FMIN=DF
    7 IF(NW*DF.GT.FMAX) GO TO 8
      FMAX=NW*DF
    8 ISTART=FMIN/DF +0.00001
      ISTOP=FMAX/DF
      J=1
      DO 18 I=ISTART,ISTOP
      FQ=I*DF
   40 IF(FQ.LT.FRES(J)) GO TO 42
      J=J+1
      GO TO 40
   42 VAL=GSOR(J-1)+(GSOR(J)-GSOR(J-1))*(FQ-FRES(J-1))/
     *(FRES(J)-FRES(J-1))
   18 G(I)=G(I)/VAL
      WRITE(6,1066) ISTART,ISTOP,DF
 1066 FORMAT(1H1,55HDATA CORRECTED FOR DISPLACEMENT RESPONSE BETWEEN IST
     *ART,I5,3H*DF,10HAND ISTOP ,I5,3H*DF,/6H DF = ,F8.3)
      RETURN
      END
@FOR,SI ,SPLOT
      SUBROUTINE SPLOT (FN,F,IBUFF,NW,LAB)
      DIMENSION IBUFF(5000),FN(500),F(500),LAB(5)
      CALL PLOT(5.0,-10.0,-3)
      CALL PLOT(0.0,+3.0,-3)
      CALL SYMBOL (-1.0,0.0,0.14,LAB,90.,30)
      FN(NW+1)=0.0
      FN(NW+2)=1.0
      F(NW+1)=-1.0
      F(NW+2)= 0.5
      CALL LINE (FN,F,NW,+1,40,3)
      CALL LGAXIS (0.0,+0.0,2HHZ, +3,6.0,90., 0.1,0.5)
      CALL AXIS (5.0,-1.0,12HLOG DIS SPEC,+12,5.0,180,,-3.0,1.0)
      RETURN
      END
@HDG,N X,M,66,0,0,
@USE 41,TPF$
@XQT
    22   97  0.04      0,0        50.        .1        AUG 2 1974 CHR EVENT,AM
00.    00.    11.    12.    28.    -42.    41.    59.    50.    18.
  63.    -5.    70.    -2.    84.    -32.   100.    30.   104.    14.    1
 112.    49.   120.   -50.   126.    44.   130.   -41.   138.   -17.
150.   -45.   158.    54.   166.    43.   171.    58.   176.   -78.
 188.    68.   193.   0.0
```

# APPENDIX V

## EARTHQUAKE HYPOCENTER PLOTS

In order to better understand the three dimentional distribution of hypocenters, four profiles of aftershock locations were constructed. These profiles were centered at 33°57.5' North Latitude and 82°30' West Longitude. Each profile was three km long. The orientations of these four profiles were NW, NE, N75°E, and N15°W.

The plots of these profiles are shown in Figures 24, 25, 26, and 27. It is felt that no single strong linear trend is apparent on Figures 24 and 27. However, there are several apparent lineations on Figures 25 and 26. In Figure 25 (the NE-SW profile) a lineation of hypocenters possibly indicating a fault plane is apparent between A and A'. A second lineation with a similar orientation (dipping about 50° SW) is apparent between C and C" on C' and C". The three hypocenters in the vicinity of C may also be interpreted as being part of a third lineation between B and B'. The lineation B-B', dipping about 60° NE, nearly orthogmal to the other two lineations (A-A' and C'-C"), and could possibly represent a faulting on a co-plane.

Figure 26 also demonstrates significant lineations. The lineation D-D' dips at about 60° SW as does the lineation E-E'. The lineation D-D' may be associated with the A-A' lineation of Figure 25, and the E-E' lineation may be associated with the C'-C" lineation of Figure 25. These lineations might represent two planes of faulting;

however, it is felt that the quality and quantity of aftershock hypocenters is insufficient at this time to make any definitive statements on fault planes.

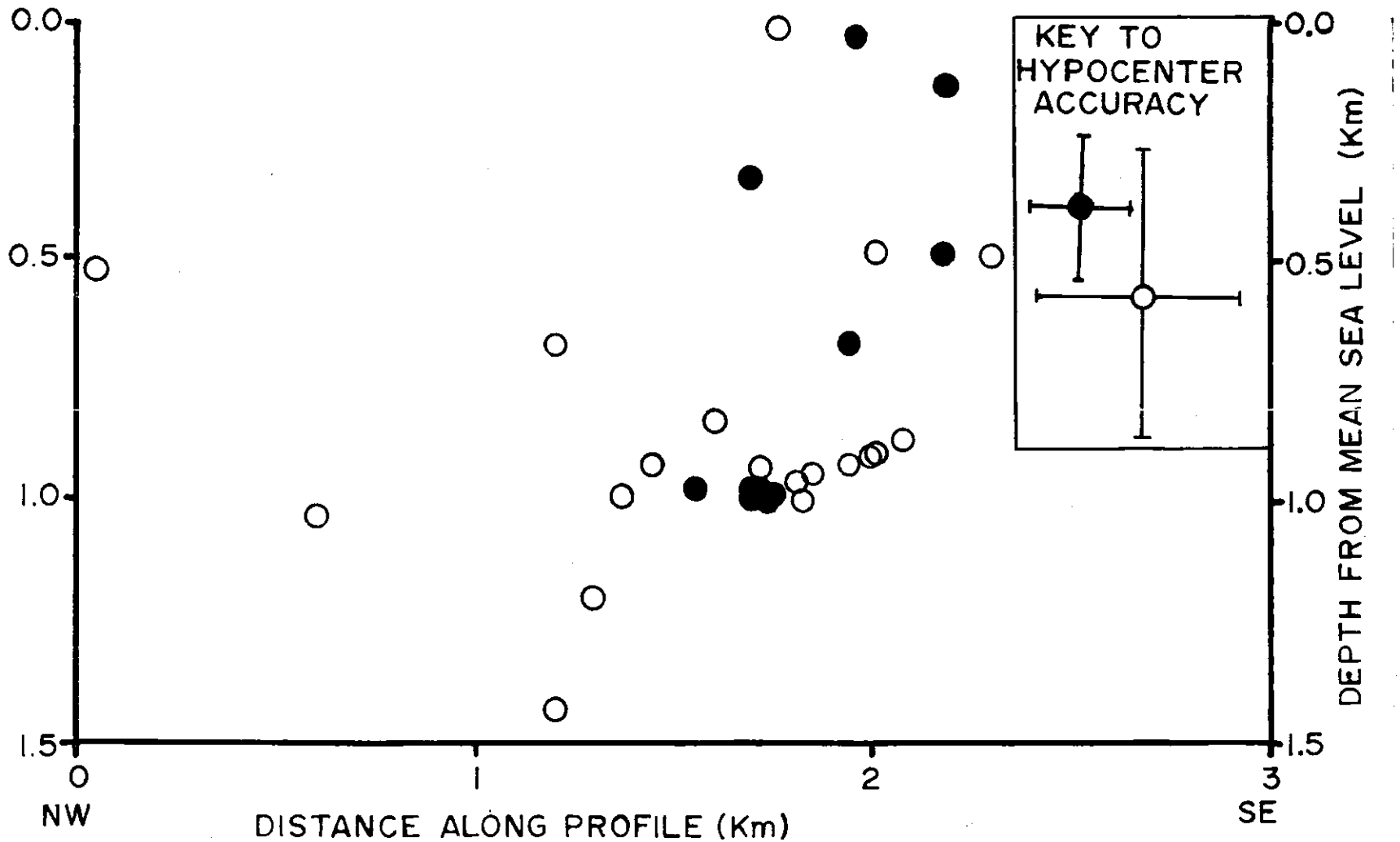


Figure 24. Projection of Hypocenters onto Vertical Plane Striking N45°W.

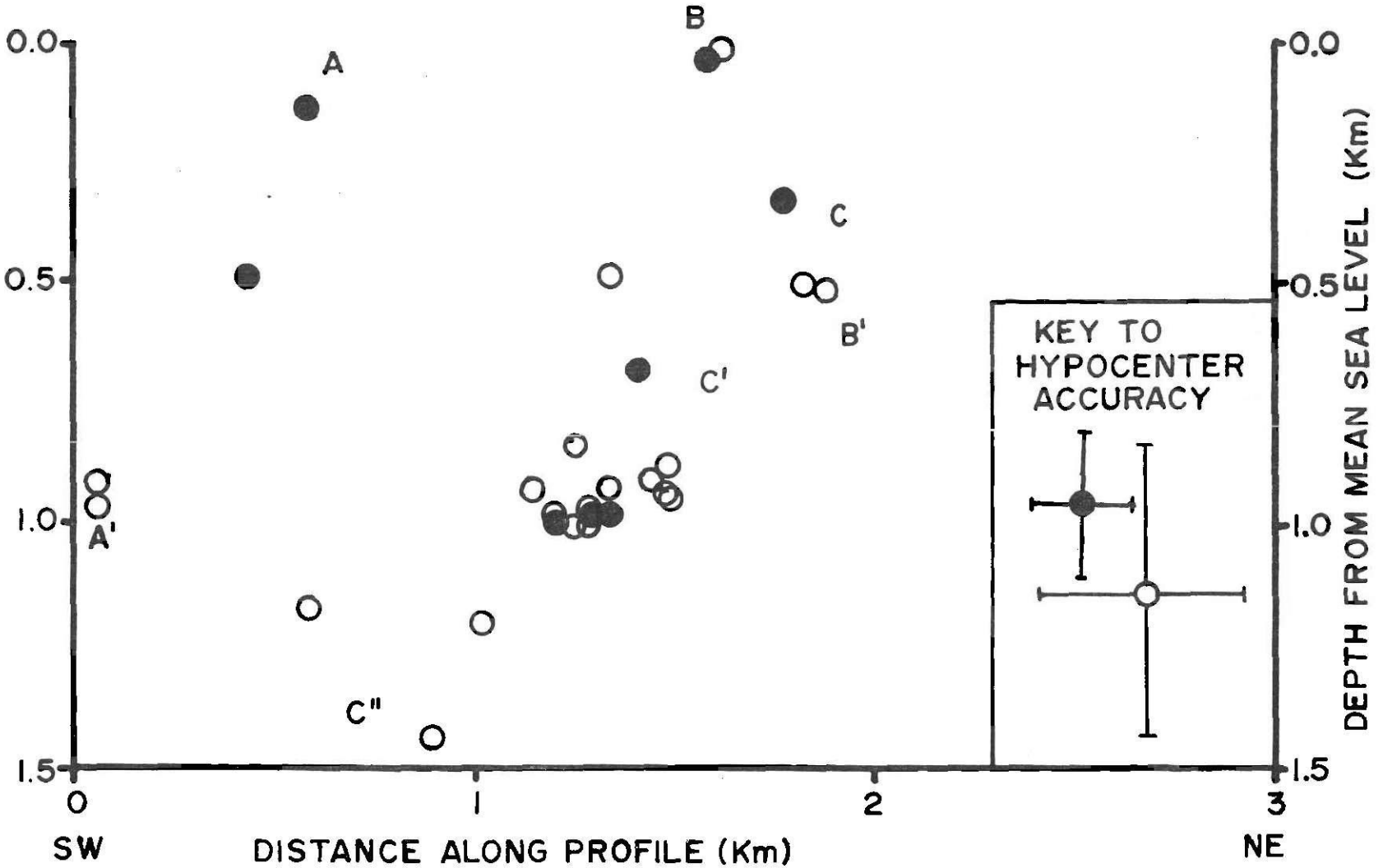


Figure 25. Projection of Hypocenters onto Vertical Plane Striking N45°E.

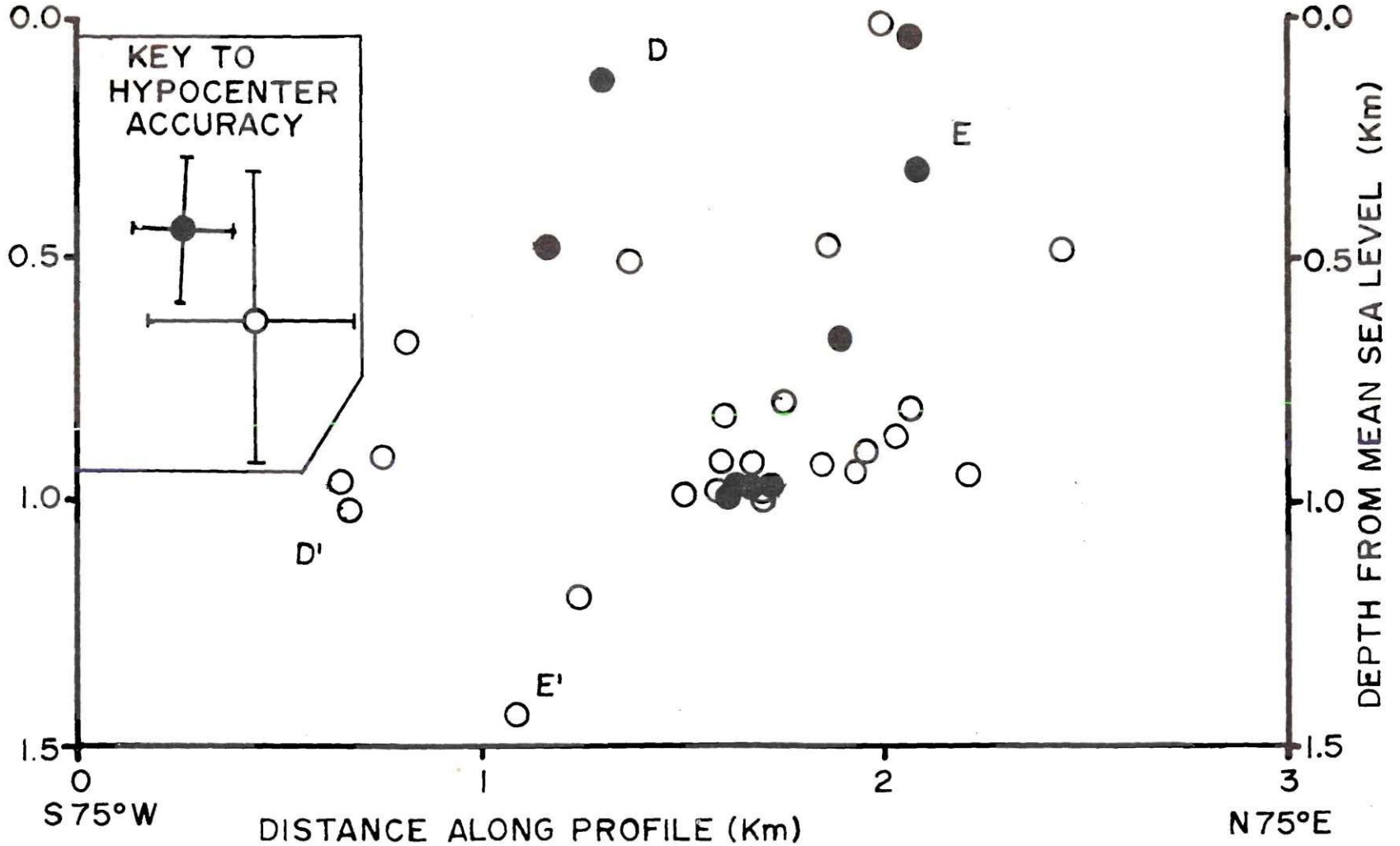


Figure 26. Projection of Hypocenters onto Vertical Plane Striking N75°E.

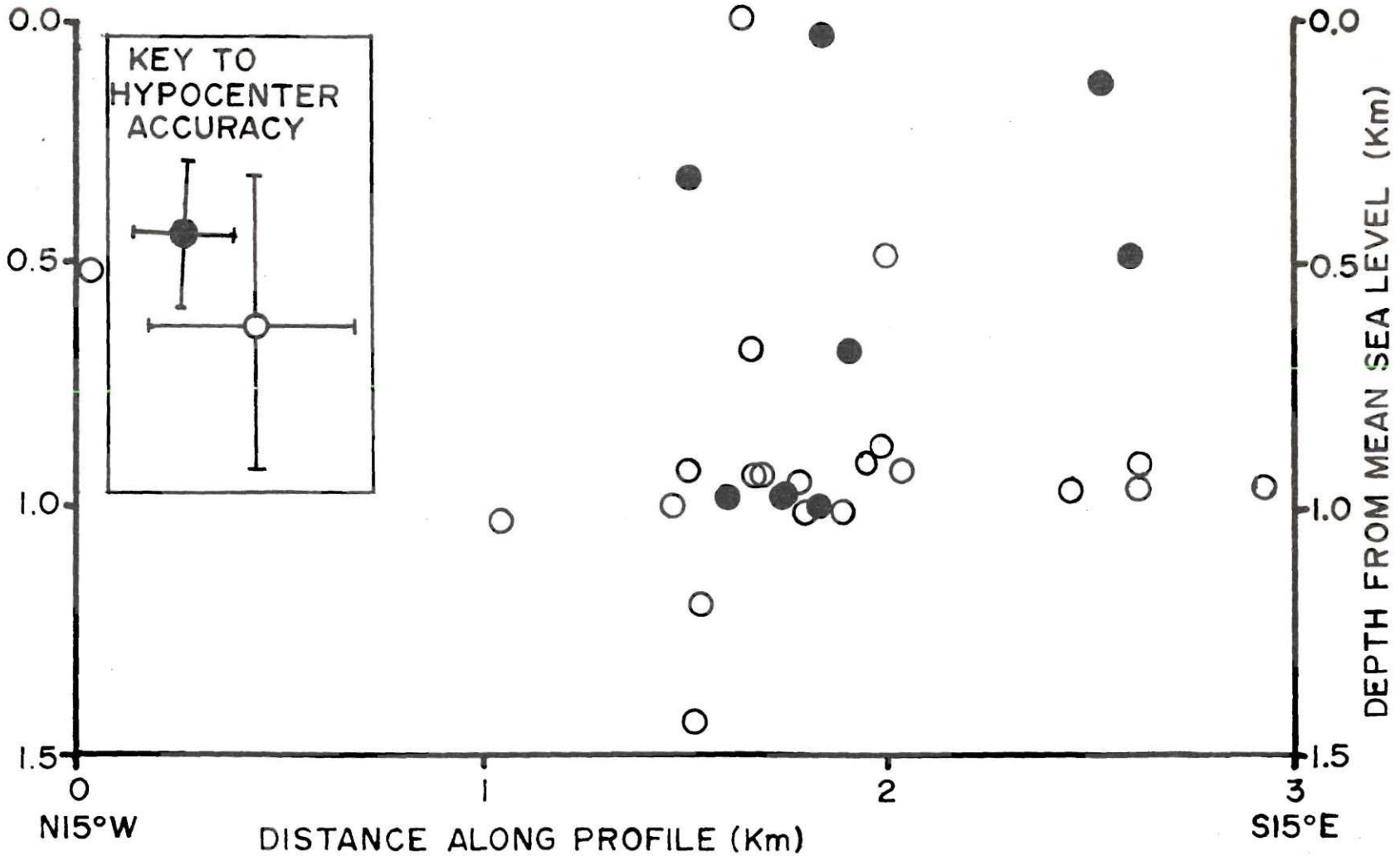


Figure 27. Projection of Hypocenters onto Vertical Plane Striking N15°W.

# BIBLIOGRAPHY


1. Atlanta Constitution, Nov. 3, 1875, p. 3, col. 1.

2. Båth, Markus (1973). Introduction to Seismology, p. 331, John Wiley and Sons, New York.

3. Bollinger, G. A. (1973). Seismicity and crustal uplift in the southeastern United States, Amer. J. of Sci. Cooper Vol. 273-A, 396-408.

4. Brune, J. N. (1970). Tectonic stress and spectra of seismic shear waves from earthquakes, J. Geophys. Res. 75, 4997-5009.

5. Crickmay, G. W. (1952). Geology of the crystalline rocks of Georgia, Ga. Geol. Sur. Bull. 58, p. 54.

6. Denman, H. E. (1974). Implications of sesimic activity at the Clark Hill Reservoir, Unpublished Masters Thesis, Georgia Institute of Technology.

7. Evernden, J. F. (1970). Study of regional seismicity and associated problems, Bull. Seis. Soc. Am. 60, 393-446.

8. Gibowicz, S. J. (1972). The relationship between teleseismic body-wave magnitude $m_b$ and local magnitude $M_L$ from New Zealand earthquakes, Bull. Seis. Soc. Am. 62, 1-11.

9. Gibowicz, S. J. (1973). Stress drop and aftershocks, Bull. Seis. Soc. Am. 63, 1433-1446.

10. Hadley, K. (1973). Laboratory studies of dilatancy and motion on fault surfaces at low confining pressures, Proceedings of the Conference on Tectonic Problems of the San Andreas Fault System, 427-435, Stanford University Press, Stanford, California.

11. Liebermann, R. C. and P. W. Pomeroy (1970). Source dimensions of small earthquakes as determined from the site of the aftershock zone, Bull. Seis. Soc. Am. 60, 879-890.

12. Lister, C. R. B. (1974). On the penetration of water into hot rock, Geophys. J. R. Astr. Soc. 39, 465-509.

13. Long, L. T. (1973). A local magnitude scale for the southeastern United States, Geol. Soc. Am. Abstracts with Programs, Vol. 5, No. 5, p. 414.

BIBLIOGRAPHY (Continued)

14. Long, L. T. (1974). Earthquake sequences and "b" values in the southeast United States, Bull. Seis. Soc. Am. 64, 267-273.

15. Long, L. T. (1975). A model for the earthquake tectonics of the Bowman and Summerville, South Carolina, epicentral zones, Geol. Soc. Am. Abstracts with Programs, Vol. 7, No. 4, p. 511.

16. Lowell, R. P. (1975). Circulation in fractures, hot springs and convective transport on mid-ocean ridge crests, Geophys. J. R. Astr. Soc. 40, 351-366.

17. Nuttli, Otto W. (1973). Seismic wave attenuation and magnitude relations for eastern North America, J. Geophys. Res. 78, 876-885.

18. Randall, M. J. (1973). The spectral theory of seismic sources, Bull. Seis. Soc. Am. 63, 1133-1144.

19. Richter, C. F. (1958). Elementary Seismology, W. H. Freeman and Co., San Francisco.

20. Rockwood, C. G. (1876). Notices of recent American earthquakes, No. 6, American Journal of Science and Arts, 28-29.

21. Sbar, Marc L., John M. W. Rynn, Frank J. Gumper and John C. Lahr (1970). An earthquake sequence and focal mechanism solution, Lake Hopatcong, northern New Jersey, Bull. Seis. Soc. Am. 60, 1231-1244.

22. Wiggins, Ralph A. (1972). The general linear inverse problem: Implication of surface waves and free oscillations for earth structure, Rev. Geophys. and Space Phys. 10, 251-285.